Multitarget Tracking Using Multistatic Sensors

MULTITARGET TRACKING USING MULTISTATIC SENSORS

BY

MAHESWARAN SUBRAMANIAM, B.Sc.Eng.(Hons.), M.A.Sc.

A THESIS

SUBMITTED TO THE DEPARTMENT OF ELECTRICAL & COMPUTER ENGINEERING

AND THE SCHOOL OF GRADUATE STUDIES

OF MCMASTER UNIVERSITY

IN PARTIAL FULFILMENT OF THE REQUIREMENTS

FOR THE DEGREE OF

DOCTOR OF PHILOSOPHY

Doctor of Philosophy (2012) McMaster University

(Electrical & Computer Engineering) Hamilton, Ontario, Canada

TITLE:	Multitarget Tracking Using Multistatic Sensors
AUTHOR:	Maheswaran Subramaniam B.Sc.Eng.(Hons.), University of Moratuwa, Sri Lanka, 2001 M.A.Sc., Ryerson University, Canada, 2004
SUPERVISOR:	Dr. T. Kirubarajan
NUMBER OF PAGES:	xv, 150

Abstract

In this thesis the problem of multitarget tracking in multistatic sensor networks is studied. This thesis focuses on tracking airborne targets by utilizing transmitters of opportunity in the surveillance region. Passive Coherent Location (PCL) system, which uses existing commercial signals (e.g., FM broadcast, digital TV) as the illuminators of opportunity for target tracking, is an emerging technology in air defence systems. PCL systems have many advantages over conventional radar systems such as low cost, covert operation and low vulnerability to electronic counter measures.

One of another opportunistic signals available in the surveillance region is multipath signal. In this thesis, the multipath target return signals from distinct propagation modes that are resolvable by the receiver are exploited. When resolved multipath returns are not utilized within the tracker, i.e., discarded as clutter, potential information conveyed by the multipath detections of the same target is wasted. In this case, spurious tracks are formed using target-originated multipath measurements, but with an incorrect propagation mode assumption. Integrating multipath information into the tracker (and not discarding it) can help improve the accuracy of tracking and reduce the number of false tracks.

However, the limitations of PCL as well as the multipath assisted tracking include lack of control over the illuminators and the reflectors, limited observability and poor

detection due to low Signalto-Noise Ratio (SNR). This leads to high clutter with low probability of detection of target. The number of reflector returns from the same target varies in multipath assisted tracking. Even though incorporating mutipath reflected signals will facilitate better estimates of the target states due to spatial diversity, one cannot use these measurements without resolving target-origin and multipath-origin uncertainties. In this thesis, these opportunistic measurements, i.e., commercial broadcast signals measurements in PCL tracking and resolvable multipath target return measurements in multipath assisted tracking are exploited.

In multipath assisted tracking, obtaining the complete knowledge of reflectors and consistently receiving resolved target originated multipath measurements are challenging. We derived tracking algorithms to handle low probability of detection and high nonlinearity in the measurement model due to high measurement error. Also, tracking algorithms are proposed to track multiple targets by removing bias on direction of arrival measurement. In multipath assisted tracking analysis, we also considered the cases where the reflector information is completely known, as well as when there are uncertainties.

We give the optimal formulations for all of the above problems as well as the performance evaluations using PCRLB. Simulation results illustrate the performance of the algorithms.

To my parents and my wife.

Acknowledgements

First, I thank my supervisor, Dr. T. Kirubarajan, for giving me an opportunity to work on this topic and for providing advice and support throughout the course of this research work. I would also like to thank my supervisory committee members, Dr. I. Bruce and Dr. S. Sirouspour, for their feedback on the ideas covered in this thesis. I thank Dr. R. Tharmarasa, a post doctoral fellow, for all the helps he extended. I thank my fellow graduate students in the ECE department for their help and support. I would like to also thank all the instructors at the ECE Department. My sincere thanks to the ECE Department staff, especially to Cheryl Gies.

I would like to thank M. Pelletier at ICx Radar Systems and Dr. M. McDonald, defence scientist in radar systems, at Defence Research Development Canada (DRDC) for their insightful comments and grants. I am grateful to DRDC and TNO (NATO C3 Agency) for providing real radar data for tracking experiment.

Finally, I would like to thank my friends, my relatives and my family. The encouragement and support by my beloved wife Mathumai, our joyful children, Dylan, Kavin and Molly, and our newly arriving little girl are powerful sources of inspiration and energy. My special thanks are for my parents and for my brother for their never-ending love and support.

Nomenclature

Acronyms

ACMA	algebraic constant modulus algorithm
AOA	angle of arrival
ARM	anti-radiation missiles
CBF	conventional beam forming
CMKF	converted measurement Kalman filter
DOA	direction of arrival
EKF	extended Kalman filter
FIM	Fisher information matrix
IRM	information reduction matrix
JPDA	joint probabilistic data association
MFT	auction algorithm based multi-mode fusion tracking
MHT	multiple hypothesis tracking
MPDA	multipath probabilistic data association
MSD	multipath S-dimensional assignment technique
MVDA	multipath Viterbi data association algorithm

NATO	north Atlantic treaty organization
NC3A	north Atlantic treaty organization consultation, command and control agency
NN	nearest neighbor
OTHR	over-the-horizon radar
PCRLB	posterior Cramer-Rao lower bound
PCL	passive coherent location
PDA	probabilistic data association
pdf	probability density function
PHD	probability hypothesis density
RMSE	root mean square error
S-D	S- dimensional assignment technique
SIR	sampling importance resampling
SMC	sequential Monte-Carlo
SN	strongest neighbor
SNR	signal-to-noise ratio
TDOA	time difference of arrivals
TMA	target motion analysis
TNO	the Netherlands organization for applied scientific research
UKF	unscented Kalman filter
VDA	Viterbi data association

Contents

List of Figures

Chapter 1

Introduction

1.1 Motivation and Contribution of the Thesis

1.1.1 Signals of Opportunity in the Environment

Active transmitters are combat targets in a war zones. Implementation of an undetected covert tracking has been essential in such an environments. Therefore, there has been high demand for building an undetectable improved surveillance systems especially in combat situations. With the latest enhanced signal processing technologies, exploiting the existing signals in the environment and tracking the target using such signals not only enable covert tracking, but also bring many additional advantages. An innovative approach uses passive signals, allow targets to be tracked without sending any active electromagnetic signals, but rather by using existing commercial broadcast signals from TV or FM radio signal around the region. Passive Coherent Location (PCL) is considered a bistatic radar or multistatic radar tracking

system which utilizes the commercial broadcast signals in the environment. The environment also has multipath reflected signals that are bounced off different sources such as buildings, mountains, the ground, clouds and moving targets.

Exploration of target return multipath signals and incorporating the target information from such signals into tracking algorithms have been studied in the literature and have become more attractive due to their inherent low cost, as this reduces the need for more sensors across the surveillance region. Also, incorporating target return multipath signals into the tracking reduces the number of bank of receivers that are needed for achieving the required accuracy of tracking. When the surveillance environment has resolvable multipath signals at the sensors, if proper measures are not taken, multiple tracks will be formed for every target. In typical radar systems, these spurious tracks are removed from tracking and therefore the information carried in such target return tracks are not utilized in tracking. Information conveyed by multipath detections of the same target may be wasted by treating these as inappropriate signals. In a multipath environment, for every multipath target return (reflection path), the sensor receives an additional measurement from the same target. In general non-multipath scenarios, in every sensor scan, there will be either one or zero measurement from every target depending on whether it is detected or undetected, respectively.

In a multipath environment, when target returns from distinct propagation modes are resolved, associating these signals appropriately into the estimation will yield better estimates of the target states. An appropriate data association of multipath reflection models has to be identified to use these measurements. Incorrect reflection model assignment will lead to errors in association and tracking. In order to utilize

these measurements appropriately, they have to be identified appropriately and a correct multipath propagation mode assignment must be performed. Uncertainty in the multipath signal propagation mode assignment adds additional complexity to data association problem. Also in multipath environments, contrary to the typical tracking scenario, in a single scan, every sensor will have more than one measurement for the same target. In addition to the multipath signal, the complexity of the problem is further increased due to missed detections, clutter, and false alarm.

Let us consider a simple phenomenon that causes a target reflected signal to be received via more than one path. This causes a time difference between the arrivals (TDOA) of the received signals at the sensor. A measurement of the TDOA received by the sensor can be used to calculate the multipath range and bistatic range. The direct and reflected signals' direction of arrival (DOA) is also used to study the geometry of the signal path, and this measurement is used for tracking.

Generally, the strength of the received multipath signals depends on the power of the transmitter, reflection environment and the signal processing capabilities of the sensor. Depending on the reflection environment, it is also possible for sensors to have resolved signals that went through more complex reflections. The multipath reflection environment and its topological geometric parameter information must be known when combining the signals received through each multipath reflection mode at the sensor. In practical scenarios, precisely knowing the coordinates of the reflection points or the surface information is not possible. That inherently increases the complexity of the multipath problem.

In this thesis the signals of opportunity, i.e., environmentally available commercial

broadcasting signals and target reflected multipath signals, are exploited and appropriately combined to track the targets. We derive algorithms for PCL tracking as well as multipath assisted multitarget tracking using environmentally available signals. These commercial multi-transmitter environment is considered as a multistatic radar environment.

1.1.2 Passive Coherent Location Tracking

Passive Coherent Location (PCL), which is a special case of bistatic radar system, is an emerging (or a re-emerging) technology in air defense systems (1) (2). In a PCL system, existing commercial signals (e.g., FM broadcast and TV telecast signals) are used as illuminators of opportunity to track airborne targets. The locations and transmission frequencies of commercial transmitters are mostly known and the receiver is designed by the user to match. Some of the signals from those transmitters of opportunity reflect off airborne targets in the vicinity and the reflected signals are also received by the receiver. Thus, bistatic measurements are obtained from the direct and target-reflected signals that are originated by the commercial transmitters.

A typical PCL system environment is described in Figure 3.1, which shows a real world PCL environment. There will be other unwanted signals such as direct signal from other transmitters and reflections from ground, buildings, trees, cloud and other moving or stationary objects. The dominant source of interference in the surveillance channel is caused by the direct in-band signals from different transmitters in the region. Multipath signals received from multiple directions are another sources of interference at the PCL radar. To efficiently remove the strong clutter signals and interference, they described an adaptive filter algorithm (2) (3) (4).

The ideal situation is that the reference signal will have only the transmitted signal. In practice, the reference signal also contains some target returns, multipath and clutter from surrounding objects such as the ground mountains, buildings and trees. These non-direct components are interference and manifest as increased clutter in the signal processor output. These clutter returns have the common property of zero Doppler effect (2) (4) (5) (6). This will create problems in direction of arrival estimation. Passive coherent detection of weak moving targets by clutter cancelation algorithm in PCL was provided in (3). Adaptive removal of strong echoes from the received signal increases PCL radar performance (7). The performance prediction of PCL system was discussed in (10). The implications of transmitter waveform and bistatic geometry on target detection, location and imaging are discussed in (9) (10) (11). In PCL, Doppler shift between direct signal and target echo result in decrease output of highest peak value with some occurrence of false peaks. A Doppler compensation method for such PCL systems was proposed (12). An enhanced accurate multiple target detection in PCL radar systems based on TV and radio ambiguity function processing is presented (13). The echo signal from the transmitters of opportunity reflected from the target is received by the PCL radar measurement antenna. A classical single-target PCL scenario is presented in Figure 1.1.

A PCL system has a number of advantages over conventional monostatic or bistatic radar systems. The monostatic or bistatic active radars quickly become combat targets themselves due to their energy emission, which can be used by the enemy target to estimate the radar's transmitter location. However, in PCL systems, there is almost no risk of being detected as the transmission sources are already out there in the environment for their intended purposes. Therefore, PCL systems increase

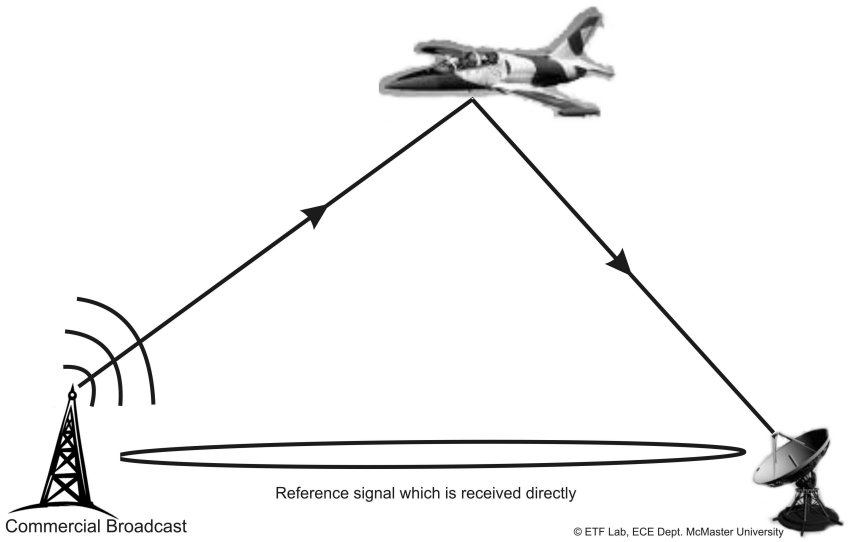

Figure 1.1: Bistatic radar PCL environment.

resilience to electronic countermeasures. Since commercial signals are freely available almost everywhere, PCL systems enjoy certain advantages such as wide coverage, low cost of operation and maintenance, and operation without a frequency clearance. The PCL system can also be used to fill blind zones of radar in an economic and effective manner.

The main disadvantage of the PCL system is that the receiver does not have control of the transmitters. Hence the transmitter location, power or waveform cannot be changed as desired. It is common to have multiple transmitters (e.g., radio broadcasting stations or relay stations) that operate in the same frequency inside the coverage region of a receiver.

This thesis analyzes the feasibility of using PCL systems for tracking multiple airborne targets. High bearing errors, low probability of detection and high false alarms rate will increase the complexity of tracking algorithm. Due to the nonlinearity in

the measurement model, these errors will highly degrade the tracking/filtering performance. In this thesis, Converted Measurement Kalman Filter (CMKF), Unscented Kalman Filter (UKF) and particle filter based Probability Hypothesis Density (PHD) filters are implemented to track the targets using nonlinear PCL radar measurements. Performances of above filters are compared on simulated data and real data collected by TNO (NATO C3 Agency (NC3A)).

The major contributions of this section in this thesis are implementation and comparison of nonlinear filters for tracking with PCL measurements and removing the bias in direction of arrival measurements.

1.1.3 Multipath Assisted Multitarget Tracking

With a single-measurement per target assumption, when resolvable multipath detections of a single target are present in the measurements, conventional tracking algorithms such as the Kalman filter with probabilistic data association (PDA) mostly produce multiple tracks for a single target. In this case, information conveyed by multipath detections of the same target may be wasted by treating some of them as clutter. The tracking algorithms may also combine several measurements belonging to different propagation modes. But combining the measurements becomes invalid unless proper accounts are taken for each such mode.

In order to move to a framework that supports the fusion of multipath measurements, it is necessary to relate the measurements from different propagation modes to a common state (14) (15) (16) (17) (18). To focus on tracking in multipath detection scenarios, we assume that the measurement models for various propagation modes are known from analysis of reflection geometry. Various propagation models due to

multipath reflections were studied in the literature in the usage of over-the-horizon radar (OTHR) systems. Tracking systems for OTHR (19) have relied on Kalman filters with the PDA (20) to track targets in slant or radar coordinates. This approach has the advantage of not requiring information about the multipath reflection point or surface information and propagation modes. However, problem arises when mapping of slant coordinates to the ground coordinates when the tracking is performed in ground coordinates. The coordinate registration procedure facilitates this mapping separately from the tracking (21). A most common problem in OTHR is the phenomenon of multipath propagation whereby radar signals scattered from the same target arrive at the receiver via different propagation paths.

A multipath probabilistic data association (MPDA) was described for initiation and tracking in OTHR is described in (22). MPDA is capable of exploiting multipath target signatures arising from discrete propagation modes that are resolvable by the radar. In (22), Pulford and Evans used the multipath target signatures in azimuth, slant range, and Doppler in a non-linear measurement model for target tracking.

In (23), a multipath Viterbi data association algorithm (MVDA) for OTHR was described. This proposed MVDA algorithm solves the problem of multiple propagation modes caused by multipath through modeling target movements in ground coordinates and implementing data association in radar coordinates (23). This MVDA algorithm extends Viterbi data association (VDA) from association between measurement and track to association among measurement, propagation mode and track.

In (24), Friedlander showed that the depth and range of an underwater source can be estimated from measurements of propagation delay differences along different

propagation paths. The accuracy of depth and range estimation by using the Cramer-Rao lower bound was studied. The formulas derived were used in conjunction with a propagation model to compute the bounds for an inhomogeneous propagation medium (nonconstant velocity profile).

In (25), airborne acoustic source signals emitted by direct and ground-reflected paths are used to measure the multipath delay and provide an instantaneous estimate of the elevation angle of the airborne target. Lo et al. formulated two methods to estimate the speed and altitude of the aircraft. Both methods require the estimation of the multipath delay as a function of time (25). In (18), Bogner proposed a pattern classification approach for associating multipath tracks caused by different ionospheric layers. Neural networks and statistical methods were applied to combine track affinities and associate pairs of tracks (18).

In (26), multi-mode fusion tracking of OTHR based on an auction algorithm (A-MFT) was proposed, which effectively solves the problem of multi-mode measurements. In (17), Blanc-Benon and Jauffret showed that target motion analysis (TMA) offers two tactical advantages over the classical bearings-only TMA. There is no requirement for any ownship maneuver and TMA can obtain this with good performance in terms of estimation error achieved in a shorter time (17). Utilization of multipath reflections is sometimes extremely helpful in improving the visibility, as it is more difficult to deploy a sensor in an enemy's territory than it is to receive multipath reflections from a surface in an enemy's territory.

In this thesis, an algorithm was proposed for initiating and tracking multiple targets using multiple transmitters and receivers. This algorithm is capable of exploiting

multipath target returns from distinct and unknown propagation modes. When multipath returns are not utilized appropriately within the tracker, (e.g., discarded as clutter or incorporated with incorrect propagation mode assumption) the potential information in the multipath returns is lost. In the initial case, it is considered that the multipath reflection points are known to the receiver. In more practical scenarios, it is more appropriate to assume that the locations of reflection points are not exactly known. In this thesis, the proposed algorithm will track the targets when there are uncertainties in the multipath reflection surface parameters.

The major contributions of this section in this thesis are implementation of a multiframe assignment algorithm and tracking with resolved multipath measurements for difference scenarios such as when the reflection point information is completely available, and when there are uncertainties in reflection surface information. This modified multiframe data association algorithms, i.e., multipath S-D or MSD, will be used for resolving the multipath reflection mode and target assignment uncertainty, and we compare the performance using PCRLB.

1.2 Organization of the Thesis

This thesis is structured as follows: Chapter 2 describes the general mutisensor multitarget tracking problem, and monostatic, bistatic and multistatic radar environment. Chapter 3 explains the multitarget tracking with PCL and the bias removal and sensor calibration in passive radar system. Chapter 4 provides algorithms for multipath assisted multitarget tracking with completely known reflector locations. Chapter 5 details the algorithms for multipath assisted multitarget tracking when uncertainty in reflector locations. This chapter also describes the performance evaluation using

PCRLB. Chapter 6 concludes the thesis with future directions.

1.3 Related Publications

1.3.1 Journal Articles

1. "Evaluations of Multipath Assisted Multitarget Tracking using Multiframe Assignment", *To be submitted to IEEE Transactions on Aerospace and Electronic Systems.*

2. "Multitarget Passive Coherent Location with Transmitter-Origin and Target-Altitude Uncertainties", *Accepted in final form for IEEE Transactions on Aerospace and Electronic Systems*, September 2011.

1.3.2 Conference Publications

1. M. Subramaniam, K. Punithakumar, R. Tharmarasa, M. McDonald and T. Kirubarajan, "Performance evaluations of multipath multitarget tracking using PCRLB", *Proceedings of the SPIE Conference on Signal and Data Processing of Small Targets*, Vol. 8137, 813714, San Diego, CA, August 2011.

2. M. Subramaniam, R. Tharmarasa, M. McDonald and T. Kirubarajan, "Multipath-Assisted Multitarget Tracking with Reflection Point Uncertainty", *Proceedings of the SPIE Conference on Signal and Data Processing of Small Targets*, Vol. 7698, pp. 76981A -12, Orlando, FL, April 2010.

3. M. Subramaniam, R. Tharmarasa, M. Pelletier and T. Kirubarajan, "Multipath-Assisted Multitarget Tracking Using Multiframe Assignment", *Proceedings of*

the SPIE Conference on Signal and Data Processing of Small Targets, Vol. 7445, pp. 74450Z-11, San Diego, CA, August 2009.

4. M. Subramaniam, K. Punithakumar, M. McDonald, and T. Kirubarajan, "Integrated Bias Removal in Passive Radar Systems",*Proceedings of the SPIE Conference on Signal and Data Processing of Small Targets*, Vol. 6969, pp. 69690Q-10, Orlando, FL, March 2008.

5. M. Subramaniam, R. Tharmarasa, M. McDonald and T. Kirubarajan, "Passive Tracking with Sensors of Opportunity using Passive Coherent Location", *Proceedings of the SPIE Conference on Signal and Data Processing of Small Targets*, Vol. 6969, pp. 69691F-12, Orlando, FL, March 2008.

1.4 Other Publications During the Course

1.4.1 Journal Articles

1. M. Subramaniam, A. Anpalagan and I. Woungang, "Performance of a distributed full inversion power control and base station assignment scheme in a cellular CDMA network with hot-spots", *Springer Wireless Personal Communications*, WIRE1949, 2011.

Chapter 2

Multitarget Tracking and Multistatic Sensors

2.1 Target Tracking

Identifying the most likely value of a quantity of interest from its incomplete, noise corrupted, inaccurate and uncertain measurements is called estimation. Target tracking is the process of performing continuous estimation of the state, such as position and velocity, of a moving object over time. This is achieved by repeated prediction of the state of the moving object at a regular interval. Prediction is the process of estimating the future state by using the current measurements. Measurements are taking at a regular interval and used for continuous prediction of the future state so that the objects can be tracked continuously.

Filtering is the estimation of the current state of a dynamic system from noise corrupted measurements. Such estimates are produced by the tracking systems with some level of accuracy. They also produce the measure of such accuracies as part of

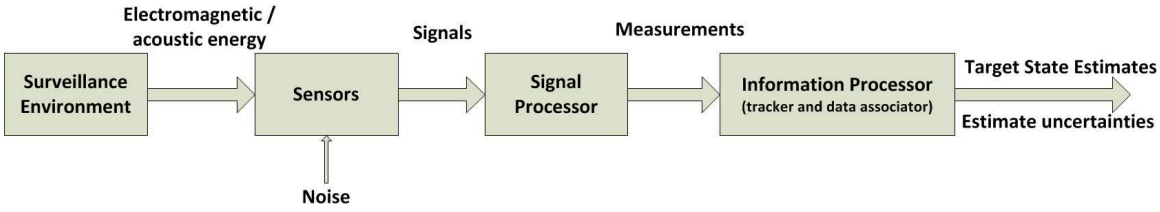

Figure 2.1: A typical tracking system.

the estimates (27) (28).

A typical tracking system is shown in Figure 2.1. The noise corrupted electro magnetic signal in the environment is received by the sensors and it is processed by going through signal processing procedures to obtain the information or measurements. These measurements are then sent to the information processor, which includes the data association and tracking algorithms, to obtain the target state estimates and its uncertainties. The data association and tracking procedure is describe below.

2.1.1 Surveillance System

A sophisticated surveillance system capable of detecting and tracking a large number of targets using various measurements received from different sensors. With high sensitive sensors, low SNR requirements and increased signal processing capabilities, numerous and more complex measurement data have become available for tracking filters. Advanced information processing filters help build sophisticated surveillance systems, which handle additional uncertainties, inaccuracies, clutter, false alarms and counter measures (16) (27).

The probability of detection P_{D} and probability of false alarms P_{FA} play an important roles and add complexities to the tracking in a surveillance environment.

- In ideal sensors:

$$P_{\mathrm{D}} = 1 \tag{2.1}$$

$$P_{\mathrm{FA}} = 0 \tag{2.2}$$

- In realistic sensors:

$$P_{\mathrm{D}} < 1 \tag{2.3}$$

$$P_{\mathrm{FA}} > 0 \tag{2.4}$$

2.1.2 State and Measurement Models

There are at least two models required for target tracking (28): a system or a state model and a measurement model. A state model describes the evolution of the state with time, whereas a measurement model relates the noisy measurements to the state. These models can be either liner or non-linear.

A linear state model can be written as:

$$x_{k+1} = F_k \; x_k + \nu_k \tag{2.5}$$

A linear measurement model can be written as:

$$z_k = H_k \; x_k + \omega_k \tag{2.6}$$

A non-linear state model can be written as:

$$x_{k+1} = f_k(x_k) + \nu_k \tag{2.7}$$

A non-linear measurement model can be written as:

$$z_k = h_k(x_k) + \omega_k \tag{2.8}$$

Here ν_k denotes the process noise and ω_k denotes the measurement noise at measurement time k. We assume that ν_k is Gaussian distributed with zero mean and covariance Γ_k. ω_k is Gaussian distributed with zero mean and covariance Σ_k. F_k and H_k denote linear state and measurement models and are known matrices, f_k and h_k are non-linear functions, x_k denotes the state of the moving target, and z_k is the received measurement vector.

2.1.3 Bayesian Filtering Approach

In filtering theory, the Bayesian approach is used to find the posterior probability distribution of the state given all the received measurements at a time. The posterior distribution provides the mean and covariance of the state at each time step. All the observations or the measurements received up to the current time are used to provide the state estimate and therefore this provides a complete solution (29). This probability density function (pdf) is repeatedly predicted, which details the target motion. This pdf is updated when a new measurement or observation becomes

available. Hence, an estimate is required as the new measurements arrives, and this processes is called filtering (30). As these measurements arrive, they are processed sequentially rather than as a set of parallel or batch processing. Therefore, neither the need for storing the previous time step measurements or observations nor the need to reprocess the existing measurement exist. This sequential process is done essentially with two important step, i.e., prediction and update.

As each new measurement arrives, an estimate is predicted and updated recursively for each time step. The state model is used to predict the state pdf forward in prediction for each time step to the next successive time step and the measurement model is used to calculate the posterior distribution according to Bayes' rule.

Let be the probability distribution function be $p(x_k|Z_k)$ at the measurement time step k is available, where $Z_k = [z_1, z_2, \ldots, z_k]$. The state model (2.7) is used for prediction to obtain the prior probability distribution function of the state at measurement time step $k+1$ and is given by

$$p(x_{k+1}|Z_k) = \int p(x_{k+1}|x_k)p(x_k|Z_k)dx_k \tag{2.9}$$

The latest measurement is used in the update stage to modify the prediction probability distribution function. At the next measurement time step $k+1$, a new measurement z_{k+1} becomes available, and with this the prior will be updated via Bayes' rule.

$$p(x_{k+1}|Z_{k+1}) = \frac{p(z_{k+1}|x_{k+1})p(x_{k+1}|Z_k)}{p(z_{k+1}|Z_k)} \tag{2.10}$$

The measurement model (2.8) is used to define the above likelihood function

$p(z_{k+1}|x_{k+1})$.

Kalman Filter

In the Kalman filter, it is assumed that the state and measurement models are linear. All the process noise and the initial state error are assumed to be Gaussian. With these assumptions it can be proved that $p(x_{k+1}|Z_{k+1})$ is Gaussian when $p(x_k|Z_k)$ is Gaussian. Hence, $p(x_k|Z_k)$ can be expressed by mean and covariance (28).

The Kalman filter algorithm is expressed by the following iterative relationship (28) when the state model and measurement models are given by (2.5) and (2.6), respectively.

$$p(x_k|Z_k) = \mathcal{N}(x_k; \hat{x}_{k|k}, P_{k|k}) \tag{2.11}$$

$$p(x_{k+1}|Z_k) = \mathcal{N}(x_{k+1}; \hat{x}_{k+1|k}, P_{k+1|k}) \tag{2.12}$$

$$p(x_{k+1}|Z_{k+1}) = \mathcal{N}(x_{k+1}; \hat{x}_{k+1|k+1}, P_{k+1|k+1}) \tag{2.13}$$

Also

$$\hat{x}_{k+1|k} = F_{k+1}\hat{x}_{k|k} \tag{2.14}$$

$$P_{k+1|k} = \Gamma_{k+1} + F_{k+1}P_{k|k}F_{k+1}^{'} \tag{2.15}$$

$$\hat{x}_{k+1|k+1} = \hat{x}_{k+1|k} + K_{k+1}(z_{k+1} - H_{k+1}\hat{x}_{k+1|k}) \tag{2.16}$$

$$P_{k+1|k+1} = P_{k+1|k} - K_{k+1}H_{k+1}P_{k+1|k} \tag{2.17}$$

and

$$S_{k+1} = H_{k+1} P_{k+1|k} H_{k+1}^{'} + \Sigma_{k+1} \tag{2.18}$$

$$K_{k+1} = P_{k+1|k} H_{k+1}^{'} S_{k+1}^{-1} \tag{2.19}$$

Here, $\mathcal{N}(x; \hat{x}, P)$ is a Gaussian density, $\hat{x}$ is the mean, argument x, and P is the covariance. Also the standard notation $[\cdot]'$ denotes the transpose.

With the above assumptions, this is the optimal solution to a tracking problem (28). That is, in a linear Gaussian environment, there is no algorithm that can do better than a Kalman filter. However, in more practical situations those assumptions are not preserved. Therefore, in typical scenarios, further approximations and additional assumptions are made.

Extended Kalman Filter (EKF)

The weakness of the Kalman Filter is that most systems in engineering are non-linear and it is not optimal for non-linear systems. The Kalman Filter was adapted for non-linear systems by approximating the model by a Taylor series expansions. An approximate linearization of the state and measurement models given by (2.7) and (2.8) respectively, may be a sufficient representation of the system. Approximate linearizations of the above state and measurement models are

$$\hat{F}_k = \frac{df_k(x)}{dx}\Big|_{x=\hat{x}_{k-1|k-1}} \tag{2.20}$$

$$\hat{H}_k = \frac{dh_k(x)}{dx}\Big|_{x=\hat{x}_{k|k-1}} \tag{2.21}$$

The probability density function $p(x_k|Z_k)$ is approximated by a Gaussian. Then all the equations of the Kalman filter can be used with this approximation and the linearized functions (28). This is the EKF, which is generally not an optimal solution unless state and measurement models are linear.

Also if the probability density function is non-Gaussian, then Gaussian representation will not be sufficient. Particle filters outperformed in performance comparison with EKF in such cases.

Particle Filtering

The probability density function $p(x_k|Z_k)$ of the target state x_k at time step k can be described by m number of particles which are sets of random samples $\{x_k^{(i)} : i = 1, 2, \ldots, m\}$ and corresponding weights of $\{w_k^{(i)} : i = 1, 2, \ldots, m\}$. As the new measurement or observations arrive, the update of these particles and the corresponding weights are performed by the Importance Sampling principle (32) (33) (34) (35) (36).

Let the Importance Density be the prior $p(x_k|x_{k-1})$. The Sampling Importance Resampling (SIR) procedure is used to generate equally weighted particles to approximate $p(x_k|Z_k)$.

$$p(x_k|Z_k) \approx \frac{1}{m}\sum_{i=1}^{m}\delta(x_k - {x_k}^{(i)}) \tag{2.22}$$

where $\delta(.)$ is the Dirac delta function.

Sampling Importance Resampling procedure

- **Prediction**
  - Each of the particles $x_{k-1}^{(i)}$ generates $\nu_{k-1}^{(i)}$ as per the known distribution of the transition noise.
  - The state propagation equation (2.7) can be used to obtain a sample $x_{k|k-1}^{(i)}$ from the prior distribution $p(x_k|x_{k-1})$.
- **Weighting**
  - Observation information can be used to find the importance weights.
  - The following formula is used to find importance weight $w_k^{(i)}$ for each particle.

$$w_k^{(i)} = p(z_k|x_{k|k-1}^{(i)}) \tag{2.23}$$

- **Resampling**
  - The particles with low weights are eliminated and the particles with high weights are multiplied and are regenerated with equal weights.
  - The m number of new particles are sampled with substitution from $\{x_{k|k-1}^{(1)}, x_{k|k-1}^{(2)}, \ldots, x_{k|k-1}^{(m)}\}$ so that
  - The sampling particle i's probability is proportional to w_k^i
  - Hence, the new $\{x_k^{(1)}, x_k^{(2)}, \ldots, x_k^{(m)}\}$ will be in equal weights $(1/m)$.

The posterior distribution's mean is used to find an estimate $\hat{x}_k$.

$$\hat{x}_k = \mathbb{E}[x_k|Z_k] \tag{2.24}$$

$$\approx \frac{1}{m}\sum_{i=1}^{m} {x_k}^{(i)} \tag{2.25}$$

Unlike the Kalman filter, Particle Filtering it is not restricted by the assumptions of linearity and Gaussian noise.

2.2 Multitarget Tracking and Data Association

The plot of the data that has been associated with the same target is an estimated state trajectory and is known as target track. In multitarget tracking, the sensor has measurements from different targets. Also there will be missed detections of targets. The measurements also have random false alarms, clutter, decoys, countermeasures, interfering targets and more.

The process that identifies which measurement belongs to which target is called data association (16) (27) (37) (38) (39). Solutions to different data association problems can be found in the literature (20) (40) (41) (42) (43) (44).

Figure 2.2 shows the fundamental elements of a typical multitarget tracking system. The sensor measurements are obtained from the signal processing unit, which converts the electro magnetic signals to measurement values. These measurements are the input for the system of multitarget tracking. The state trajectories are the

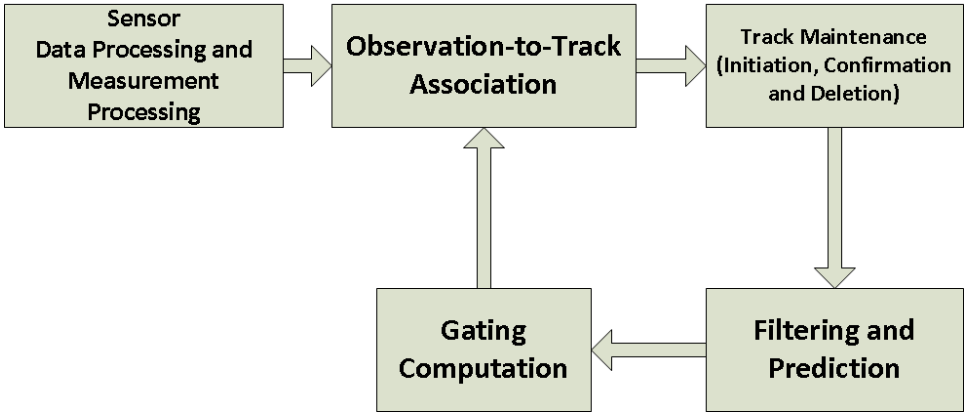

Figure 2.2: A system of multitarget tracking and data association.

representation of moving targets. The continuous measurement input is used for maintaining the track. Tracks are initialized and maintained by confirming, and inappropriate tracks are deleted (16) (27).

Unassigned measurements to any established tracks can initiate new tracks. When these newly initiated tracks meet the confirmation condition, they are confirmed. The tracks that are not updated within an interval become degraded and then deleted.

A validation region is defined for existing track and any measurements away from this validation region is ignored as inappropriate measurements for the existing track. A validation gate is set up around the predicted measurement. When the validation region has more than one measurement, a data association technique is used to find the assignment. Different data association techniques will implement different methods to update validated measurements to the track. However all data association techniques use gates to reduce the expensive computational cost. Then the track is updated with the newly associated measurement. The tracks will be predicted for the next set of measurements and gates are used on these predicted positions and the track maintenance cycle is iterated.

When the actual measurement conditioned on the past is Gaussian or normally distributed, and if its pdf is given by

$$p(z_{k+1}|Z_k) = \mathcal{N}[z_{k+1}; \hat{z}_{k+1|k}, S_{k+1}] \tag{2.26}$$

the actual measurement will be under the following region

$$\mathcal{V}(k+1,\gamma) = \{z : [z - \hat{z}_{k+1|k}]' S_{k+1}^{-1} [z - \hat{z}_{k+1|k}] \leq \gamma\} \tag{2.27}$$

and the gate threshold γ calculates the probability. Here, the predicted measurement at time $k+1$ is $\hat{z}_{k+1|k}$. The measurement prediction covariance S_{k+1} is given by (2.18). The region (2.27) is known as the validation, association region or the gate. In a given time interval, a range gate is found and the detections or the measurements within the gate is associated with the target.

Typically measurements will have higher dimension because in a time scan, there will different measurements such as range, azimuth or bearing, elevation, range rate and time difference of arrival. In such cases a multidimensional gate is found so that the entire measurements space is not searched to track the target of interest. In a typical tracking problem, the validation regions contain sets of validated measurements. A measurement in the gate is a valid association candidate. A gate has correct measurement if target is detected and the measurement fell in the validation gate. The gate may also have unwanted measurements from clutter or false-alarms.

Well-separated targets

Figure 2.3 shows validation regions of well-separated targets. Assume that at most one measurement is target generated in the validation region in Figure 2.3. When

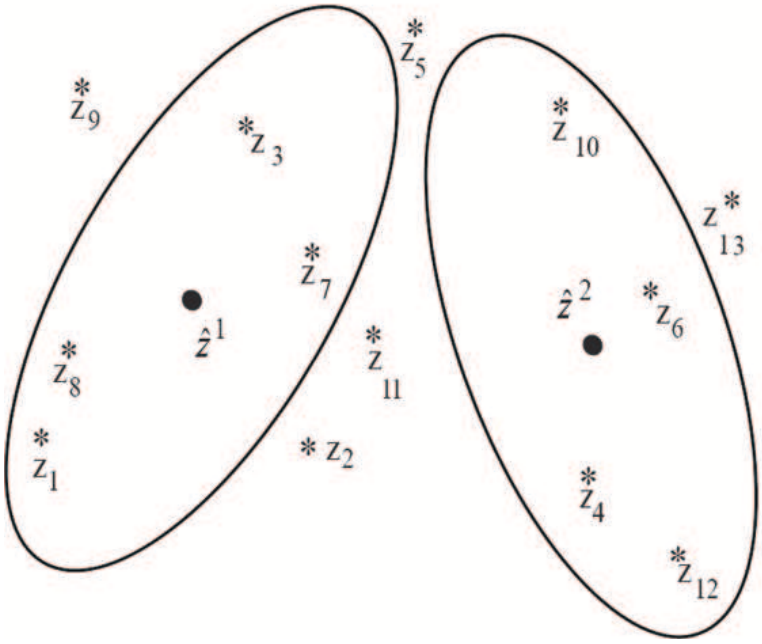

Figure 2.3: Well-separated targets' association gate. • expected measurement, ∗ received measurement.

there is more than one association candidate in the validation gate, the problem arises in finding which measurement was target originated. In the detection or measurement space, if the targets are well separated, the validation regions will not overlap as shown in Figure 2.3. In this case the problem is that of a single target tracking.

The problem of tracking well-separated multiple targets in clutter considers the situation where there are possibly several measurements in the validation region of each target.

Assume that the targets are detected and measurements have fallen in the validation region, then the validated measurements consist of actual measurements from the targets as well as false alarms in the case of tracking well separated multitarget in clutter. It is assumed that the spatial distribution of false alarms is uniform within the surveillance region and are independent across time. Then there are different

approaches for associating these validated measurements to the appropriate target tracks (16).

The Nearest Neighbor (NN) technique chooses the measurement nearest to the predicted measurement, whereas the Strongest Neighbor (SN) chooses the strongest measurement in the validation region. Probabilistic Data Association (PDA) associates all the measurements that are in the validation region to the targets probabilistically to the target of interest (20). PDA is a Bayesian approach (45) (46) and the standard method used for data association that is used with Kalman filter or the extended Kalman filter. The NN algorithm requires comparatively less computation and therefore widely used with the particle filtering algorithms.

Closely-spaced targets

Validation regions of two closely spaced targets and the measurements inside those validation region are shown in Figure 2.4. In the detection or measurement space, if the targets are closely spaced, the validation regions will overlap as shown in Figure 2.4. In this case the measurement contains detections from other targets in addition to the clutter and false alarms. In this case, the data association process resolves the measurement origin uncertainty.

The problem of tracking closely spaced multiple targets in clutter considers the situation where there are possibly several measurements in the validation region of each target, and a measurement could originate from any one of the target or clutter. It is assumed that one measurement originates from at most one target and one target can generate at most one measurement. It is also assumed that the spatial distribution of false alarms is uniform within the surveillance region and is independent across

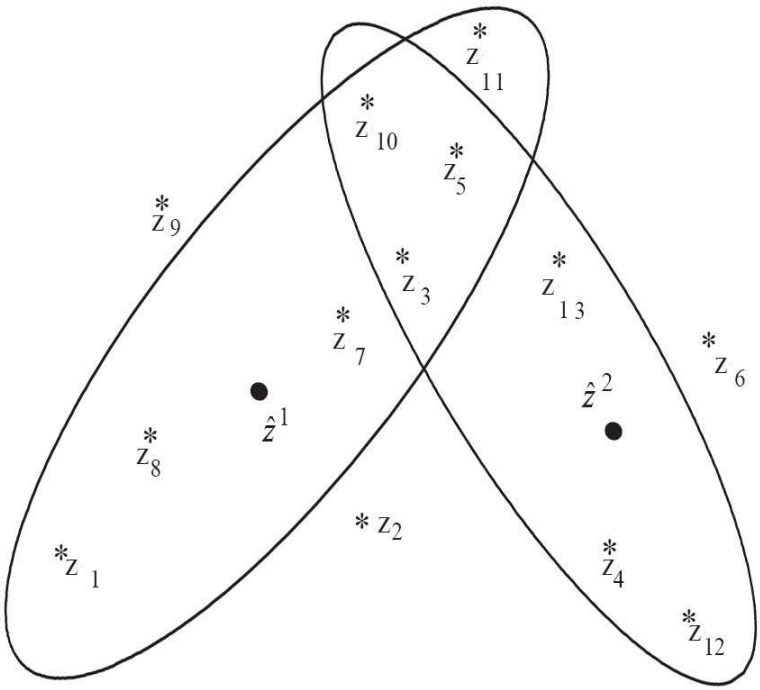

Figure 2.4: Two closely spaced targets and the measurements in association gate. • expected measurement, ∗ received measurement.

time.

Joint Probabilistic Data Association (JPDA) is a target oriented technique (37) (41). This is an extended form of the PDA technique. JPDA can only be used for the tracks that are already established. JPDA and its implementations have been widely studied in the literature (47) (48) (49) (50) (51).

Multiple Hypothesis Tracking (MHT) is another data association technique for closely spaced multiple targets in clutter. Probability of a measurement sequence is originated from an established target or a new target is calculated for MHT technique and it is a measurement oriented technique. Track initiation and maintenance may be performed by MHT. MHT is not practically feasible when considering the large measurement steps. Therefore, an S-D (S- Dimensional) assignment technique is used. This S-D assignment algorithm is a suboptimal version of MHT and the mostly used data association technique.

2.3 Monostatic, Bistatic and Multistatic Radar

Tracking problems have been widely studied, and currently the radar developments and implementations become a matured discipline (52). Target tracking is widely used in many applications such as ballistic missile defense, military surveillance, air traffic control of military and civilian aviation (46) (53), and highway vehicle surveillance (54) (55). Radar (RAdio Detection And Ranging) transmits electromagnetic pulses, which bounce off any objects or target in their path. The reflected signal's energy is scattered in all directions from the target or object. A sensor receives such target return signals and processes them to find the measurements such as range, azimuth and Doppler.

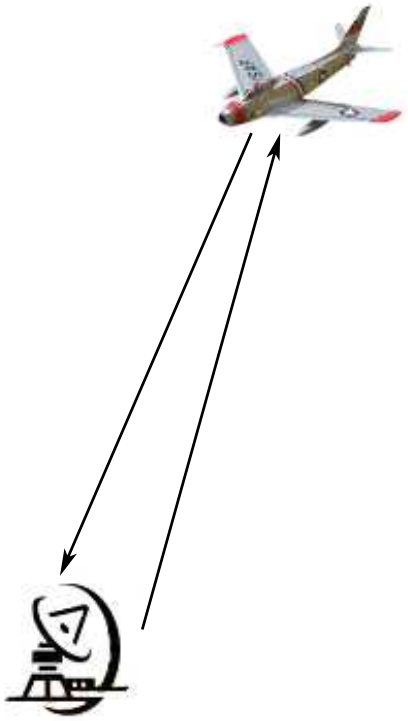

Figure 2.5: Monostatic radar.

The transmitter and the sensor are collocated in a typical radar system, which is also known as monostatic radar as shown in Figure 2.5. When these transmitter and sensor are physically separated, then such radar system is known as bistatic radar as shown in Figure 2.6. Additional advanced references about bistatic radars can be found at (71) (72) (73) (74). When the physically apart sensor receives the target reflected signals, which were originally sent by more than one transmitters this configuration is known as multistatic radar system as shown in Figure 2.7 (75).

In a bistatic radar configuration, instead of using the radar transmitter, if a system uses transmitters of opportunity in the environment such as commercial broadcast signals (FM or TV signals), then it is known as passive coherent location (PCL)

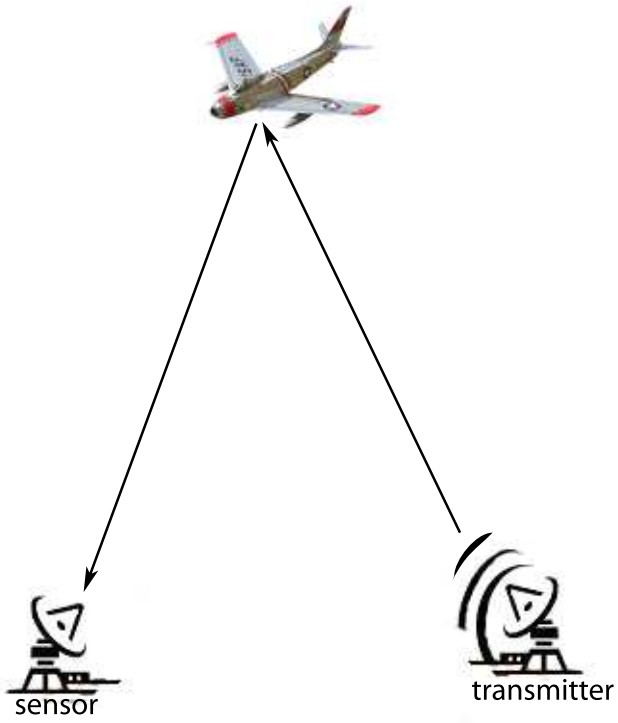

Figure 2.6: Bistatic radar.

system. Therefore, the primary difference between bistatic and monostatic radar is that of geometry. A bistatic radar consisting of a PCL receiver and a transmitter of opportunity separated by a distance L is shown in Figure 3.2.

2.4 Evolution of PCL Radar

In the evolution of bistatic radars, different methods of transmissions were exploited. This exploration leads to the research of exploiting the transmitters of opportunity in the environment, and that leads to the research of PCL radars and tracking. PCL radar configuration is a bistatic or multistatic radar configuration. Environmentally

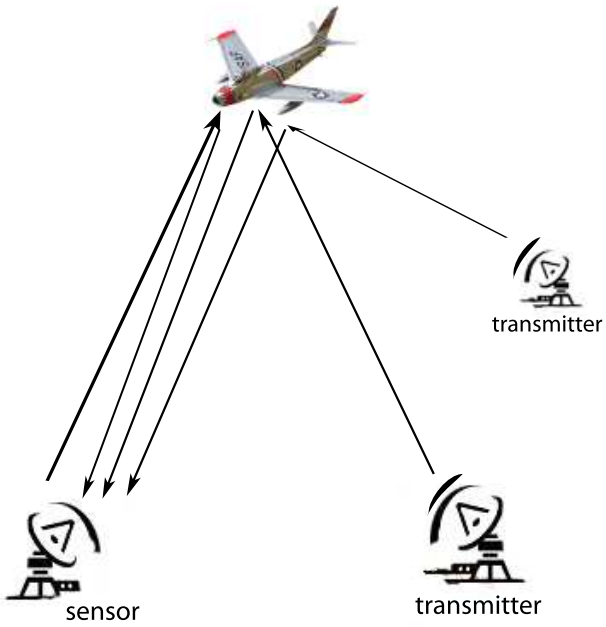

Figure 2.7: Multistatic radar.

available source of illuminations are used as transmitters to develop PCL radar. High definition television transmission signals, cellular phone base station signals, FM radio signals, analog television signals, digital audio broadcasting signals and digital video broadcasting signals are some of the examples.

The satellite signals have the advantage of expanded coverage, however, the received power levels at the ground receivers are very less. The satellite transmissions may not be frequent enough to track fast moving targets. However, tracking targets with satellite radio systems was exploited.

A PCL radar system detects the target reflected signals from the transmitter of

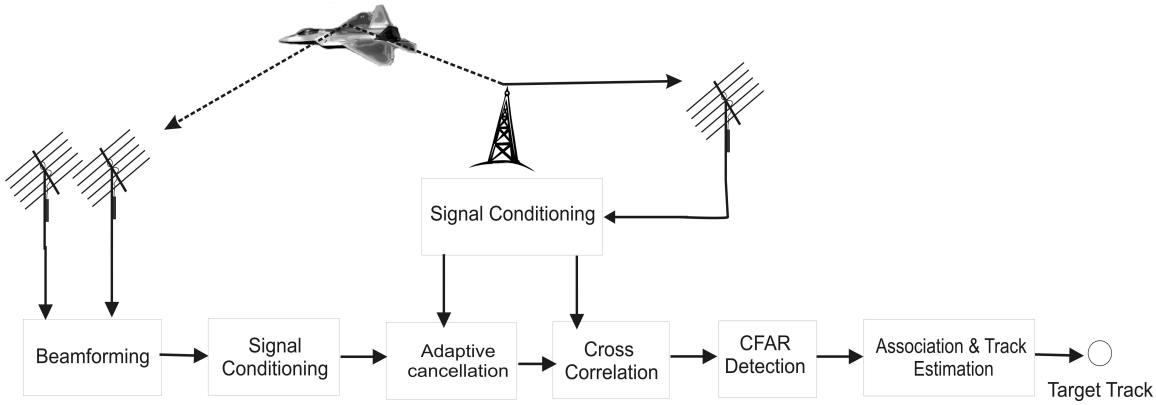

Figure 2.8: Signal processing scheme of PCL radar.

opportunity by low noise receivers. Due to the direct signal interference from the transmitters and the other signals from the in band transmitters, PCL systems are highly limited by noise.

Digitized and sampled signals are given as output from PCL receiver systems. A typical PCL radar signal processing schedule is given in Figure 2.8. Generally the PCL receivers have higher number of antenna elements. Standard beamforming technique is generally used to calculate the DOA measurements. Pair of antenna elements and phase difference of arrival of the echoes can be used to generate the DOA measurements.

Based on what types of transmitters or signals are used for the PCL tracking, some transmitter specific conditioning are done before the cross-correlation processing. Generally the signal conditioning is performed using some channel equalizers and band-pass filters. In some cases, unwanted signal patterns are removed from the transmitter signals or complete restructuring of the transmitter signals are performed.

Due to the higher interference by the direct signals received from the transmitters, the signal to interference ratio becomes the limiting factor of PCL systems.

Adaptive filters are used to remove the direct signals received from the transmitters. Then the signals are sent to the cross-correlation processing. An appropriate adaptive threshold is given and target detection is performed. Generally, a cell averaged constant false alarm rate algorithm is used for the detection process. Then this information is sent to the tracker for processing the target track.

PCL systems' transmitters are generally non-cooperative, i.e., the PCL receiver does not have control over the transmitters. The nature of the environmentally available signals differ based on operating frequency range, type of transmission such as voice or video, duration of the transmission such as day time, night time, or 24x7 broadcast. Therefore, it is more appropriate to call these transmitters as the transmitters of opportunity. A commercially available multistatic PCL radar system developed by Lockheed Martin is Silent Sentry® (76). This system uses FM radio broadcast transmitters.

Advantages of PCL Systems

- The transmitters are already out there in the environment. Therefore, there is no need to build expensive transmitters or towers. The signals are ready to be used in the environment.
- The passive receivers cannot be located by any methods by the enemies.

- Since PCL systems use the environmentally available transmitters of opportunity, they enable covert tracking.
- Due to the passive nature, jamming the PCL radar operating frequency is difficult.
- Able to cover the vast amount of territory without massively deploying the transmitters. Therefore, cost per surveillance region is very low.
- Fast deployment with a very low cost.
- PCL radar can be even operated using enemy's transmitters silently. Therefore, snooping form the enemy's territory is possible with PCL.

Disadvantages of PCL Systems

- Signals are not designed for the radar but for a different purposes. Therefore, the signals may not be very suitable for radar processing.
- The receiver design is more complex as it needs to abide for the available transmitted waveforms characteristics.
- Lack of control over the transmitters and therefore no control over the waveform design, frequency band, transmit power and antenna orientation.
- Low signal to noise ratio at PCL receivers affects the accuracy of tracking.

- No control over the other inband signal frequencies and therefore the interference will be high. It is difficult to remove such frequencies completely and therefore the signal to interference ratio will be low.
- Challenges in tracking long range targets due to low signal to noise ratio.

Chapter 3

Multitarget Passive Coherent Location Tracking using Transmitters of Opportunity and Bias Removal in Direction of Arrival

PCL systems, which use existing commercial signals (e.g., FM broadcast, digital TV) as the illuminators of opportunity, is an emerging technology in air defence systems. PCL systems have many advantages such as low cost, covert operation and low vulnerability to electronic counter measures over conventional radar systems. However, the limitations of PCL include lack of control over illuminators, limited observability and poor detection due to low Signal-to-Noise Ratio (SNR). This leads

to high clutter with low probability of detection of target. In this chapter, multiple target tracking algorithms for PCL systems are derived to handle low probability of detection and high nonlinearity in the measurement model due to high measurement error. The major contributions of this chapter are the new algorithms for tracking using PCL systems in high clutter with low probability of detection and false alarm environment. The feasibility of using transmitters of opportunity for tracking airborne targets in such environment is shown on simulated and real data sets.

A sample multistatic PCL configuration is shown in Figure 3.1. The environment has multiple transmitters-of-opportunity in the area of interest, where all the transmitters transmit the same signal at the same frequency. This may happen because of multiple radio station transmitters operating at the same frequency within the surveillance region.

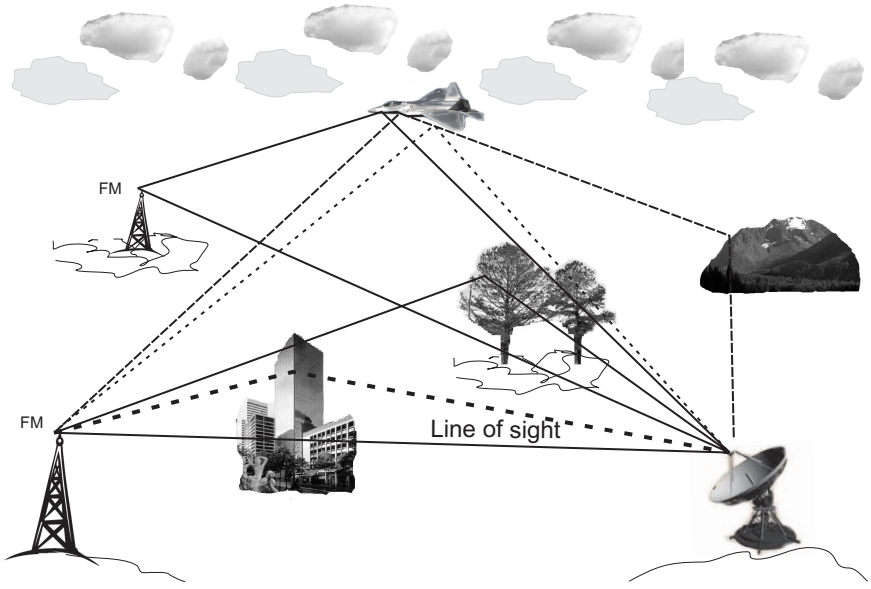

Figure 3.1: Multistatic PCL system.

Note that the bistatic range measurements can be calculated from the time-difference-of-arrival.

While there have been continuous improvements in radar technology, the development of anti-radiation missiles (ARM) has added new challenges to trackers that rely on radar returns. In bistatic radar systems, the transmitter and receiver pairs are widely separated, while they are co-located in monostatic radars (77) (83) (84). Since the receiver locations are passive and cannot be identified by the target, bistatic radars are generally less susceptible to ARM. PCL is a specific case of bistatic or multistatic radar surveillance systems.

In general, a simple PCL system consists of one illuminator of opportunity (the transmitter) and a PCL receiver. This bistatic configuration of PCL is illustrated in Figure 1.1. The direct signals and the echoes from the target that originate from the commercial transmitters like TV and radio stations are received by the PCL receiver. In most cases, the locations of the commercial transmitters are known accurately. In this chapter, it is assumed that the exact transmitter locations are known. Hence, signal origination time can be calculated from the direct signal and distance between the receiver and the transmitter. Then, signal origination time can be used to calculate the bistatic measurement from the received signals.

In the literature, different aspects of PCL systems are analyzed. In (5), a signal processing scheme that allows airborne targets to be detected and tracked using only the vision or sound carrier of the television broadcast was presented. It used the Doppler shift and the bearing of target echoes to estimate the target's track. The Doppler-bearing information from the television video signals was used to track the aircraft ranges up to 260 km. In (56), an overall discussion on PCL systems with

simulated data sets was given. In (2), it was shown that an FM radio based bistatic radar system can detect and track targets at ranges in excess of 150 km.

3.1 Measurement Model in PCL

The primary difference between bistatic and monostatic radar is that of geometry. A bistatic radar consisting of a PCL receiver and a transmitter of opportunity separated by a distance L is shown in Figure 3.2.

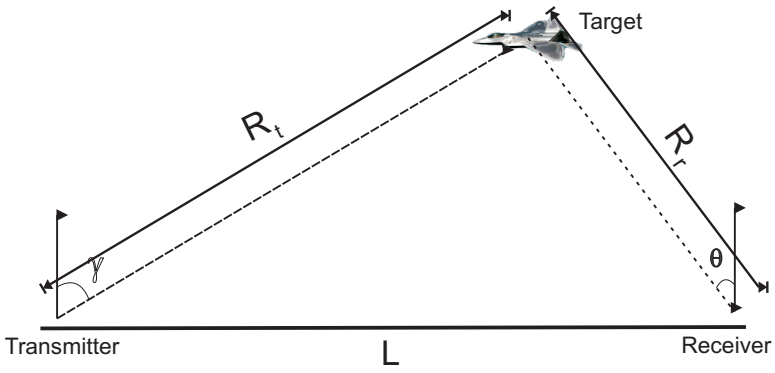

Figure 3.2: Bistatic radar geometry.

In this chapter, it is assumed that the PCL system's measurements are bistatic range r_b, bistatic rage rate $\dot{r}_b$ and bearing θ (from north). The Measurement equations are given by

$$\begin{pmatrix} r_b \\ \dot{r}_b \\ \theta \end{pmatrix} = \begin{pmatrix} R_r + R_t - L \\ \left(\dot{R}_r + \dot{R}_t\right) \\ \text{atan}\left(\frac{x-x_r}{y-y_r}\right) \end{pmatrix} + \omega \tag{3.1}$$

where

$$L = \sqrt{(x_t - x_r)^2 + (y_t - y_r)^2} \tag{3.2}$$

$$R_r = \sqrt{(x - x_r)^2 + (y - y_r)^2} \tag{3.3}$$

$$R_t = \sqrt{(x - x_t)^2 + (y - y_t)^2} \tag{3.4}$$

$$\dot{R}_r = \frac{(x - x_r)}{R_r}\dot{x} + \frac{(y - y_r)}{R_r}\dot{y} \tag{3.5}$$

$$\dot{R}_t = \frac{(x - x_t)}{R_t}\dot{x} + \frac{(y - y_t)}{R_t}\dot{y} \tag{3.6}$$

x and y are the Cartesian coordinates of the target, and $\dot{x}$ and $\dot{y}$ are velocities of the targets in the X and Y coordinate directions, respectively. Similarly, (x_t, y_t) and (x_r, y_r) are the positions of transmitter and receiver, respectively. Also, atan($\cdot$) is the four-quadrant arctangent, and ω is the measurement noise, which is zero-mean Gaussian random variable with covariance $\Sigma = \text{diag}[\sigma_{\text{r}}^2, \sigma_{\dot{\text{r}}}^2, \sigma_{\theta}^2]$. False alarms are assumed to be uniformly distributed throughout the surveillance region.

3.2 Tracking Algorithms for Bistatic PCL Systems

The Kalman filter is the optimal filter when the target state and measurement models are linear and the noise are Gaussian. When nonlinearities are present, converted measurement Kalman filter, Extended Kalman Filter (EKF), unscented Kalman filter, particle filter or the Probability Hypothesis Density filter can be used (34) (57) (58) (59). In this chapter, CMKF, UKF and particle filter based PHD filters are analyzed for multitarget tracking using PCL systems. An Interacting Multiple Model (IMM) estimator with two constant velocity models with different

process noises is used to handle the target maneuvers (16) (60) (61).

A PCL system's measurements have measurement origin uncertainty due to false alarms and missed detections. In addition to filtering, multitarget tracking with low probability of target detection and high false alarm rate requires data association and track maintenance logic in order to initialize and maintain the tracks.

3.2.1 Track Maintenance

The tracks are classified into two categories: 1) Tentative tracks and 2) Confirmed tracks. Tentative tracks are the ones formed with fewer initial measurement associations than required for confirmation tracks within a certain time limit. Upon receiving more measurements, the tentative tracks are promoted to confirmed tracks. If an inadequate number of measurements are associated with a tentative track, then the tentative tracks are deleted. Logic based track maintenance is used as follows (16):

- For track initialization: out of the last N_{init} measurement frames
  - if at least M_{init} measurements are associated together, then form a track and mark it tentative
  - otherwise, do nothing
- For a tentative track: out of the last N_{tent} measurement frames
  - if at least M_{tent} measurements are associated to the track, then promote it as confirmed
  - otherwise, delete the track
- For a confirmed track: out of the last N_{conf} measurement frames

– if at least M_{conf} measurements are associated to the track, then do nothing

– otherwise, delete it

In order to get better association results, the measurements are first associated to the confirmed tracks. Then, the unassociated measurements are used to update the tentative tracks. Finally, the measurements that are not associated to the confirmed or tentative tracks are used to initialize new tracks. It is possible to use track quality for track confirmation and termination logic (62). We have found that M-out-of-N logic performs well for real data.

Track Initialization

Bistatic range and bearing measurements are used to initialize the target positions, and the related equations are given in Section 3.2.3. The range rate measurements are used to initialize the target velocity, is given by (63):

$$\dot{x} = \frac{\sigma_p^2}{(A^2+B^2)\sigma_p^2+\sigma_{\dot{r}}^2} A\ \dot{r}_r \tag{3.7}$$

$$\dot{y} = \frac{\sigma_p^2}{(A^2+B^2)\sigma_p^2+\sigma_{\dot{r}}^2} B\ \dot{r}_r \tag{3.8}$$

The corresponding covariance is

$$P = \sigma_p^2 \begin{pmatrix} \left(1-\frac{\sigma_p^2 A^2}{(A^2+B^2)\sigma_p^2+\sigma_{\dot{r}}^2}\right) & -\frac{\sigma_p^2 AB}{(A^2+B^2)\sigma_p^2+\sigma_{\dot{r}}^2} \\ -\frac{\sigma_p^2 AB}{(A^2+B^2)\sigma_p^2+\sigma_{\dot{r}}^2} & \left(1-\frac{\sigma_p^2 B^2}{(A^2+B^2)\sigma_p^2+\sigma_{\dot{r}}^2}\right) \end{pmatrix} \tag{3.9}$$

where σ_p^2 is the variance of prior information about the target speed, $A = \sin(\theta) + \sin(\gamma)$ and $B = \cos(\theta) + \cos(\gamma)$, with $\gamma = \text{atan}\left(\frac{x-x_t}{y-y_t}\right)$.

3.2.2 Data Association

Data association makes decisions as to which of the received measurements should be used to update each track. To associate the measurements to already established targets, two dimensional data association based on the auction algorithm is used for CMKF and UKF (58). Note that simpler association techniques such as the nearest neighbor association will be sufficient in most cases for the particle filter, and no data association is necessary for the PHD filter.

2-D Assignment

The fundamental idea behind 2-D assignment is that the measurements from the scan list $\mathcal{M}(k)$ are matched with the tracks in list $\mathcal{T}(k-1)$ by formulating the matching as a constrained global optimization problem. The optimization is carried out to minimize the "cost" of associating (or not associating) the measurements to tracks.

To present the 2-D assignment, define a binary assignment variable $a(k,m,n)$ such that

$$a(k,m,n) = \begin{cases} 1 & m\text{-th measurement is assigned to track } \mathcal{T}^n(k-1) \\ 0 & \text{otherwise} \end{cases} \tag{3.10}$$

The indices $m = 0$ and $n = 0$ correspond to the non-existent (or "dummy") measurement and track.

The objective of the assignment is to find the optimal assignment $\mathbf{a}^*(k)$, which minimizes the global cost of association

$$C\left(k|\mathbf{a}(k)\right) = \sum_{m=0}^{M(k)} \sum_{n=0}^{N(k-1)} a(k,m,n)\; c(k,m,n) \tag{3.11}$$

subject to

$$\sum_{m=0}^{M(k)} a(k,m,n) = 1, \quad n = 1, 2, \ldots, N(k-1) \tag{3.12}$$

$$\sum_{n=0}^{N(k-1)} a(k,m,n) = 1, \quad m = 1, 2, \ldots, M(k) \tag{3.13}$$

where $c(k,m,n)$ is the cost of the assignment $a(k,m,n)$, $M(k)$ and $N(k-1)$ are the cardinalities of the measurement and track sets, respectively.

The costs $c(k,m,n)$ are the negative of the logarithm of the dimensionless likelihood ratio of the measurement-to-track associations, namely,

$$c(k,m,n) = -\ln \Lambda(k,m,n) \tag{3.14}$$

where

$$\Lambda(k,m,n) = \begin{cases} P_d p\left[\nu_m^n(k)\right]/\lambda & m > 0, \quad n > 0 \\ 1 & m > 0, \quad n = 0 \\ (1 - P_d) & m = 0, \quad n > 0 \end{cases} \tag{3.15}$$

where $p\left[\nu_m^n(k)\right]$ is the probability density function of the corresponding innovation and λ is the spatial density of the false alarm.

The above 2-D assignment optimization problem is solved using the auction algorithm (78).

3.2.3 Converted Measurement Kalman Filter

In this section, the converted measurement Kalman filter is described for a PCL system with bistatic range, bearing and bistatic range rate measurements.
The range sum r can be calculated from bistatic range as:

$$r = r_b + L \tag{3.16}$$

The range of the target from the receiver, R_r, can be calculated as:

$$R_r = \frac{r^2 - L^2}{2\left(r - L\cos(\beta)\right)} \tag{3.17}$$

where

$$\beta = \text{atan}\left(\frac{x_t - x_r}{y_t - y_r}\right) - \theta \tag{3.18}$$

From R_r and θ, the measurements can be converted into Cartesian coordinates as follows:

$$x = x_r + R_r \sin(\theta) \tag{3.19}$$

$$y = y_r + R_r \cos(\theta) \tag{3.20}$$

The corresponding covariance is (82)

$$\sigma_x^2 = \left(H_1^2\sigma_r^2 + H_2^2\sigma_\theta^2\right)/H_3^4 \tag{3.21}$$

$$\sigma_y^2 = \left(H_4^2\sigma_r^2 + H_5^2\sigma_\theta^2\right)/H_3^4 \tag{3.22}$$

$$\sigma_{xy}^2 = \left(H_1H_4\sigma_r^2 + H_2H_5\sigma_\theta^2\right)/H_3^4 \tag{3.23}$$

where

$$H_1 = \sin(\theta)(r^2 + L^2 - 2rL\cos(\beta)) \tag{3.24}$$

$$H_2 = (r^2 - L^2)\left(r\cos(\theta) - L(\cos(\theta)\cos(\beta) - \sin(\theta)\sin(\beta))\right) \tag{3.25}$$

$$= (r^2 - L^2)\left(r\cos(\theta) - L\cos(\theta + \beta)\right) \tag{3.26}$$

$$H_3 = \sqrt{2}(r - L\cos(\beta)) \tag{3.27}$$

$$H_4 = \cos(\theta)(r^2 + L^2 - 2rL\cos(\beta)) \tag{3.28}$$

$$H_5 = (r^2 - L^2)\left(-r\sin(\theta) + L(\sin(\theta)\cos(\beta) + \cos(\theta)\sin(\beta))\right) \tag{3.29}$$

$$= (r^2 - L^2)\left(-r\sin(\theta) + L\sin(\theta + \beta)\right) \tag{3.30}$$

In the presence of large bearing measurement errors and long sensor-to-target distances, the above measurement conversion introduces a bias and a debiasing technique is required. The unbiased conversion can be obtained by (63) (64):

$$x = x_r + e^{\sigma_\theta^2/2}R_r\sin(\theta) \tag{3.31}$$

$$y = y_r + e^{\sigma_\theta^2/2}R_r\cos(\theta) \tag{3.32}$$

Then, the converted measurement equation is given by

$$\underbrace{\begin{pmatrix} x \\ y \\ \dot{r}_b \end{pmatrix}}_{z} = \underbrace{\begin{pmatrix} 1 & 0 & 0 & 0 \\ 0 & 0 & 1 & 0 \\ 0 & A & 0 & B \end{pmatrix}}_{H} \begin{pmatrix} x \\ \dot{x} \\ y \\ \dot{y} \end{pmatrix} + w_c \tag{3.33}$$

where w_c is the converted measurement noise, which is zero-mean Gaussian random variable with covariance Σ_c. The variance of error in $\dot{r}_b$ due to the uncertainties in θ and γ can be approximated as

$$\tilde{\sigma}_{\dot{r}}^2 = \left(\frac{\partial \dot{r}_b}{\partial \theta}\sigma_\theta\right)^2 + \left(\frac{\partial \dot{r}_b}{\partial \gamma}\sigma_\gamma\right)^2 \tag{3.34}$$

$$= \sigma_\theta^2(\dot{x}\cos(\theta) - \dot{y}\sin(\theta))^2 + \sigma_\gamma^2(\dot{x}\cos(\gamma) - \dot{y}\sin(\gamma))^2 \tag{3.35}$$

where

$$\sigma_\gamma^2 = \sigma_{xx}^2\frac{\cos(\gamma)^2}{r^2} + \sigma_{yy}^2\frac{\sin(\gamma)^2}{r^2} - 2\frac{\sigma_{xy}\cos(\gamma)\sin(\gamma)}{\sqrt{r^2}} \tag{3.36}$$

Then, the covariance of the converted measurement noise is given by

$$\Sigma_c = \begin{bmatrix} \sigma_x^2 & \sigma_{xy}^2 & 0 \\ \sigma_{xy}^2 & \sigma_y^2 & 1 \\ 0 & 0 & \sigma_{\dot{r}}^2 + \tilde{\sigma}_{\dot{r}}^2 \end{bmatrix} \tag{3.37}$$

3.2.4 Kalman Filter

The constant velocity model is used for state dynamics:

$$\mathbf{x}(k+1) = F(k)\mathbf{x}(k) + v(k) \tag{3.38}$$

where $\mathbf{x}(k) = [x(k)\ \dot{x}(k)\ y(k)\ \dot{y}(k)]'$ is the target state, $F(k)$ is the state transition matrix and $v(k)$ is the process noise, which is zero-mean Gaussian random variable with covariance $Q(k)$. The measurement equation is given by (3.33). Note that the algorithm is not restricted to the constant velocity model. A multiple model estimation can be used instead to handle maneuvering targets (28).

The Kalman filter recursions for state estimate $\hat{x}(k|k)$ and covariance $P(k|k)$ are given by

$$\hat{\mathbf{x}}(k+1|k) = F(k)\hat{\mathbf{x}}(k|k) \tag{3.39}$$

$$P(k+1|k) = Q(k) + F(k)P(k|k)F(k)' \tag{3.40}$$

$$\hat{\mathbf{x}}(k+1|k+1) = \hat{\mathbf{x}}(k+1|k) + W(k+1)(z(k+1) - \hat{z}(k+1|k)) \tag{3.41}$$

$$P(k+1|k+1) = P(k+1|k) - W(k+1)S(k+1)W(k+1)' \tag{3.42}$$

with

$$\hat{z}(k+1|k) = H(k+1)\hat{\mathbf{x}}(k+1|k) \tag{3.43}$$

$$S(k+1) = H(k+1)P(k+1|k)H(k+1)' + \Sigma_c(k+1) \tag{3.44}$$

$$W(k+1) = P(k+1|k)H(k+1)'S(k+1)^{-1} \tag{3.45}$$

3.2.5 Unscented Kalman Filter

When the state transition and/or observation models are highly nonlinear, the EKF may perform poorly. The unscented Kalman filter does not approximate the nonlinear functions of state and measurement models as required by the EKF. Instead, the UKF uses a deterministic sampling technique known as the unscented transform to pick a minimal set of sample points called sigma points around the mean. Here, the propagated mean and covariance are calculated from the transformed samples (65). The steps of the UKF are described below.

Sigma Point Generation

The state vector $\hat{\mathbf{x}}(k)$ with mean $\hat{\mathbf{x}}(k|k)$ and covariance $P(k|k)$ is approximated by $2n+1$ weighted sigma points, where n is the dimension of the state vector, as

$$\chi^0(k|k) = \hat{\mathbf{x}}(k|k), \qquad w_0 = \frac{\kappa}{(n+\kappa)} \tag{3.46}$$

$$\chi^i(k|k) = \hat{\mathbf{x}}(k|k) + \left(\sqrt{(n+\kappa)P(k|k)}\right)_i, w_i = \frac{1}{2(n+\kappa)} \tag{3.47}$$

$$\chi^{i+n}(k|k) = \hat{\mathbf{x}}(k|k) - \left(\sqrt{(n+\kappa)P(k|k)}\right)_i, w_{i+n} = \frac{1}{2(n+\kappa)} \tag{3.48}$$

where w_i is the weight associated with the i-th point, κ is a scaling parameter, $i = 1, 2, ...n$, and $\left(\sqrt{(n+\kappa)P(k|k)}\right)_i$ is the i-th row or column of the matrix square root of $(n+\kappa)P(k|k)$.

Recursion

The predicted target state $\hat{\mathbf{x}}(k+1|k)$ and corresponding covariance $P(k+1|k)$ are found as follows:

(a) The Sigma points are transformed using the process model

$$\chi^i(k+1|k) = f(k, \chi^i(k|k)) \tag{3.49}$$

(b) The mean of the predicted state is given by

$$\hat{\mathbf{x}}(k+1|k) = \sum_{i=0}^{2n} w_i \chi^i(k+1|k) \tag{3.50}$$

(c) The covariance of the predicted state is given by

$$P(k+1|k) = Q(k) + \sum_{i=0}^{2n} w_i[\chi_i(k+1|k) - \hat{\mathbf{x}}(k+1|k)][\chi_i(k+1|k) - \hat{\mathbf{x}}(k+1|k)]' \tag{3.51}$$

The predicted measurement $\hat{z}(k+1|k)$ and the corresponding covariance $S(k+1)$ are found as follows:

(a) Sigma points $\chi_i(k+1|k)$ are regenerated using the mean $\hat{\mathbf{x}}(k+1|k)$ and covariance $P(k+1|k)$ in order to incorporate the effect of $Q(k)$. If $Q(k)$ is zero, the resulting $\chi_i(k+1|k)$ will be the same as in (3.49). If the process noise is correlated with the state, then the noise vector must be stacked with the state vector $\hat{\mathbf{x}}(k|k)$ before generating the sigma points (65).

(b) The mean of predicted measurement $\hat{z}(k+1|k)$ is calculated as

$$\hat{z}(k+1|k) = \sum_{i=0}^{2n} w_i \varphi^i(k+1|k) \tag{3.52}$$

where

$$\varphi^i(k+1|k) = h(k, \chi^i(k+1|k)) \tag{3.53}$$

(c) The innovation covariance $S(k+1)$ and gain $W(k+1)$ are calculated as

$$S(k+1) = \Sigma(k+1) + \sum_{i=0}^{2n} w_i[\varphi^i(k+1|k) - \hat{z}(k+1|k)][\varphi^i(k+1|k) - \hat{z}(k+1|k)]' \tag{3.54}$$

$$W(k+1) = \sum_{i=0}^{2n} w_i[\chi^i(k+1|k) - \hat{\mathbf{x}}(k+1|k)][\varphi^i(k+1|k) - \hat{z}(k+1|k)]' S(k+1)^{-1} \tag{3.55}$$

The state $\hat{\mathbf{x}}(k+1|k+1)$ and the corresponding covariance $P(k+1|k+1)$ are updated using (3.41) and (3.42), respectively.

3.2.6 PHD Filter

The PHD is the factorial moment density found in point process theory (59), and provides a straightforward method of estimating the number of targets in a region under surveillance. The PHD filter automatically handles the non-trivial tasks of both target number estimation and data fusion (66). In this work, the Sequential Monte Carlo (SMC) PHD filter is used (67). The SMC approach provides a mechanism to represent the posterior probability hypothesis density by a set of random samples or particles, which consists of state information with associated weights.

Let the posterior PHD, given all the measurement $Z_{1:k-1}$ up to time step $k-1$, $D_{k-1|k-1}(\mathbf{x}_{k-1}|Z_{1:k-1})$ be represented by a set of particles $\left\{w_{k-1}^{(s)}, \mathbf{x}_{k-1}^{(s)}\right\}_{s=1}^{L_{k-1}}$. That is,

$$D_{k-1|k-1}(\mathbf{x}_{k-1}|Z_{1:k-1}) = \sum_{s=1}^{L_{k-1}} w_{k-1}^{(s)} \delta(\mathbf{x}_{k-1} - \mathbf{x}_{k-1}^{(s)}) \tag{3.56}$$

where $\delta(\cdot)$ is the Dirac Delta function.

In contrast to particle filters, the total weight $\sum_{s=1}^{L_{k-1}} w_{k-1}^{(s)}$ is not equal to one. Instead, it gives the expected number of targets n_{k-1}^{X} at time step $(k-1)$.

Prediction

Generate L_{k-1} samples for existing targets and J_k number of particles for new-born targets. To generate the samples for existing targets, sample $\mathbf{x}_{k|k-1}^{(s)}$ from proposal density $q_k(\cdot|\mathbf{x}_{k-1}^{(s)}, Z_k)$, for $s = 1, \ldots, L_{k-1}$, with associated weights

$$w_{k|k-1}^{(s)} = \frac{e_{k|k-1}(\mathbf{x}_{k|k-1}^{(s)}) f_{k|k-1}(\mathbf{x}_{k|k-1}^{(s)}|\mathbf{x}_{k-1|k-1}^{(s)})}{q_k(\mathbf{x}_{k|k-1}^{(s)}|\mathbf{x}_{k-1|k-1}^{(s)}, Z_k)} w_{k-1}^{(s)} \tag{3.57}$$

where $e_{k|k-1}$ is the target survival probability.

To generate the samples for new-born targets, sample $\mathbf{x}_{k|k-1}^{(s)}$ from another proposal density $p_k(\cdot|Z_k)$, for $s = L_{k-1}+1, \ldots, L_{k-1}+J_k$ with associated weights

$$w_{k|k-1}^{(s)} = \frac{\gamma_k(\mathbf{x}_{k|k-1}^{(s)})}{p_k(\mathbf{x}_{k|k-1}^{(s)}|Z_k)} \tag{3.58}$$

where $\gamma_k(\cdot)$ is the PHD of new born spontaneous targets.

Update

With the available set of measurements Z_k at time step k, the updated particle weights can be calculated by

$$w_k^{*(s)} = \left[(1 - p_d(\mathbf{x}_{k|k-1}^{(s)})) + \sum_{i=1}^{N_k^Z} \frac{p_d(\mathbf{x}_{k|k-1}^{(s)}) f_{k|k}(\mathbf{z}_k^i|\mathbf{x}_{k|k-1}^{(s)})}{\lambda_k c_k(\mathbf{z}_k^i) + \Psi_k(\mathbf{z}_k^i)}\right] w_{k|k-1}^{(s)} \quad (3.59)$$

where

$$\Psi_k(z_k^i) = \sum_{s=1}^{L_{k-1}+J_k} p_d(\mathbf{x}_{k|k-1}^{(s)}) f_{k|k}(\mathbf{z}_k^i|\mathbf{x}_{k|k-1}^{(s)},) w_{k|k-1}^{(s)} \quad (3.60)$$

The single-target/single-sensor measurement likelihood function $f_{k|k}(\cdot)$ in (3.59) and (3.60) are written as conditioned on the model, considering a general case in which the measurement model can also be mode dependent.

Resample

To perform resampling, since the weights are not normalized to unity in PHD filters, the expected number of targets is calculated by summing up the total weights, i.e.,

$$\hat{n}_k^X = \sum_{s=1}^{L_{k-1}+J_k} w_k^{*(s)} \quad (3.61)$$

Then the updated particle set is resampled to get $\left\{w_k^{(s)}/n_k^X, \mathbf{x}_k^{(s)}\right\}_{s=1}^{L_k}$ such that the total weight after resampling remains n_k^X. Now, the discrete approximation of the updated posterior PHD at time step k is given by

$$D_{k|k}(\mathbf{x}_k|Z_{1:k}) = \sum_{s=1}^{L_k} w_k^{(s)} \delta(\mathbf{x}_k - \mathbf{x}_k^{(s)}) \quad (3.62)$$

Birth Model

Since the surveillance region is very large, if the particles for new targets are distributed uniformly throughout the surveillance region, then a large number of particles will be necessary to initialize new targets. Therefore, the particles are generated by converting the measurement at the last time step to the state space, which are in turn predicted to the current time step. For each measurement that is unassociated at the last time step, J_k particles are generated by adding noises to the converted measurement state. The association of the measurement is determined by finding the sum of the weights of particles updated by that measurement. For the associated measurement, $(1 - A_c)J_k$ particles are generated for new target as described above and $A_c J_k$ particles are generated using the particles of the target to which the measurement is associated, where A_c is the association confidence.

Clustering and Cluster-to-Track Association

Track labeling with k-mean clustering is used for track association (68). Each particle is labeled with a track number. After updating the particles, particles are clustered using the k-mean clustering algorithm. After clustering, the labels of the particles in each cluster are set to the dominating track ID in its cluster. If the new target, which is labeled zero, is dominating, then a new ID is assigned to that target, and labels are set to the assigned target ID.

When there are false alarms, the clusters may have some particles corresponding to false tracks, and this will affect the target estimate, which is found by taking the mean of the particles. In order to avoid such a problem, first cluster the particles into smallest integer, which is greater than $\hat{n}_k^X$, groups. Then for each cluster find

the mean and covariance, and remove the particles that are outside a gate that was formed using the mean and covariance.

3.3 Integrated Bias Removal and Sensor Calibration in Passive Radar Systems

In a passive radar system, a variety of measurements can be used to estimate target states such as DOA or angle of arrival (AOA), time difference of arrival (TDOA) or Doppler shift. Noise and the precision of DOA estimation are main issues in a PCL system and methods such as conventional beam forming (CBF) algorithm, algebraic constant modulus algorithm (ACMA) are widely analyzed in literature to address them. In practical systems, although it is necessary to reduce the directional ambiguities, the placement of receivers closed to each other results in larger bias in the estimation of DOA of signals, especially when the targets move off bore-sight. This phenomenon leads to degradation in the performance of the tracking algorithm. In this chapter, we present a method for removing the bias in DOA and calibrating the senor simultaneously to alleviate the aforementioned problem. The simulation results are presented to show the effectiveness of the proposed algorithm with an example of tracking airborne targets.

Multisensor systems use data fusion of multiple sensors to form accurate estimate of a target track. To fuse multiple sensor data, each sensor data must be expressed in a common reference frame. The problem encountered in multisensor system is the presence of errors due to sensor bias, antenna orientation, site position uncertainties or any measurement related bias. Problem of reference frame misalignment, also

known as tilt error (92), also cause an error in the measurements.

The smaller errors in the direction of arrival measurement will create large degradation in the tracking accuracy. Especially for a large bistatic range measurement, it will give larger errors and therefore, the DOA accuracy becomes a very important limiting factor in long range target detection. Hence, it will create large errors in detection and estimation of high range targets. Therefore, it is very essential to reduce the angular errors in DOA estimation. The DOA measurement will have noise and bias errors due to mutual coupling in antenna elements and antenna orientation. Therefore, in this chapter, we propose a method for removing the bias in DOA and calibrating the senor simultaneously to alleviate the aforementioned problem. An SMC implementation of Probability Hypothesis Density (PHD) filter (59) (66) (88) based technique is used to estimate and remove the DOA bias. The simulation results are presented to show the effectiveness of the proposed algorithm with an example of tracking airborne targets.

In (5), Howland developed a signal processing scheme that allows airborne targets to be detected and be tracked using only the vision or sound carrier of the television broadcast. They used Doppler shift and DOA of the target echoes to estimate the target's track. The Doppler-DOA information on the television video career signal can track the aircraft ranges up to 260 km. Target tracking was performed in range-Doppler-DOA domain. To efficiently remove the strong clutter signals and interference, an adaptive filter algorithm was described in (2) (3).

The direct signal and the echo from the target are received and processed for the measurements such as bistatic range, range rate, and target DOA. However, in order to eliminate the ambiguities in bistatic range, bistatic Doppler and DOA, a

PCL system can use more than one illumination source and receiver. Therefore, a multistatic PCL configuration yields an enhanced robust and redundant information, and therefore reduces the ambiguity and enhance the tracking accuracy.

3.3.1 Direction of Arrival

Figure 3.2 shows an isorange ellipsoids for a particular bistatic range measurement in a PCL system. The DOA estimation helps to determine on which point of the isorange ellipsoid the target is located. The smaller errors in the direction of arrival measurement will create large errors when the bistatic range measurement increases. Hence, will create large errors in detection and estimation of high range target. Therefore, it is very essential to reduce the angular errors in DOA estimation. The DOA measurement will have noise and bias errors due mutual coupling in antenna elements and antenna orientation. Also the errors can be caused due to many reasons such as errors in electromagnetic related issues, hardware or software related issues, mechanical and positioning related issues and signal processing based issues.

Since the accuracy of the DOA plays a major role in target tracking in PCL systems, this chapter focus on estimating and removing the bias in DOA measurement. In this chapter, we assume a bistatic multitarget environment to track the target. We consider the two dimensional environment and ignore the altitudes of the target.

Howland estimated the DOA using phase interferometry (5). The DOA of a target echo, Φ, is related to the phase difference of arrival at two surveillance antenna, Θ can be given by the following equation.

$$\Phi = \frac{2\pi d}{\lambda} \sin\Theta \tag{3.63}$$

where d is the distance between the dipoles and λ is the wavelength.

3.3.2 Problem Formulation

In general, a passive radar measures bistatic range, bistatic Doppler and direction of arrival of the signal.

Direction of arrival

The direction of arrival associated with j th target at the PCL radar receiver can be given by,

$$\theta_k^j = \tan^{-1}\left(\frac{y_k^j - y_R}{x_k^j - x_R}\right) + b_k^j + v_{1,k-1}^j \tag{3.64}$$

where b_k^j is the bias associated with the measurement θ_k^j and v_{k-1}^j is the measurement noise corresponding the DOA measurement.

Bistatic range

From PCL radar, the bistatic range measurement can be obtained, and the target will be located in a point at the ellipse given by the following equation.

$$R = \sqrt{(x_k^j - x_T)^2 + (y_k^j - y_T)^2} + \sqrt{(x_k^j - x_R)^2 + (y_k^j - y_R)^2} + v_{2,k-1}^j \tag{3.65}$$

Bistatic Doppler

From PCL radar also gives the bistatic Doppler measurement, and it can be given by

$$\dot{R} = \frac{(x_k^j - x_T)\dot{x}_k^j + (y_k^j - y_T)\dot{y}_k^j}{\sqrt{(x_k^j - x_T)^2 + (y_k^j - y_T)^2}} + \frac{(x_k^j - x_R)\dot{x}_k^j + (y_k^j - y_R)\dot{y}_k^j}{\sqrt{(x_k^j - x_R)^2 + (y_k^j - y_R)^2}} + v_{3,k-1}^j \tag{3.66}$$

Target Dynamics

The general parameterized target dynamics of the j th target is given by

$$\mathbf{x}_k^j = a_k(\mathbf{x}_{k-1}^j, \mathbf{w}_{k-1}) \qquad j = 1, \ldots, N_k^X, \tag{3.67}$$

where $\mathbf{x}_k^j$ is the target state vector at time step k, N_k^X is the number of targets at time step k, a_k, in general, is a nonlinear function and $\mathbf{w}_{k-1}$ is the process noise vector of known statistics.

$$\mathbf{x}_k^j = \begin{bmatrix} 1 & T & 0 & 0 & 0 \\ 0 & 1 & 0 & 0 & 0 \\ 0 & 0 & 1 & T & 0 \\ 0 & 0 & 0 & 1 & 0 \\ 0 & 0 & 0 & 0 & 1 \end{bmatrix} \mathbf{x}_{k-1}^j + \mathbf{w}_k^j \tag{3.68}$$

where $\mathbf{x}_k^j = [x_k^j, \dot{x}_k^j, y_k^j, \dot{y}_k^j, b_k^j]$ is the state of the j th target, which consists of target position (x_k^j, y_k^j) and target velocity $(\dot{x}_k^j, \dot{y}_k^j)$ at time step k and $\mathbf{w}_k^j$ is i.i.d sequence of

zero-mean Gaussian variable with covariance

$$\Sigma_k^j = \begin{bmatrix} \frac{T^3 l_1}{3} & \frac{T^2 l_1}{2} & 0 & 0 & 0 \\ \frac{T^2 l_1}{2} & T l_1 & 0 & 0 & 0 \\ 0 & 0 & \frac{T^3 l_1}{3} & \frac{T^2 l_1}{2} & 0 \\ 0 & 0 & \frac{T^2 l_1}{2} & T l_1 & 0 \\ 0 & 0 & 0 & 0 & T l_2 \end{bmatrix} \tag{3.69}$$

where the levels of the power spectral densities are l_1 and l_2 corresponding to state and bias estimates, respectively.

3.4 Results

3.4.1 Bistatic PCL System

Simulations

In this simulation, the parameter settings are: transmitter position = [49925, -10899]m; receiver position = [0, 0]m; measurement interval is 1 second; measurement variances $\sigma_r^2 = 400$ m^2 and $\sigma_{\dot{r}}^2 = 1$ m^{2}s^{-2}; probability of detection is 0.98; on average, 10 false alarms occur at each sampling time. The target trajectories, transmitter and receiver locations are given in Figure 3.3. There are two targets in the surveillance region, one enters the region at $k = 1$ and the other enters at $k = 15$.

In the first scenario, a low bearing error of $\sigma_\theta^2 = 0.0001$ radians^2 is considered. The Root Mean Square Errors (RMSEs) of the CMKF, UKF and the PHD filter are given in Figures 3.4, 3.5 and 3.6, respectively.

From these figures it can be seen that the performances of UKF and PHD filters

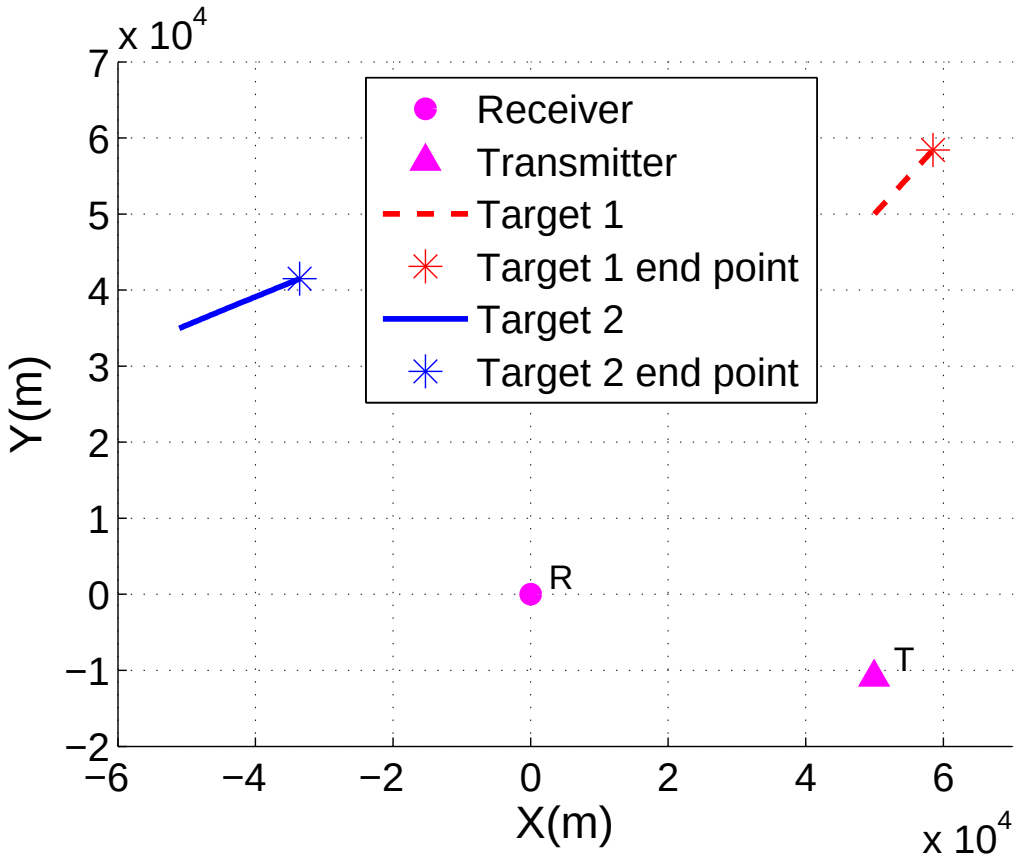

Figure 3.3: Target trajectories and locations of transmitter and receiver.

are better than that of the CMKF.

The performance of the PHD filter was almost equal to the one of CMKF when the number particles used in PHD filter was 1000. Around 4000 particles were required to match the performance of the UKF.

Because of the low computational complexity of the UKF compared to the particle filter based PHD filter, the UKF is the best choice for the errors considered in this scenario.

In the second scenario, a high bearing error with $\sigma_\theta^2 = 0.01$ radians^2 is considered.

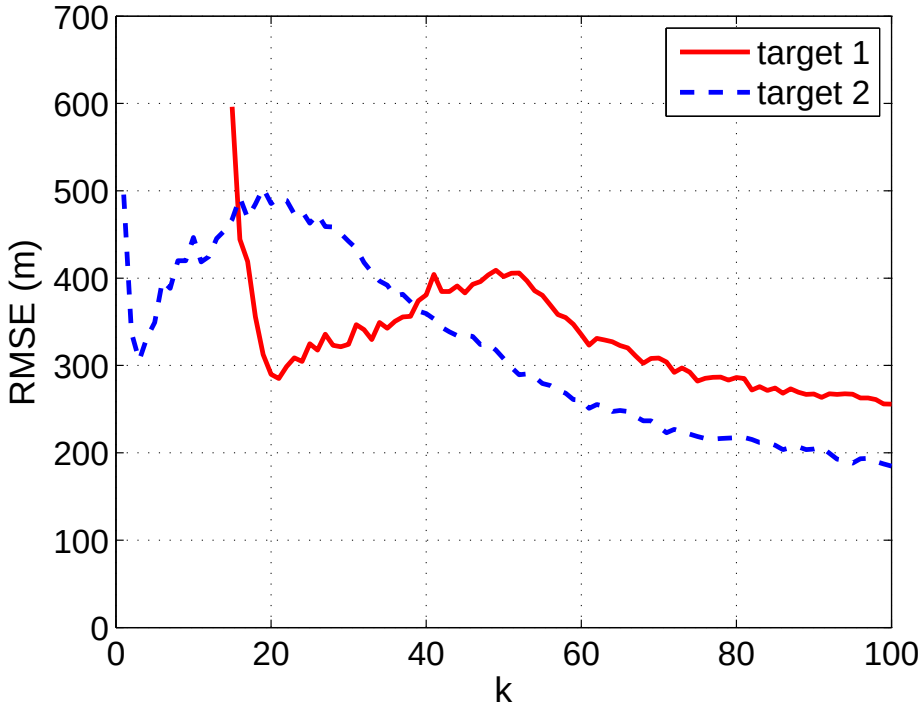

Figure 3.4: RMSE comparison of CMKF with variances $\sigma_r^2 = 400$ m^2, $\sigma_\theta^2 = 0.0001$ radians^2 and $\sigma_{\dot{r}}^2 = 1$ m^{2}s^{-2}.

The RMSEs of the CMKF, UKF and PHD filter are shown in Figures 3.7, 3.8 and 3.9, respectively.

The number of times in which the tracks are found within 5000 m distance from the target out of 100 runs is shown in Figures 3.10, 3.11 and 3.12. From these figures it can be seen that PHD filter outperforms CMKF and UKF.

While the PHD filter detects the targets, on average, in 96% of the runs, the CMKF and UKF detect the targets only in 41% and 59% of the runs respectively. Tracks are missed due to track losses for the UKF and due to track breakages for the CMKF.

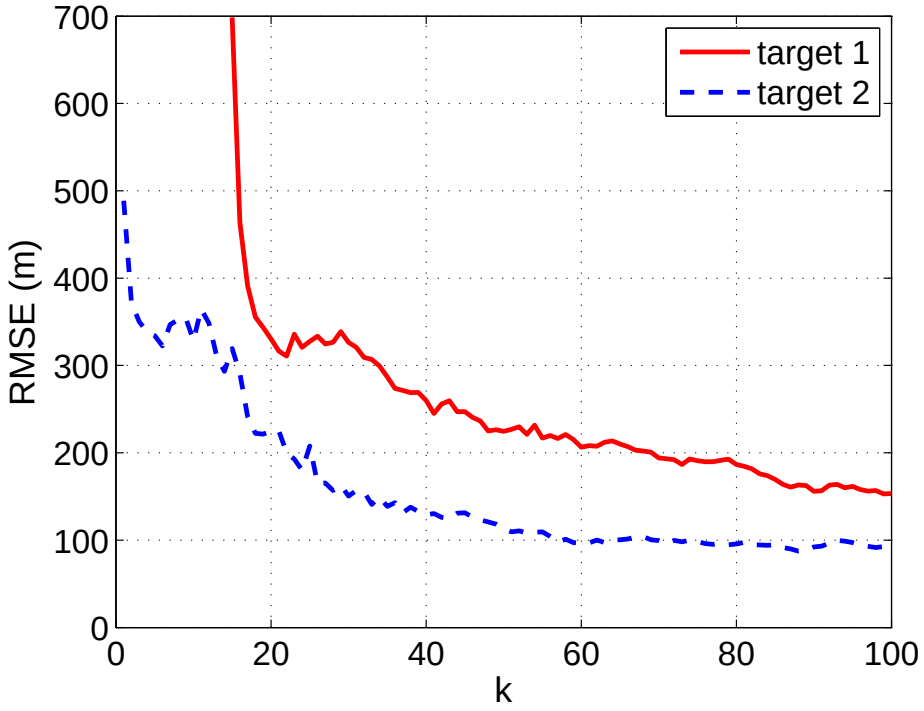

Figure 3.5: RMSE comparison of UKF with variances $\sigma_r^2 = 400$ m^2, $\sigma_\theta^2 = 0.0001$ radians^2 and $\sigma_{\dot{r}}^2 = 1$ m^{2}s^{-2}.

Real Data

The real data provided by TNO is shown in Figure 3.13. In the TNO system, only one transmitter and one receiver are used. A large number of false alarms are observed in a narrow region. The reason for the appearance of this clutter is unknown and it may be an artifact due to processing errors. For simplicity, the high false alarm region is ignored during the processing. Integrated clutter modeling and target tracking can be used to handle the non-uniform clutter. The position-dependent measurement variances are in the range of 400^2–1000^2 m^2 for σ_r^2, around 1 m^{2}s^{-2} for $\sigma_{\dot{r}}^2$ and in the range of 0.0004 – 0.008 radians^2 for σ_θ^2.

The tracker parameter settings are: tentative track formation logic is 2 out of 2,

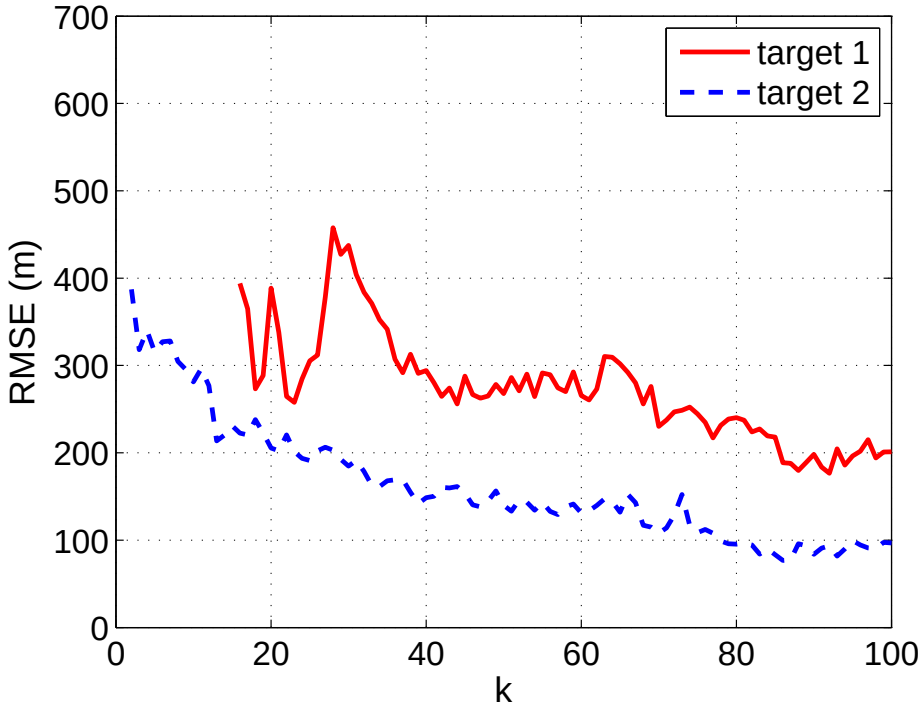

Figure 3.6: RMSE comparison of PHD filter with variances $\sigma_r^2 = 400$ m^2, $\sigma_\theta^2 = 0.0001$ radians^2 and $\sigma_{\dot{r}}^2 = 1$ m^{2}s^{-2}.

tentative track maintenance logic is 4 out of 8 and confirmed track deletion logic is 1 out of 15.

The tracks formed using the UKF are shown in Figure 3.14. Tracks are formed only for the targets within the coverage region of the PCL system. Even the formed tracks are not smooth due to the low probability of detection and target maneuvers. It can be seen that there are gaps between the tracks and the ground truth.

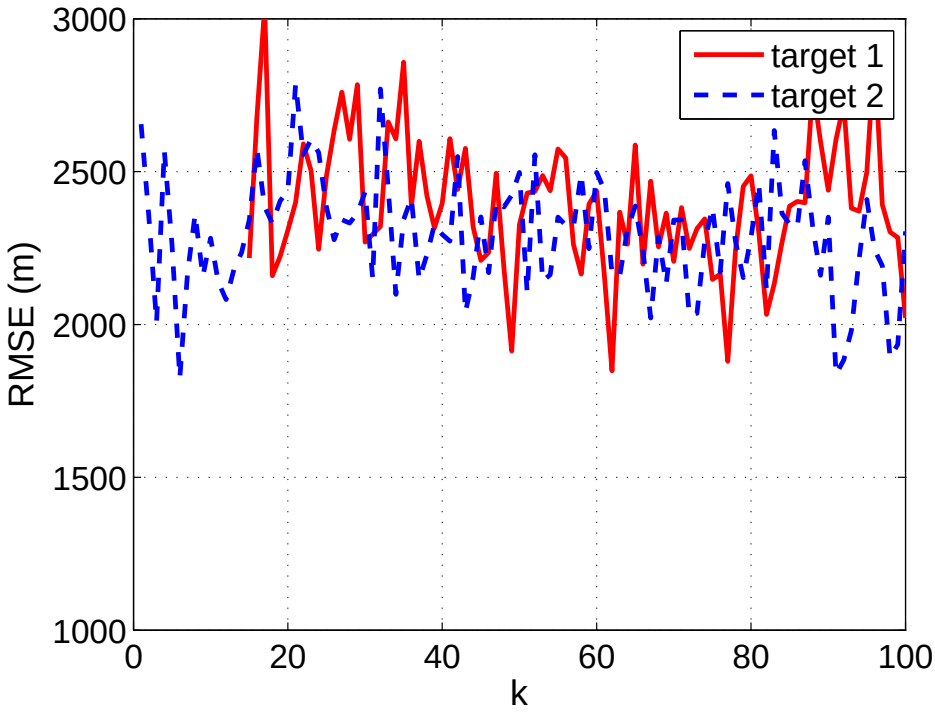

Figure 3.7: RMSE comparison of CMKF with variances $\sigma_r^2 = 400$ m^2, $\sigma_\theta^2 = 0.01$ radians^2 and $\sigma_{\dot{r}}^2 = 1$ m^{2}s^{-2}.

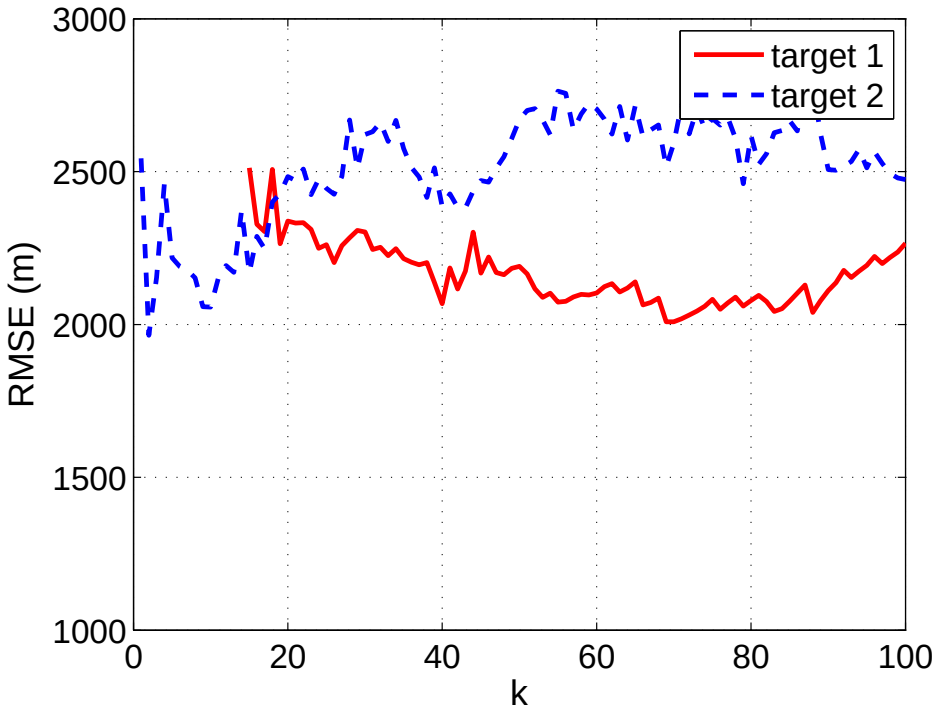

Figure 3.8: RMSE comparison of UKF with variances $\sigma_r^2 = 400\ \mathrm{m}^2$, $\sigma_\theta^2 = 0.01\ \mathrm{radians}^2$ and $\sigma_{\dot{r}}^2 = 1\ \mathrm{m}^2\mathrm{s}^{-2}$.

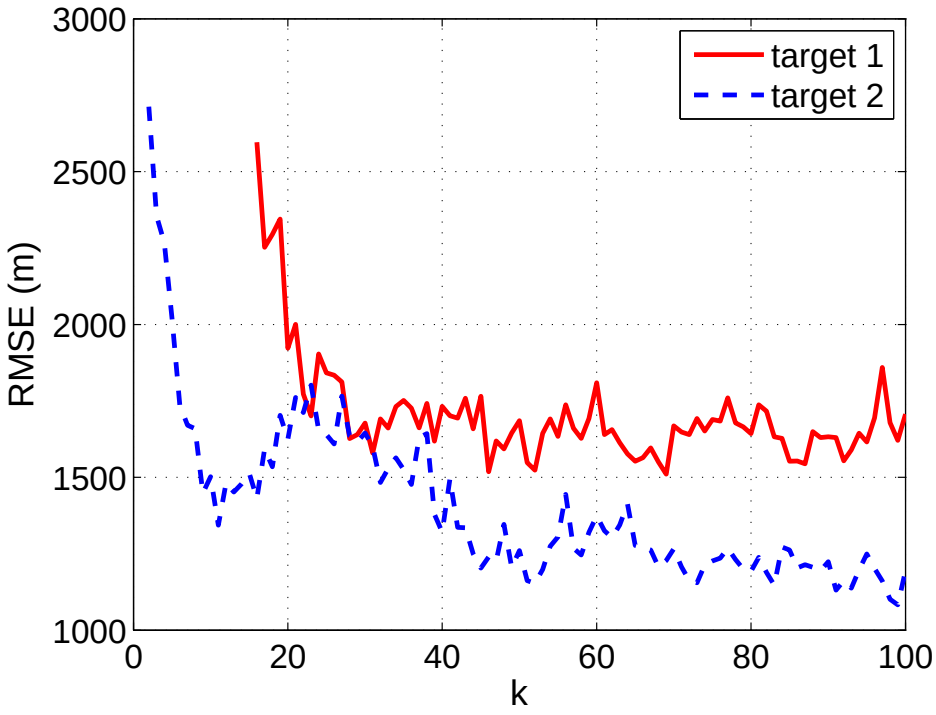

Figure 3.9: RMSE comparison of PHD filter with variances $\sigma_r^2 = 400$ m^2, $\sigma_\theta^2 = 0.01$ radians^2 and $\sigma_{\dot{r}}^2 = 1$ m^{2}s^{-2}.

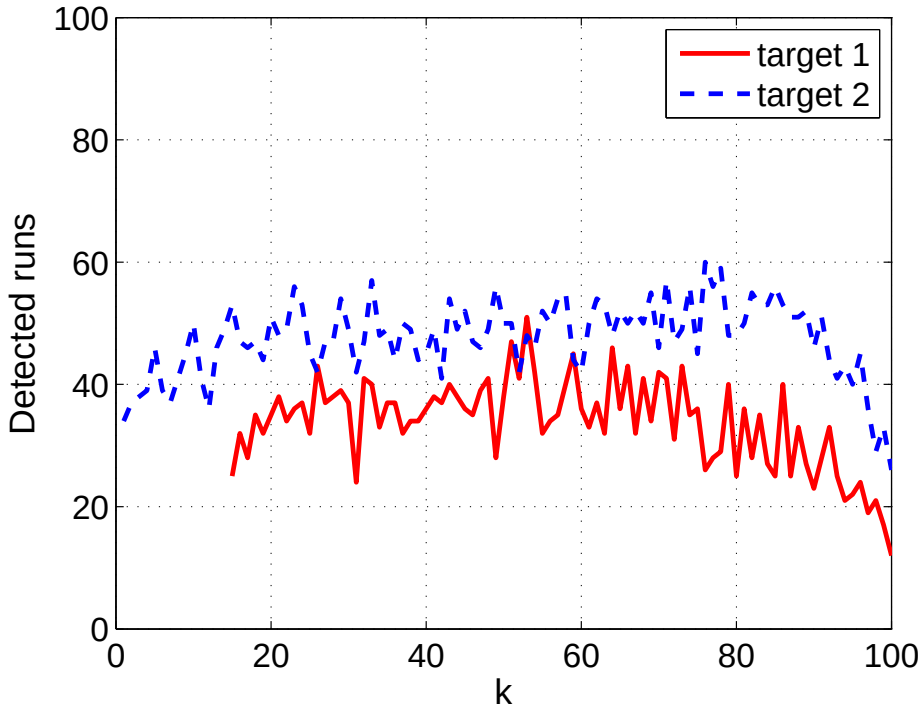

Figure 3.10: CMKF: Number of runs in which tracks are found within 5000 m distance from the target out of 100 runs with variances $\sigma_r^2 = 400$ m^2, $\sigma_\theta^2 = 0.01$ radians^2 and $\sigma_{\dot{r}}^2 = 1$ m^{2}s^{-2}.

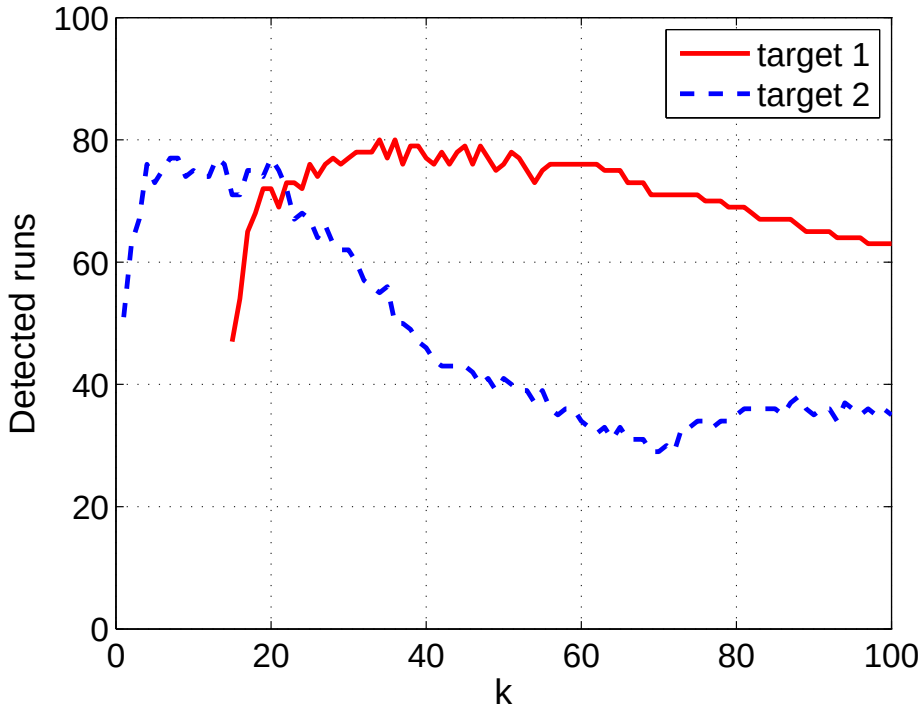

Figure 3.11: UKF: Number of runs in which tracks are found within 5000 m distance from the target out of 100 runs with variances $\sigma_r^2 = 400$ m^2, $\sigma_\theta^2 = 0.01$ radians^2 and $\sigma_{\dot{r}}^2 = 1$ m^{2}s^{-2}.

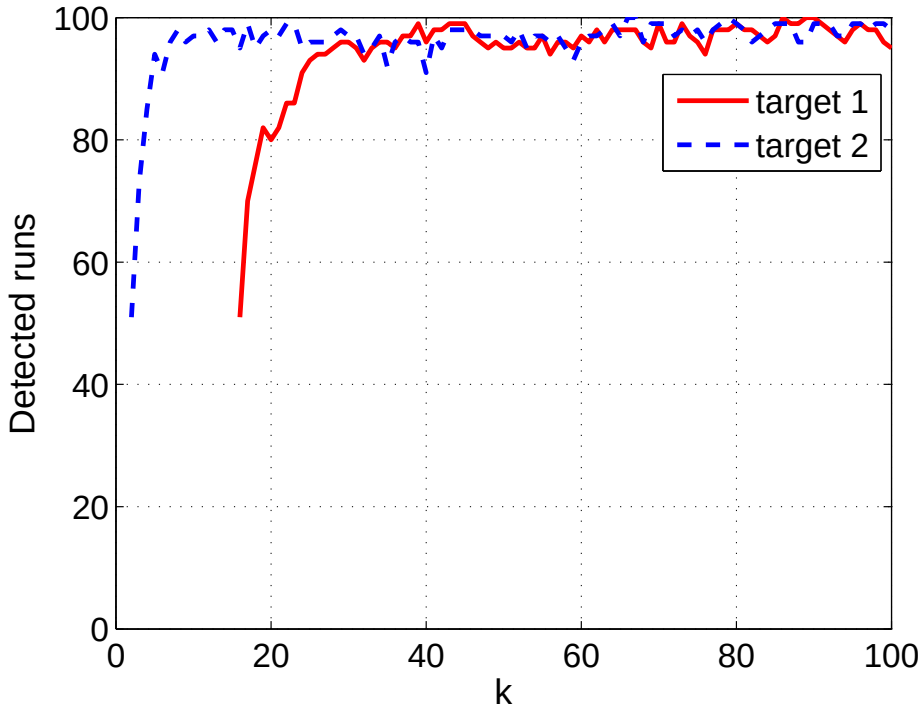

Figure 3.12: PHD: Number of runs in which tracks are found within 5000 m distance from the target out of 100 runs with variances $\sigma_r^2 = 400$ m^2, $\sigma_\theta^2 = 0.01$ radians^2 and $\sigma_{\dot{r}}^2 = 1$ m^{2}s^{-2}.

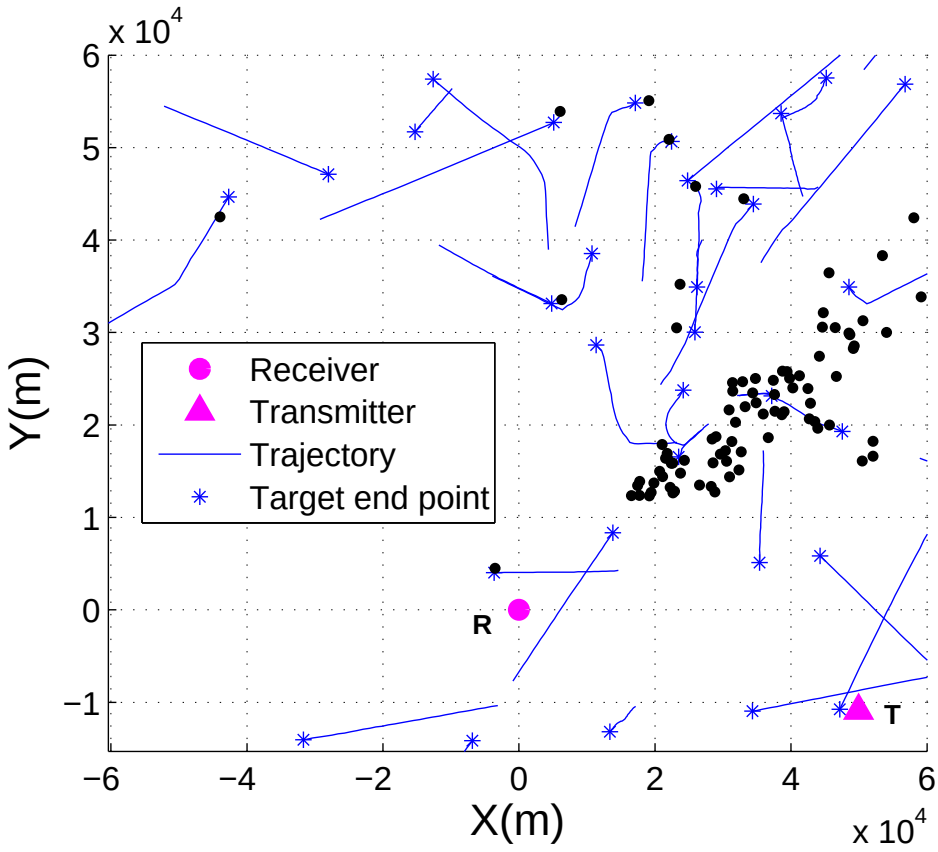

Figure 3.13: TNO data.

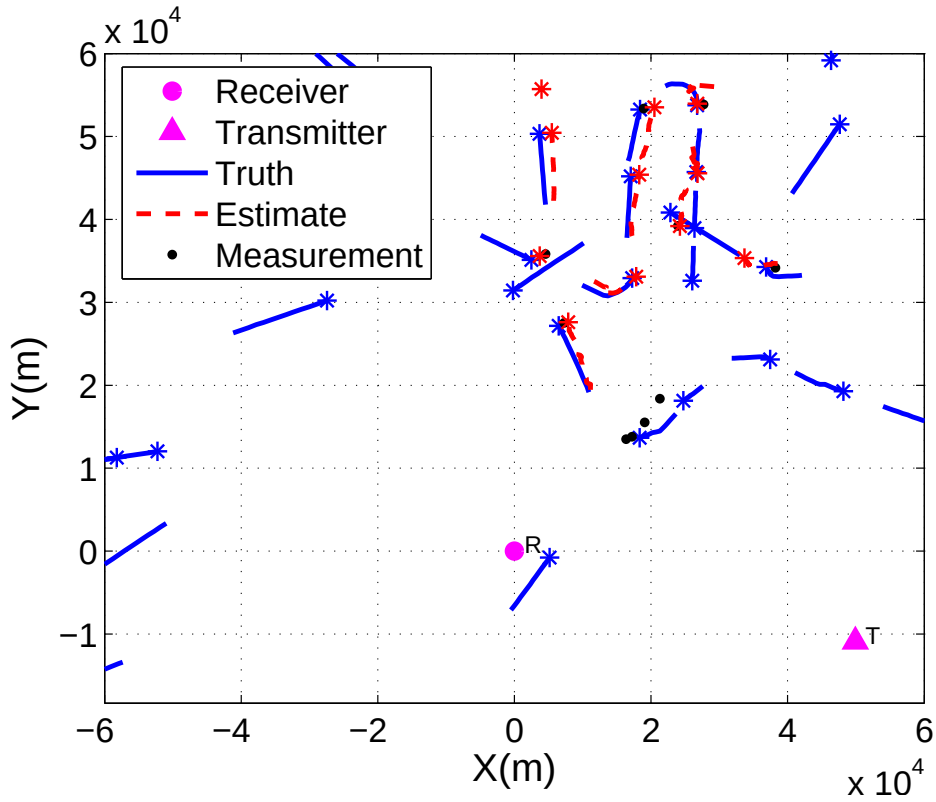

Figure 3.14: Estimated trajectories and ground truth for TNO data.

3.4.2 Bias Removal in PCL System

In this section, a two dimensional tracking example is presented to demonstrate the performance of the bias removal algorithm. The example consists of a transmitter and two receivers, which are shown in Figure 3.15 by T, R1 and R2, respectively. The measurements are received at both receivers synchronously at an interval of 1s. The covariance associated with measurements is $\text{diag}([400\,m^2\ 0.0001\,\text{radians}^2\ 1\,m^2s^{-2}])$. It is assumed that bias in the direction of arrival is characterized by random walk model with initial value 0.1 radians. The noise associated with the random walk model is zero mean Gaussian with variance 0.000001 radians^2. In this scenario, two targets enter the surveillance region at time steps $k = 1$ and $k = 30$.

The PHD filter is constructed with the following parameters: the number of particles per target = 5000; the number of particles associated with new targets = 100; the probability of target birth = 0.01; the probability of target death = 0.001.

In this example, the performances of the algorithms with and without estimating the bias are compared.

Figures 3.17 shows the root mean square values of the estimates when the bias is ignored.

Figures 3.18 shows the root mean square values of the estimates when the bias is estimated. It could be seen that estimating the bias yields significant improvement on the performance of the tracking algorithm.

Figure 3.18 shows that the bias estimation takes around 10 steps to converge. Sudden peak at $k = 31$ due to clustering issues when new target enters, which should be accounted towards the clustering part of the algorithm and should not be related to the performance of the bias estimation.

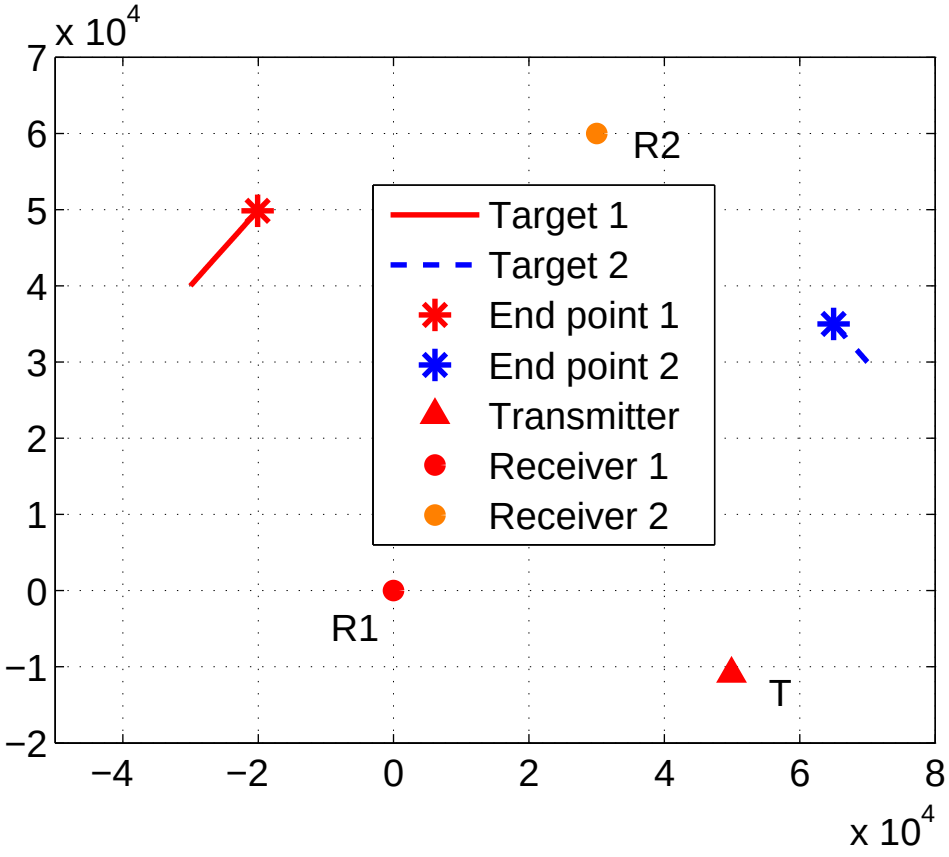

Figure 3.15: Target trajectories and locations of transmitter and receivers.

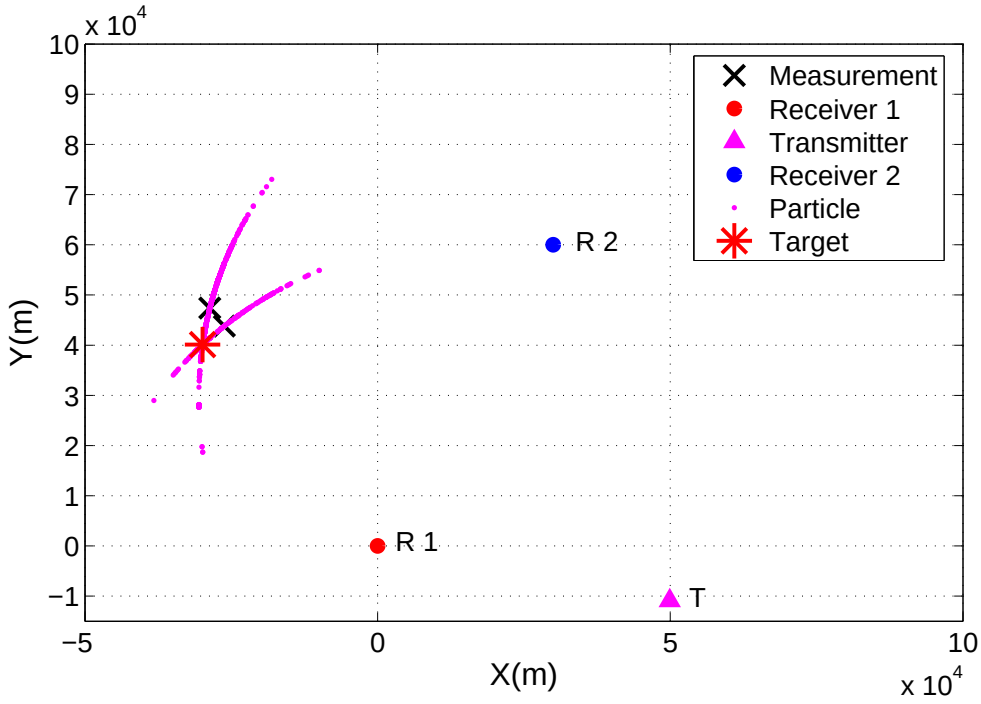

Figure 3.16: Particles at the initial time step.

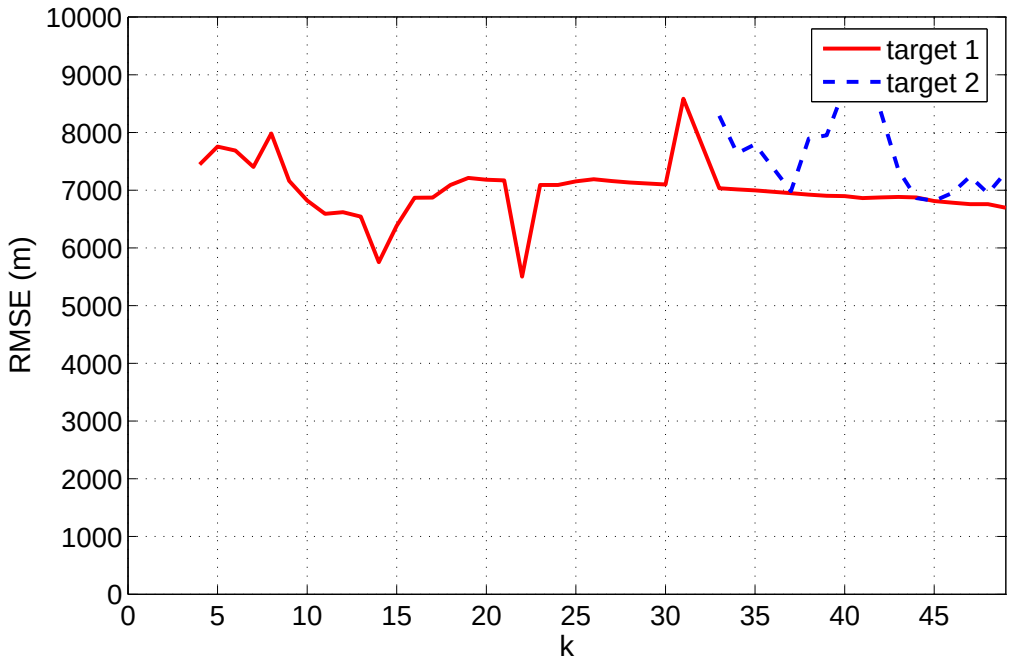

Figure 3.17: RMSE of target with no bias consideration.

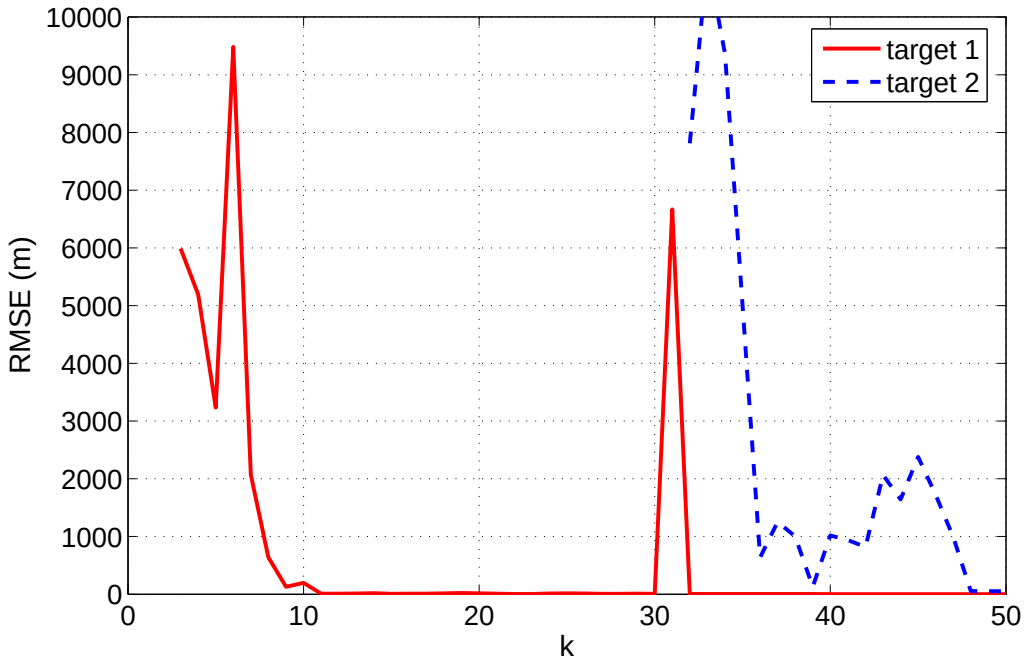

Figure 3.18: RMSE of target with bias estimation.

Chapter 4

Multipath Assisted Tracking with Known Reflection Points

4.1 Multipath Reflections in Tracking Environment

In this chapter an algorithm for multipath-assisted multitarget tracking using multi-frame assignment is proposed for initiating and tracking multiple targets using one or more transmitters and receivers. This algorithm is capable of exploiting multipath target returns from distinct propagation modes that are resolvable by the receiver. When resolved multipath returns are not utilized within the tracker, i.e., discarded as clutter, potential information conveyed by the multipath detections of the same target is wasted. In this case, spurious tracks are formed using target-originated multipath measurements, but with an incorrect propagation mode assumption. Integrating multipath information into the tracker instead of discarding can help improve the accuracy of tracking and reduce the number of false tracks. The challenge in improving tracking results using multipath measurements is the fusion of direct and

multipath measurements from the common target. The problem will be considered in an environment with false alarms and missed detections. We propose a multiframe assignment technique to incorporate multipath information. The simulation results are presented to show the effectiveness of the proposed algorithm with an example of tracking ground targets.

4.2 Incorporating Multipath in Tracking

4.2.1 System Model in Multipath Reflection Environment

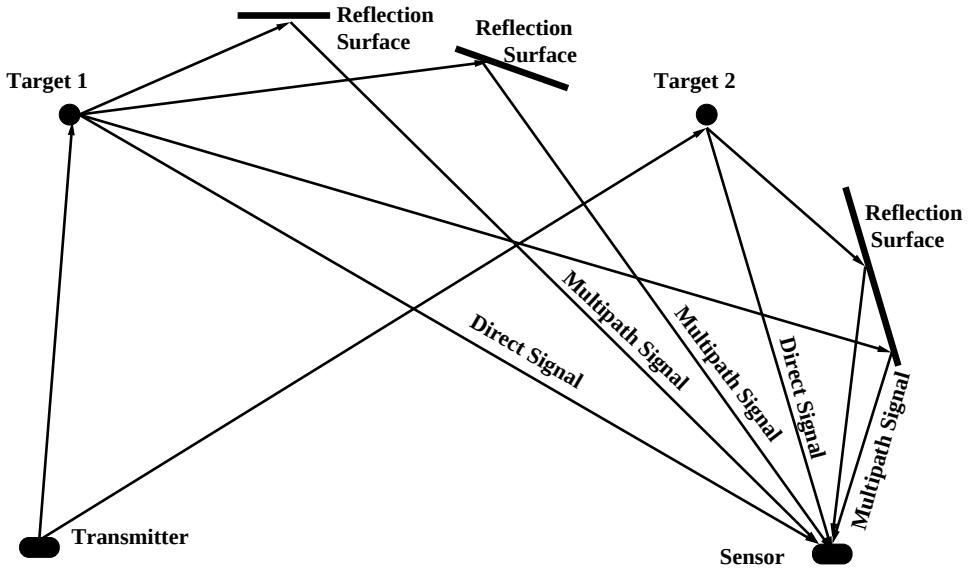

Figure 4.1: Multipath reflection model in target tracking.

In this chapter, we considered a bistastic multipath model in which the transmitter and the receiver are separated by a large distance. The direct signal from the transmitter and the echo from the target are received and processed for the bistatic range and multipath range measurements. In this model a transmitter and a receiver are

used for target detection and tracking. The simple configuration of multipath model is illustrated in Figure 4.1. In this model, bistatic range, multipath range and bearing are used to track the target. A multipath configuration yields additional information about the target through the reflected signals. In a real world multipath signal propagation mode environment, the echo signals are buried deep in noise. There will be other unwanted signals such as measurements from unmodeled multipath reflections, clutter, and unwanted echoes such as reflections from ground, buildings, trees, clouds and other moving or stationary objects.

In system model, the reflected signals from the target reach the sensor by different ways such as direct path and multipath reflections. In this work, we utilize the multipath signal information for improving the tracking accuracy. We consider a system with a single transmitter and a single receiver to detect and track multiple targets with a direct and a multipath reflected signals. In this model, the multipath signals reflected from the target reflect at most once before they arrive at the sensor. Figure 4.1 depicts the geometry of the radar sensor system when separate transmitter and receiver arrays are used. We assume that transmitter, target, reflection surface and receiver are on the same (ground) level. For simplicity we assume that the ground surface is flat and vertical to the ground plane and tracking is performed on the ground coordinates.

When multipath target returns from distinct propagation modes are resolved, spurious tracks are formed. Associating these signals facilitate better estimates of the target states. However, in order to use this measurement an appropriate association of multipath reflection model has to be identified. Incorrect reflection model assignment will lead to errors in association and tracking. Hence, to utilize these measurements

appropriately, it is important to have the measurements resolved appropriately in multipath propagation mode assignment uncertainties. Multipath signal propagation mode assignment uncertainty adds another level of complexity to the standard data association problem. That is, there is more than one uncertainty that needs to be resolved in order to track multiple targets. One is the measurement-to-target association and the other is the measurement-to-multipath propagation mode association. In this work a tracking algorithm is proposed to track multiple targets using more than one target originated returns due to direct signal and a multipath reflection.

In this model $(x(k), y(k))$ denotes the moving target position at time step k. It is assumed that the sensor and the transmitter locations are known and they are denoted by $(x_r(k), y_r(k))$ and $(x_t(k), y_t(k))$, respectively. The reflection model index is denoted by rs. Based on the reflection surface information, using ray optics geometry, the reflection points can be evaluated. The reflection point coordinate $(x_{rs}(k), y_{rs}(k))$ denotes the reflection point at k^{th} time step in rs^{th} multipath reflection model (reflection surface). The received signals are either direct signal from the target or signals with one reflection at the reflection surface rs before it arrives at the sensor.

Key Assumptions

- In addition to the direct signal detection, the sensor measurements contain resolved multipath detections.
- The transmitted signal directly hit the target and there is no other reflection point between the target and the transmitter.
- The signals reflected from the target reflect at most once before they arrive at the sensor.

- Complete knowledge of the reflection surface information such as the geometry of the surface or the reflection points, and reflection coefficients are known.

The measurements are bistatic range $r_d(k)$, multipath range $r_m(k)$, bearing from direct signal $\theta_d(k)$, and multipath reflected signal $\theta_m(k)$. The measurement equations are given below. At a given time step k, the bistatic range measurement from the direct target return can be given by

$$\begin{aligned} r_d(k) &= \left(\sqrt{(x(k)-x_t(k))^2+(y(k)-y_t(k))^2}\right)+ \\ &+\left(\sqrt{(x(k)-x_r(k))^2+(y(k)-y_r(k))^2}\right)+ \\ &-\left(\sqrt{(x_t(k)-x_r(k))^2+(y_t(k)-y_r(k))^2}\right)+ \\ &+\omega_\tau(k) \end{aligned} \tag{4.1}$$

The direction of arrival (DOA) of the signal received directly from the target is given by

$$\theta_d(k) = \tan^{-1}\left[\frac{(y(k)-y_r(k))}{(x(k)-x_r(k))}\right]+\omega_\theta(k) \tag{4.2}$$

In the above case, there is no multipath reflection between the target and the sensor in the signal propagation path. When there is a reflection between target and the sensor, the multipath range measurement can be given by

$$\begin{aligned} r_m(k) &= \left(\sqrt{(x(k)-x_t(k))^2+(y(k)-y_t(k))^2}\right)+\left(\sqrt{(x_{rs}(k)-x(k))^2+(y_{rs}(k)-y(k))^2}\right)+ \\ &+\left(\sqrt{(x_{rs}(k)-x_r(k))^2+(y_{rs}(k)-y_r(k))^2}\right)+ \\ &-\left(\sqrt{(x_t(k)-x_r(k))^2+(y_t(k)-y_r(k))^2}\right)+ \\ &+\omega_m(k) \end{aligned} \tag{4.3}$$

In this case, the direction of arrival (DOA) of the signal received by the sensor after reflected from a point on the reflection surface is given by

$$\theta_m(k) = \tan^{-1}\left[\frac{(y_{rs}(k)-y_r(k))}{(x_{rs}(k)-x_r(k))}\right]+\omega_\theta(k) \tag{4.4}$$

Therefore, the measurement $z(k)$ can be given by the following equation.

$$z(k) = \begin{bmatrix} r(k) \\ \theta(k) \end{bmatrix} \tag{4.5}$$

where $r(k) = r_d(k)$ and $\theta(k) = \theta_d(k)$ when the target return signal propagation mode is direct and $r(k) = r_m(k)$ and $\theta(k) = \theta_m(k)$ when the target return signal propagation mode is multipath.

4.2.2 Multipath Reflection Points on Smooth Surface

Based on the ray optical geometry, it is possible to evaluate the reflection points $(x_{rs}(k), y_{rs}(k))$ on the reflection surface when the reflection surface information is known. Consider a flat

smooth reflecting surface leant in an angle α as shown in Figure 4.2 is defined by $y = mx+c$. Figure 4.2 also shows the ray reflection path geometry where $(\frac{\pi}{2} - \phi)$ is the incident angle on the smooth surface, $\theta_m(k)$ is the DOA of the wall-reflected signal at the receiver $(x_r(k), y_r(k))$, and $\theta_m^{rs}(k)$ is the direction of arrival angle at the reflection point. Then the reflection points $(x_{rs}(k), y_{rs}(k))$ on the surface can be defined by the following way.

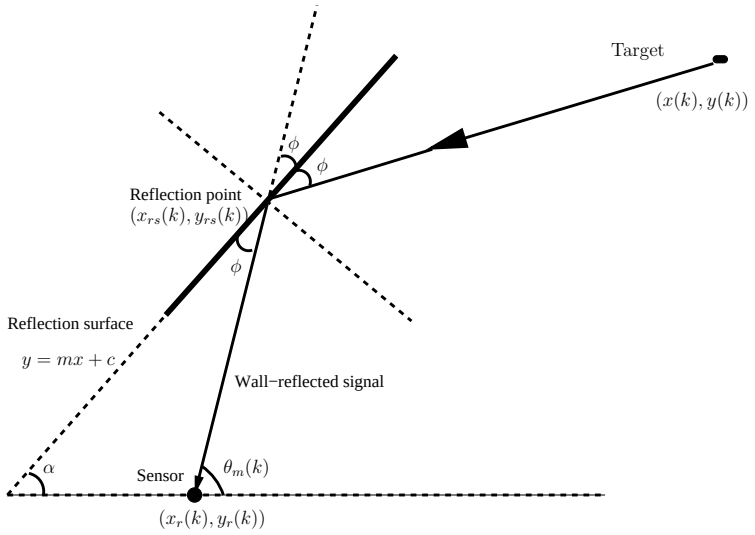

Figure 4.2: Ray optical geometry.

$$\theta_m(k) = \phi + \alpha \tag{4.6}$$

$$\theta_m^{rs}(k) = \alpha - \phi \tag{4.7}$$

$$\alpha = \tan^{-1}(m) \tag{4.8}$$

$$y = mx + c \tag{4.9}$$

$$\begin{aligned} \theta_m(k) &= \tan^{-1}\left[\frac{(y_{rs}(k) - y_r(k))}{(x_{rs}(k) - x_r(k))}\right] + \omega_\theta(k) \\ &= \tan^{-1}(m'_{rp}) \end{aligned} \tag{4.10}$$

$$x_{rs}(k) = \frac{y_r(k) - m'_{rp}x_r(k) - c}{(m - m')} \tag{4.11}$$

$$y_{rs}(k) = \frac{my_r(k) - mm'_{rp}x_r(k) - m'c}{(m - m')} \tag{4.12}$$

In the tracking and data association, the uncertainty in reflection point estimation due to bearing error must be considered. However, in this chapter it is assumed that reflection points are known to the receiver. Incorporating the reflection point uncertainty in target tracking is considered in the next chapter.

4.3 Tracking Algorithm

The target motion model and measurement models are using the following non-linear relationship in the Cartesian coordinate system.

$$x(k+1) = f_k\left(x(k)\right) + v(k) \tag{4.13}$$

$$z(k) = h_k\left(x(k)\right) + w(k) \tag{4.14}$$

where $x(k) = [x(k)\ \dot{x}(k)\ y(k)\ \dot{y}(k)]^T$ is the state of the moving target at discrete time step k. Here $x(k)$ and $y(k)$ are the positions and $\dot{x}(k)$ and $\dot{y}(k)$ are the velocities in the direction

of X and Y coordinates. Here, f_k and h_k are state and measurement models defining the non-linear functions, and $v(k)$ and $w(k)$ are process and measurement noise, which are assumed to be drawn from a zero mean, statically independent and Gaussian white noise with covariances Q_k and R_k, respectively.

To initialize the targets, we form a tentative track for each unassociated measurements at last time step and perform the 2-D data association with current measurements. If any association is found, then the tentative track is confirmed as an initial track, and it is deleted otherwise. Bistatic range and bearing measurements from the direct signal are used to initialize the target positions.

The Kalman filter is the optimal filter when the target state and measurement models are linear and noises are Gaussian. When nonlinearities are present the extended Kalman filter (EKF), the unscented Kalman filter (UKF), particle filter or probability hypothesis density (PHD) filter can be used (34) (59). Multitarget tracking becomes more difficult since which reports from a particular sensor were generated by which targets must be determined. Since more than one measurement from the same sensor need to be associated to the target and to the different propagation path modes the complexity further increases. As we consider a multitarget multipath system with the presence of false alarms and missed detections the complexity increases further. How many targets are present and how it should keep track of it are the important issues to be addressed. The primary focus is to estimate the target kinematic state (position and velocity) from noise corrupted measurements. In this chapter, we implemented the UKF to track the targets using multipath measurements.

The problem is to associate the measurements to targets and to the appropriate signal propagation path mode. One of the approach is tracking the targets in the measurement space by assuming that all the measurements from direct path signal model. In this case, more than one track may be formed for each target, and then tracks must be fused by finding the appropriate multipath signal propagation model assignment. Furthermore, one

of the other approach is tracking the targets in the state space and add one more dimension in the S-D assignment for the signal propagation model. In both approaches, multiframe assignment must be used. The data association gives decisions as to which of the received measurements and propagation modes should be used to update each track.

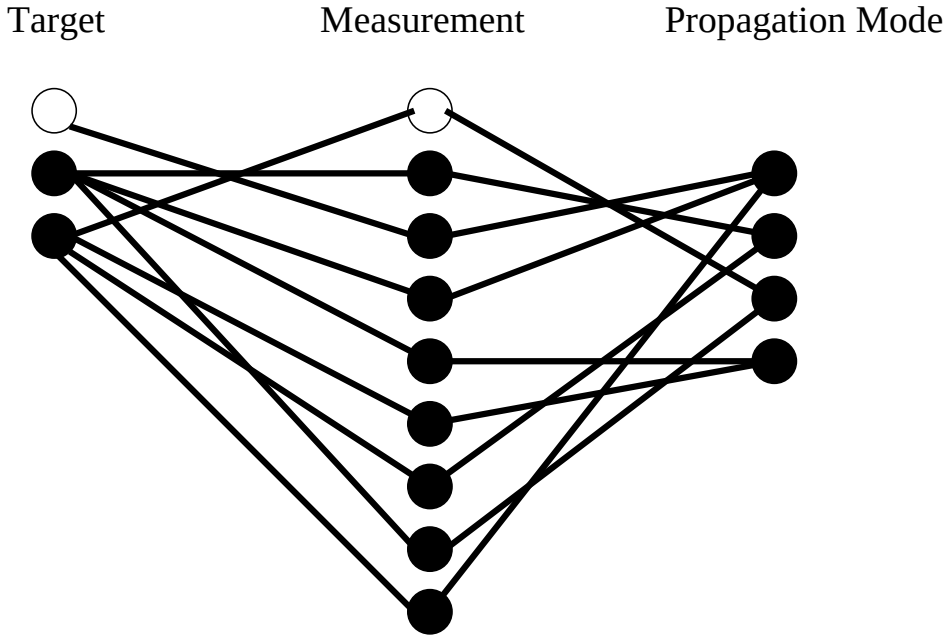

Figure 4.3: Multipath uncertainty in assignment tree.

4.4 Data Association based on Multiframe Assignment

Tracking multiple targets in noisy measurements of the target together with spurious observations created by the background noise and clutter has been studied for many years (46). Data association problem becomes more difficult to handle when multiple targets compete for measurements. Identification of which measurement belongs to which target is the conventional data association problem. However, in this work, the complexity of the problem

is increased in such a way that the the measurements compete for target and the multipath distinct propagation mode. The multipath signal propagation mode measurements add more complexity to the data association problem.

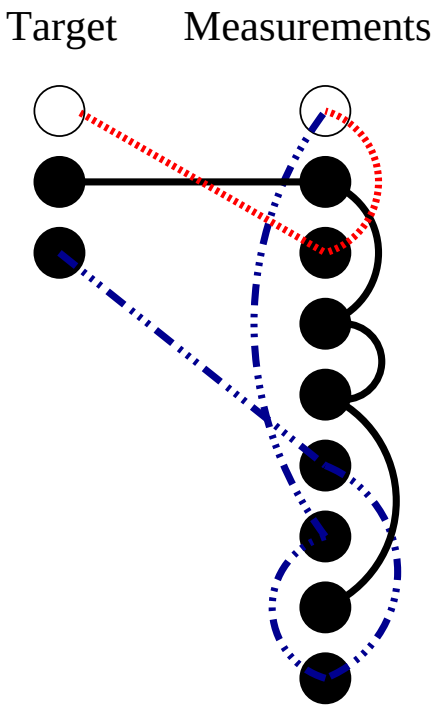

Figure 4.4: Assignment tree of multipath model.

4.4.1 Formulation of the MSD Problem and Solution Technique

At a time step k, data association based on multipath multiframe assignment where a single sensor measurements in the last scan with $(S-1)$ multiple modes are associated with the list of established tracks (S lists - S-dimensional association, denoted as S-D). Every possible $S-$ tuple is assigned a cost $C(k|\chi(k))$. When we have r number of sensors and considering $\mathbb{N}_{S-1}$ number of distinct propagation modes, then the multipath multiframe data association problem will be an $r \times \mathbb{N}_{S-1} + 1$ dimensional problem (i.e., $S = r \times \mathbb{N}_{S-1} + 1$).

In order to associate the existing measurements to each reflection path mode and each target, every sensor measurements are stacked to the number of distinct propagation modes times (i.e., $\mathbb{N}_{S-1}$ times), and an association is found in such a way that it minimizes the total cost. In this current work, we assume that there is only one sensor ($r = 1$) and $\mathbb{N}_{S-1} = S-1$ (i.e., there is $S-1$ number of distinct propagation modes ($i = 1, 2, ..., \mathbb{N}_{S-1}$). In order to formulate the multipath S-D problem, we formulate the assignment tree diagrams as shown in Figure 4.3 and Figure 4.4. Since the assignment tree diagram in Figure 4.4 is too complicated to understand and solve, we draw an equivalent assignment tree diagram as shown in Figure 4.5. We stack the same sensor measurement to the number of distinct propagation modes times as shown in Figure 4.5. The objective is to detect and track an unknown number of targets by estimating their positions using the $S-1$ lists of stacked measurements. The sensor provides scans of detected and resolved signals at a discrete time step $k = 1, 2, ..., K$. With each detection, there is an associated measurement of bearing and bistatic range by direct signal or multipath range by multipath reflected signal. For every multipath S-D problem, $\mathbb{N}_{S-1}$ lists of stacked measurements are associated with established tracks, and each stacked measurement list has $n_{\mathbb{N}}$ (the number of sensors $\mathbb{N} = 1, 2, ..., r$ measurements at time k. In this case, the stacked measurement list has n_1 (as we consider one sensor) measurements. It is assumed that the sensor has a known nonunity detection probability P_D.

A likelihood ratio test that involves the target state estimate for the candidate associations is used to assign cost to each feasible $S-$ tuple of measurements, i.e., candidate association, and then S-D is used to minimize the cost globally. The measurement $\mathbf{z}_{ij_i}$, $j_i = 1, 2, ...n_{\mathbb{N}_{S-1}}$($\mathbf{z}_{1j_1}$ and $j_1 = 1, 2, ...n_1$ in our case as the number of sensors are 1). A target may not be detected at every scan. For the simplification of the notation for incomplete measurement to target association occurred by miss-detection from the direct or multipath reflected signal, a dummy measurement $\mathbf{z}_{i0}$ is added to each list. A dummy measurement

from multipath reflection propagation mode measurement list $\mathbb{N}_{S-1}$ assigned to target p implies that this target was not detected by the sensor r (i.e., in this case $r = 1$). That is, it can be a miss-detection from the direct signal propagation mode, or a miss-detection from the multipath reflection propagation modes. The likelihood that an $r \times \mathbb{N}_{S-1}$- tuple of measurements $Z_{i_1 j_2 j_3 \cdots j_{\mathbb{N}_{S-1}}}$, originated from target p, with the known state $\mathbf{x}_p$ at a time step k, is the joint pdf:

$$\Lambda(Z_{j_1 j_2 j_3 \cdots j_{\mathbb{N}_{S-1}}}|p) = \prod_{i=1}^{r \times \mathbb{N}_{S-1}} \left\{ [1 - P_D]^{1-u(j_i)} [P_D p(\mathbf{z}_{ij_i}|\mathbf{x}_p)]^{u(j_i)} \right\} \tag{4.15}$$

where $u(j_i)$ is an indicator function. That is

$$u(j_i) = \begin{cases} 0 & \text{if } j_i = 0 \\ 1 & \text{otherwise} \end{cases} \tag{4.16}$$

The likelihood that the measurements are all spurious or irrelevant to this target (i.e., $p = 0$) is given by

$$\Lambda(Z_{j_1 j_2 j_3 \cdots j_{\mathbb{N}_{S-1}}}|p = 0) = \prod_{i=1}^{r \times \mathbb{N}_{S-1}} \left[\frac{1}{\Psi_i} \right]^{u(j_i)} \tag{4.17}$$

where Ψ_i is the false alarm probability in a cell multiplied by the volume of the resolution cell.

The cost of associating the $r \times \mathbb{N}_{S-1}$ ($r = 1$ in our case) tuple to target p is given by the negative log-likelihood ratio.

$$c_{j_1 j_2 j_3 \cdots j_{\mathbb{N}_{S-1}}} = -\ln \frac{\Lambda(Z_{j_1 j_2 j_3 \cdots j_{\mathbb{N}_{S-1}}}|p)}{\Lambda(Z_{j_1 j_2 j_3 \cdots j_{\mathbb{N}_{S-1}}}|p = 0)} \tag{4.18}$$

However, $\mathbf{x}_p$ is unknown in Eq. (4.15) therefore, will be replaced by its ML estimate and is given by

$$\hat{\mathbf{x}}_p = \arg\max_{\mathbf{x}_p} \Lambda(Z_{j_1 j_2 j_3 \ldots j_{\mathbb{N}_{S-1}}} | p) \tag{4.19}$$

Therefore (4.18) becomes a generalized likelihood ratio. Hence, we get the cost of the candidate association of the $\mathbb{N}_{S-1}$ tuple of measurements $(j_1, j_2, j_3, ..., j_{\mathbb{N}_{S-1}})$ to a target is

$$\begin{aligned} c_{j_1 j_2 j_3 \ldots j_{\mathbb{N}_{S-1}}} = \sum_{i=1}^{\mathbb{N}_{S-1}} \Bigg\{ & [u(j_i) - 1] \ln(1 - P_D) - u(j_i) \ln \left(\frac{P_D \Psi_i}{|2\Pi\Sigma_i|^{\frac{1}{2}}} \right) + \\ & u(j_i) \left(\frac{1}{2} [\mathbf{z}_{ij_i} - H(\hat{\mathbf{x}}_p, \mathbf{y}_{ij_i})]^T \Sigma_i^{-1} [\mathbf{z}_{ij_i} - H(\hat{\mathbf{x}}_p, \mathbf{y}_{ij_i})] \right) \Bigg\} \end{aligned} \tag{4.20}$$

The objective is to find the most likely set of $\mathbb{N}_{S-1}$ - tuples such that each measurement is assigned to unique one target one propagation mode combined pair, or declared false, and each target receives at most one measurement from each list for every propagation mode, or declared false, and each target receives at most one measurement from each stacked list and not the corresponding same measurement is used in the other stacked list. That is, the same corresponding measurement from the other stacked list should not be arranged to any target. This can be reformulated as the following assignment problem.

The multipath multidimensional assignment problem is a constraint optimization problem. The solution to the problem is to associate the measurements to appropriate targets and the multipath propagation modes. In order to find the appropriate assignment to the existing targets, an assignment variable $\chi_t^{(j,i)}(k)$ can be defined in such a way that it can take either 0 or 1 depending on the different constraints and scenarios. It can be defined in the following way

$$\chi_t^{(j,i)}(k) = \begin{cases} 1 & \text{if the measurement } z_{ij_i}(k) \text{ is assigned to a track } \mathfrak{t}^t(k-1) \\ & \text{and the multipath model } i \\ 0 & \text{otherwise} \end{cases} \tag{4.21}$$

The constraints can be defined as given below.

$$\sum_{j=0}^{n_{\mathbb{N}_{S-1}}} \chi_t^{(j,i)}(k) = 1 \tag{4.22}$$

where $t = 1, 2, ...T$ and $i = 1, 2, ...\mathbb{N}_{S-1}$

The target and multipath mode uncertainty constraints can be written as

$$\sum_{t=0}^{T} \chi_t^{(j,i)}(k) = 1 \tag{4.23}$$

where $j = 1, 2, ...n_{\mathbb{N}_{S-1}}$ and $i = 1, 2, ...\mathbb{N}_{S-1}$

$$\sum_{i=1}^{\mathbb{N}_{S-1}} \chi_t^{(j,i)}(k) = 1 \tag{4.24}$$

where $j = 1, 2, ...n_{\mathbb{N}_{S-1}}$ and $t = 1, 2, ...T$

The above last two constraints can be combined as given below.

$$\sum_{i=1}^{\mathbb{N}_{S-1}} \sum_{t=0}^{T} \chi_t^{(j,i)}(k) \quad = \quad 1 \tag{4.25}$$

where $j = 1, 2, ...n_{\mathbb{N}_{S-1}}$.

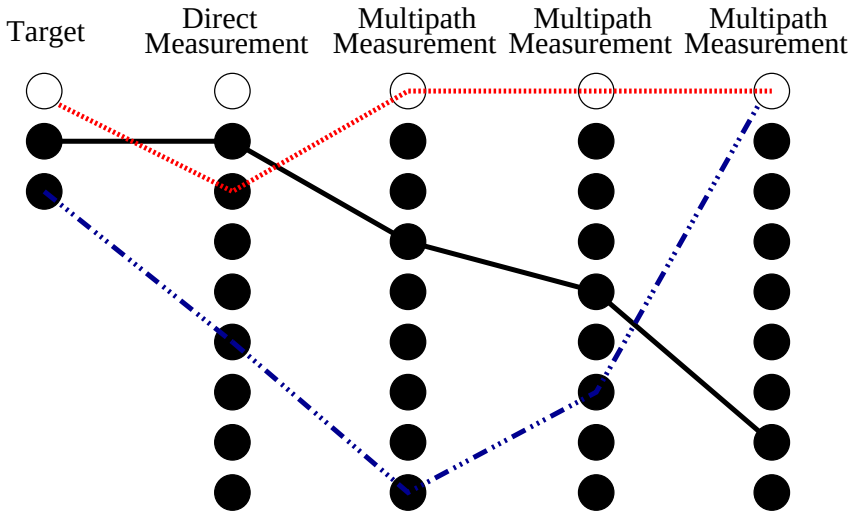

Figure 4.5: Multipath model assignment tree by stacking the same measurement.

Since we assume that all the signal propagation modes are known, there is no dummy propagation path mode. But since there are miss-detections, we have dummy targets and dummy measurements in our problem. Now the solution for the problem is to find the optimal assignment $\chi^{\mathbf{opt}}(k)$ that minimizes the global cost of assignment.

$$C(k|\chi(k)) \quad = \quad \sum_{j=0}^{n_{\mathbb{N}_{S-1}}} \sum_{i=1}^{\mathbb{N}_{S-1}} \sum_{t=0}^{T} \chi_t^{(j,i)}(k)\ \psi_t^{(j,i)}(k) \tag{4.26}$$

where $\psi_t^{(j,i)}(k)$ is the appropriate cost assignment of $\chi_t^{(j,i)}(k)$.

The above objective function can give a suboptimal solution if $\psi_t^{(j,i)}(k)$ are calculated

independently of any other measurements that can be associated to the same target. To find the optimal cost, the following equation is used:

Minimize:

$$C(k|\chi(k)) = \sum_{t=0}^{T} \sum_{j_1=0}^{n_{\mathbb{N}_{S-1}}} \sum_{j_2=0}^{\mathbb{N}_{S-1}} \ldots \sum_{j_i=\mathbb{N}_{S-1}}^{\mathbb{N}_{S-1}} \varphi_t^{(j_i)i=1\ldots\mathbb{N}_{S-1}}(k)\psi_t^{(j_i)_{i=1\ldots\mathbb{N}_{S-1}}}(k) \quad (4.27)$$

where $\varphi_t^{(j_i)i=1..\mathbb{N}_{S-1}}(k)$ is the assignment variable and $\mathbb{N}_{S-1}$ is the total number of multipath target originated signal propagation mode. We need to find the optimal assignment tree by satisfying the following constraints.

Subject to:

$$\sum_{t=0}^{T}\sum_{j_2=0}^{n_{\mathbb{N}_{S-1}}}\sum_{j_3=0}^{n_{\mathbb{N}_{S-1}}}\sum_{j_4=0}^{n_{\mathbb{N}_{S-1}}}\cdots\sum_{j_{\mathbb{N}_{S-1}-1}=0}^{n_{\mathbb{N}_{S-1}}}\sum_{j_{\mathbb{N}_{S-1}}=0}^{n_{\mathbb{N}_{S-1}}}\varphi_t^{(j_i)i=1..\mathbb{N}_{S-1}}(k) = 1,\ j_1=1,2,...,n_{\mathbb{N}_{S-1}} \tag{4.28}$$

$$\sum_{t=0}^{T}\sum_{j_1=0}^{n_{\mathbb{N}_{S-1}}}\sum_{j_3=0}^{n_{\mathbb{N}_{S-1}}}\sum_{j_4=0}^{n_{\mathbb{N}_{S-1}}}\cdots\sum_{j_{\mathbb{N}_{S-1}-1}=0}^{n_{\mathbb{N}_{S-1}}}\sum_{j_{\mathbb{N}_{S-1}}=0}^{n_{\mathbb{N}_{S-1}}}\varphi_t^{(j_i)i=1..\mathbb{N}_{S-1}}(k) = 1,\ j_2=1,2,...,n_{\mathbb{N}_{S-1}} \tag{4.29}$$

.

.

$$\sum_{t=0}^{T}\sum_{j_1=0}^{n_{\mathbb{N}_{S-1}}}\sum_{j_2=0}^{n_{\mathbb{N}_{S-1}}}\sum_{j_3=0}^{n_{\mathbb{N}_{S-1}}}\cdots\sum_{j_{\mathbb{N}_{S-1}-2}=0}^{n_{\mathbb{N}_{S-1}}}\sum_{j_{\mathbb{N}_{S-1}}=0}^{n_{\mathbb{N}_{S-1}}}\varphi_t^{(j_i)i=1..\mathbb{N}_{S-1}}(k) = 1,\ j_{\mathbb{N}_{S-1}-1}=1,2,...,n_{\mathbb{N}_{S-1}} \tag{4.30}$$

$$\sum_{t=0}^{T}\sum_{j_1=0}^{n_{\mathbb{N}_{S-1}}}\sum_{j_2=0}^{n_{\mathbb{N}_{S-1}}}\sum_{j_3=0}^{n_{\mathbb{N}_{S-1}}}\cdots\sum_{j_{\mathbb{N}_{S-1}-2}=0}^{n_{\mathbb{N}_{S-1}}}\sum_{j_{\mathbb{N}_{S-1}-1}=0}^{n_{\mathbb{N}_{S-1}}}\varphi_t^{(j_i)i=1..\mathbb{N}_{S-1}}(k) = 1,\ j_{\mathbb{N}_{S-1}}=1,2,...,n_{\mathbb{N}_{S-1}} \tag{4.31}$$

where $\{\varphi_t^{(j_i)i=1..\mathbb{N}_{S-1}}(k)\}$ are binary association variables such that $\{\varphi_t^{(j_i)i=1..\mathbb{N}_{S-1}}(k)\} =$ 1 if $\mathbb{N}_{S-1}$ tuple $Z_{j_1 j_2 j_3 \cdots j_{\mathbb{N}_{S-1}}}$ is associate with a candidate target.

Its value is equal to zero otherwise. The same measurement cannot be associated with itself. Hence,

$$\varphi_t^{(j_i)i=1..\mathbb{N}_{S-1}}(k) = 0 \text{ if } j_p = j_q, \forall\ p \neq q, \text{ and } p,q \in \{1,2,...,n_{\mathbb{N}_{S-1}}\} \tag{4.32}$$

$$\sum_{t=0}^{T}\sum_{j_1=0}^{n_{\mathbb{N}_{S-1}}}\sum_{j_2=0}^{n_{\mathbb{N}_{S-1}}}\sum_{j_3=0}^{n_{\mathbb{N}_{S-1}}}\cdots\sum_{j_{\mathbb{N}_{S-1}-1}=0}^{n_{\mathbb{N}_{S-1}}}\sum_{j_{\mathbb{N}_{S-1}}=0}^{n_{\mathbb{N}_{S-1}}}\varphi_t^{(j_i)i=1..\mathbb{N}_{S-1}}(k)\times\left(j_1\text{or}j_2\text{or}j_3\text{or}...\text{or}j_{n_{\mathbb{N}_{S-1}}}==j\right) = 1, \tag{4.33}$$

where $j = 1, 2, ..., n_{\mathbb{N}_{S-1}}$.

This multipath multiframe assignment problem is formulated similar to a generalized S-D problem. Therefore, we solve the multipath multiframe assignment problem as a series of relaxed 2-D subproblems in two phases such as constraint relaxation phase and the multiplier update and constraint enforcement phase (46).

4.5 Simulation and Results

In the simulation, parameter setting are: transmitter position = [49925, -10899]m; receiver position = [0, 0]m; the reflection point = [30000, 5000]m; the measurement interval is 1 second; measurement variances $\sigma_r^2 = 10$ m^2 and $\sigma_\theta^2 = 0.0001$ radians^2; probability of detection is 0.98; 10 false alarms at each sampling. The target trajectories, transmitter and receiver locations are given in Figures 4.6 and 4.7. There are two targets in the surveillance region, one enters the region at $k = 3$ and the other enters at $k = 6$.

Figures 4.6 and 4.7 show the S-D association comparison of the tracking by considering and not considering the multipath reflection model. In both cases S-D association and multipath S-D association are used.

Figure 4.6 shows that when the multipath measurements are available and if they are not utilized within the tracker, then there are spurious tracks formed.

But Figure 4.7 shows that with a correct propagation mode assumption, integrating multipath information into the tracker can help improve the accuracy of tracking and reduce

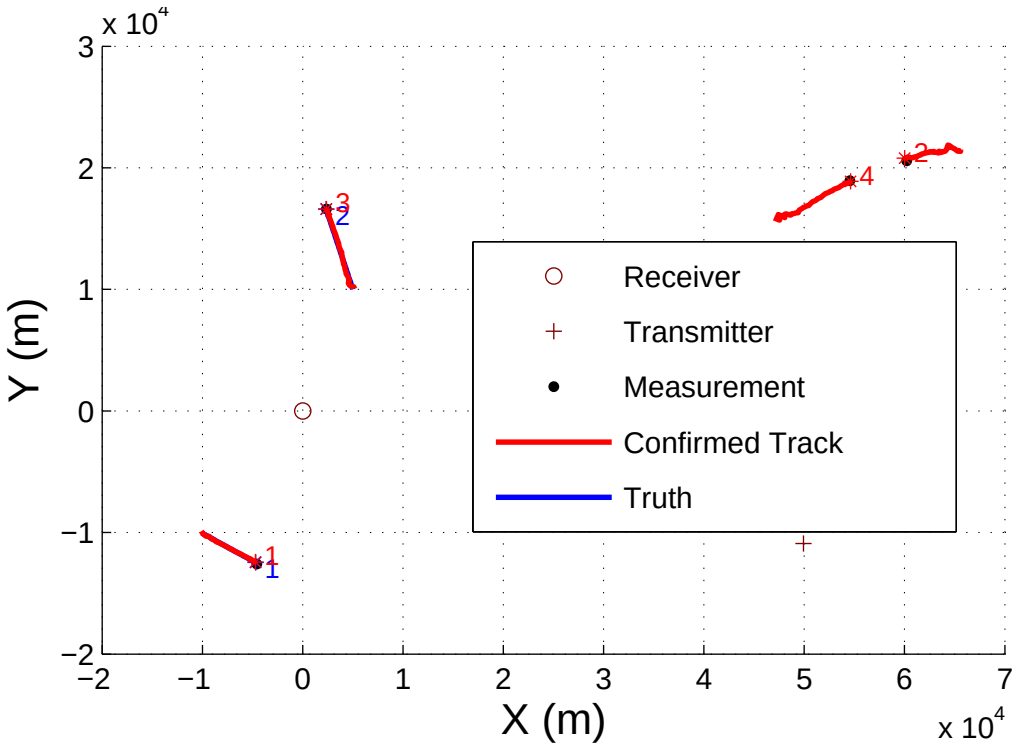

Figure 4.6: Estimated target tracks without incorporating multipath.

the number of false tracks.

The root mean square error (RMSE) values are compared in Figure 4.8 or Figure 4.9. The RMSE values are lower for fused tracks that were obtained through multipath multi-frame assignment technique. It shows that the multipath S-D association based tracking algorithm converges as the RMSE goes lower over the time. The RMSE curves show that multipath S-D association filter outperform when the multipath reflection modes information is incorporated in tracking.

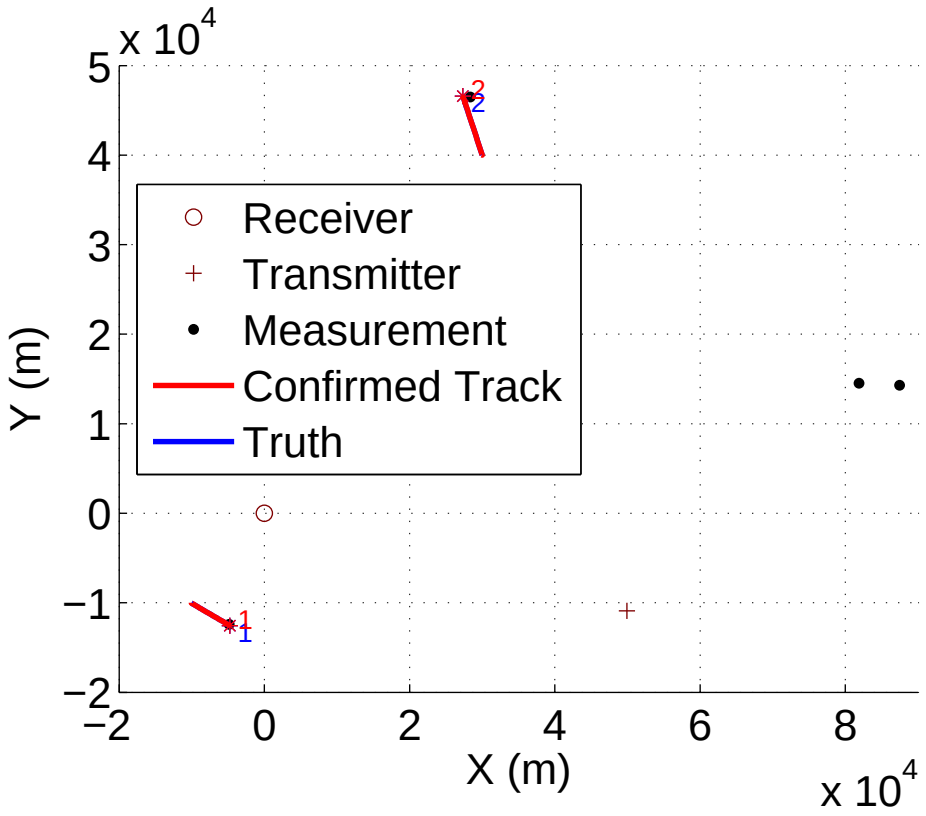

Figure 4.7: Estimated target tracks with incorporating multipath.

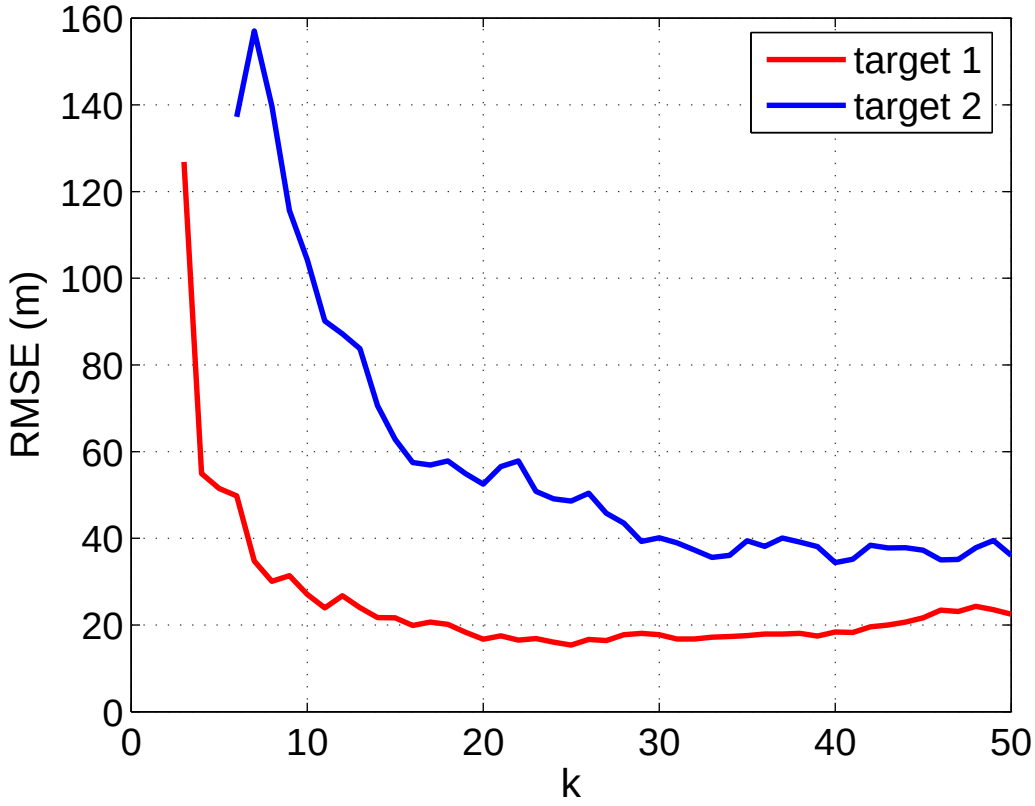

Figure 4.8: RMSE values without incorporating multipath.

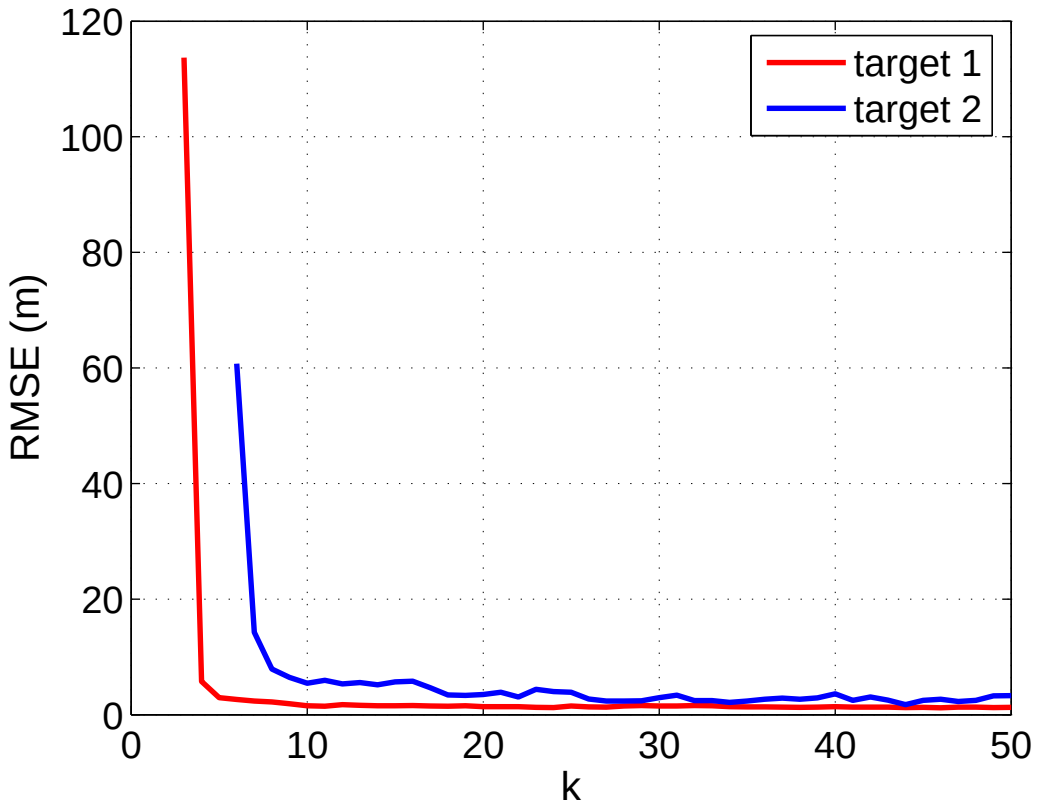

Figure 4.9: RMSE values with incorporating multipath.

Chapter 5

Multipath Assisted Multitarget Tracking with Reflection Point Uncertainty

In this chapter, the previous work multipath-assisted multitarget tracking using multiframe assignment is extended to the case where there are uncertainties in multipath reflection points at the receiver. An algorithm is proposed for initiating and tracking multiple targets using multiple transmitters and receivers. This algorithm is capable of exploiting multipath target returns from distinct and unknown propagation modes. When multipath returns are not utilized appropriately within the tracker, (e.g., discarded as clutter or incorporated with incorrect propagation mode assumption) the potential information in the multipath returns is lost. In real scenarios, it is more appropriate to assume that the locations of the reflection points/surfaces are not accurately known.

Integrating multipath information into the tracker by correctly identifying the multipath mode and identifying the reflection point can help improve the accuracy of tracking. The

challenge in improving tracking results using multipath measurements is the fusion of direct and multipath measurements from the common target when the multipath-reflection mode is unknown. The problem becomes even more challenging with false alarms and missed detections. We propose an algorithm to track the target with uncertainty in multipath reflection points/surface using the multiframe assignment technique. Simulation results are presented to show the effectiveness of the proposed algorithm on a ground target tracking problem.

In the previous chapter, the multipath-assisted multitarget tracking using multiframe assignment was studied. An algorithm was proposed for initiating and tracking multiple targets using multiple transmitters and receivers. This algorithm is capable of exploiting multipath target returns from distinct and unknown propagation modes. When multipath returns are not utilized appropriately within the tracker, (e.g., discarded as clutter or incorporated with incorrect propagation mode assumption) the potential information in the multipath returns is lost. In the previous work the multipath reflection points are known to the receiver. In real scenarios, it is more appropriate to assume that the locations of reflection points are not exactly known. In this chapter, the proposed algorithm will track the targets when there are uncertainties in the multipath reflection surface parameters.

This chapter mainly focuses on formulating the multipath tracking problem with reflection points or surface uncertainties for ground or airborne targets and deriving an assignment based data association filter. In this chapter, errors in bearing and uncertainties in reflection surface's angle and distance from the sensor are incorporated in measurements and tracking capabilities are analyzed.

5.1 Multipath Reflection Surface Uncertainty

When multipath target returns from distinct propagation modes are resolved, spurious tracks are formed. Associating these signals facilitate better estimates of the target states. However, in order to use these measurements, appropriate association of multipath reflection models have to be identified. Incorrect reflection model assignment will lead to errors in association and tracking.

Hence, to utilize these measurements appropriately, it is important to have the measurements resolved appropriately in multipath propagation mode assignment. Multipath signal propagation mode assignment uncertainty adds another level of complexity to the standard data association problem. This problem was solved in the previous chapter. In the previous chapter, the association uncertainties were in the measurement-to-target association and in the measurement-to-multipath propagation mode association. In typical scenarios, it is more appropriate to assume that the reflection surface parameters are not accurately known (i.e.,there are uncertainties associated with reflection surface parameters). Therefore, in this work we considered the case where there are uncertainties associated with reflection surface parameters. Hence, in such situations tracking is performed when the reflection points are unknown.

5.1.1 System Model

Since the reflection surface parameters are not accurately known, another level of uncertainty is added to the existing problem. In this model, we assume that the reflection surface is smooth and can be described by a line $y = mx + c$ in the tracking plane, where $m = (m' + e_{m'}), c = (c' + e_{c'})$. Here $e_{m'}$ and $e_{c'}$ are the error covariance of m' and c' added in the form of uncertainties. That is, the reflection surface's geometry is not accurately known to the receiver in this system model as described in Figure 5.1.

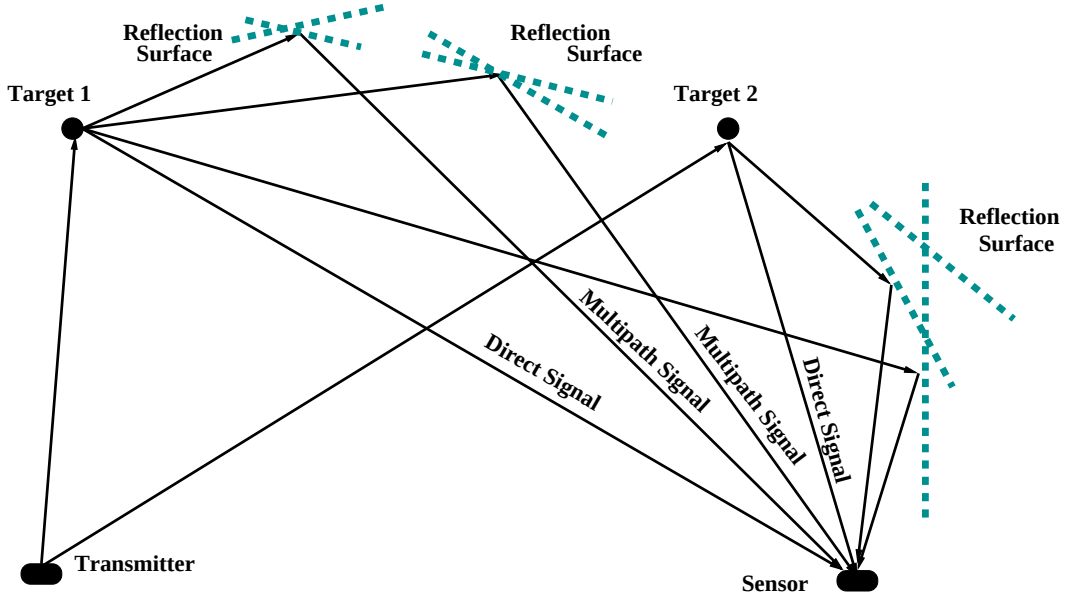

Figure 5.1: Uncertainty in reflection surface parameters.

When considering the target tracking with reflection surface uncertainty, it is also important to make assumptions on reflection scenarios. Figure 5.2 shows that the signals directly hit the target first, and then the target returns are received by the sensors directly and through the multipath reflections.

Figure 5.3 shows that the signals reflected at the wall first before hitting the target. Then the target returns are received by the sensor through direct and multipath propagation modes.

Figure 5.4 shows that the signals reflect at different walls first before hitting the target. Then the target returns are received by the sensor through direct and multipath propagation modes.

Figure 5.5 shows that the signals reflect at different walls and or clutter and received by sensor. These signals are non-target returns. The Doppler shift measurements can be used to differentiate the target originated returns from clutter.

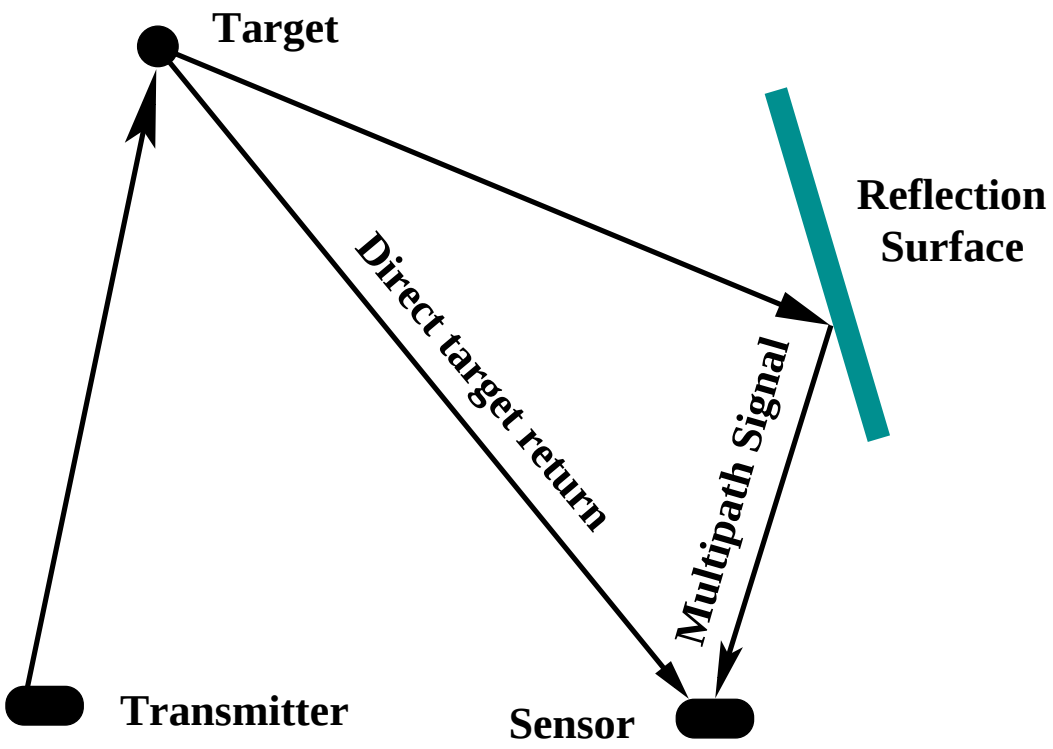

Figure 5.2: Multipath reflection scenarios: Transmitter-target.

Figure 5.6 shows a complex target reflection scenario. The sensor receives more complex signals such as Transmitter-Target-Sensor, Transmitter-Target-Multiple Walls-Sensor, Transmitter-Multiple Walls-Target-Sensor and Transmitter-Multiple Walls-Target-Multiple Walls-Sensor.

Figure 5.7 shows the scenario of complex multipath target returns from another target return signal.

In this model $(x(k), y(k))$ denotes the moving target position at time step k. It is assumed that the sensor and the transmitter locations are known and they are denoted by $(x_r(k), y_r(k))$ and $(x_t(k), y_t(k))$, respectively. The reflection model index is denoted by rs. Based on the reflection surface information, using ray optics geometry, the reflection points can be evaluated. The reflection point coordinate $(x_{rs}(k), y_{rs}(k))$ denotes the reflection point at k^{th} time step in rs^{th} multipath reflection model (reflection surface). For simplicity,

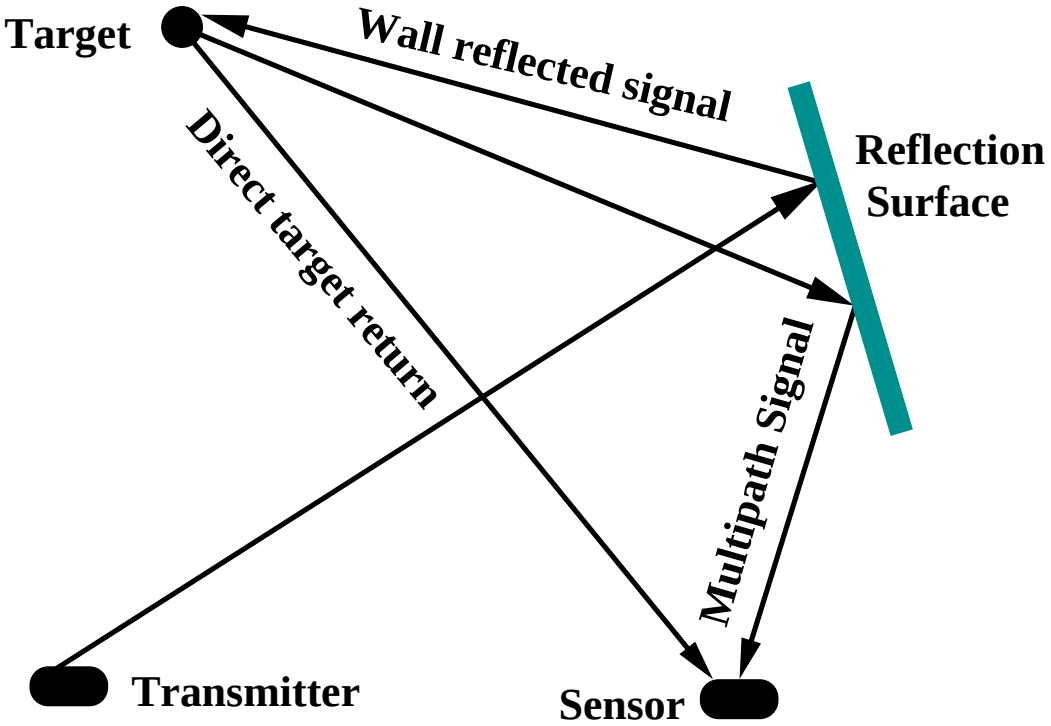

Figure 5.3: Multipath reflection scenarios: Transmitter-wall-target.

it is assumed that the received signals are either direct signal from the target or target reflected signals with one reflection at the reflection surface rs before it arrives the sensor.

Key Assumptions and Scenario Description

- Transmitter is located on the axis of the receiver, and the motion of the target is in the same plane.
- The distance between the transmitter and receiver is large enough to satisfy the bistatic range ellipse and multipath range ellipse as these are along the transverse diameter.
- In addition to the direct signal detection, the sensor measurements contain resolved multipath detections.

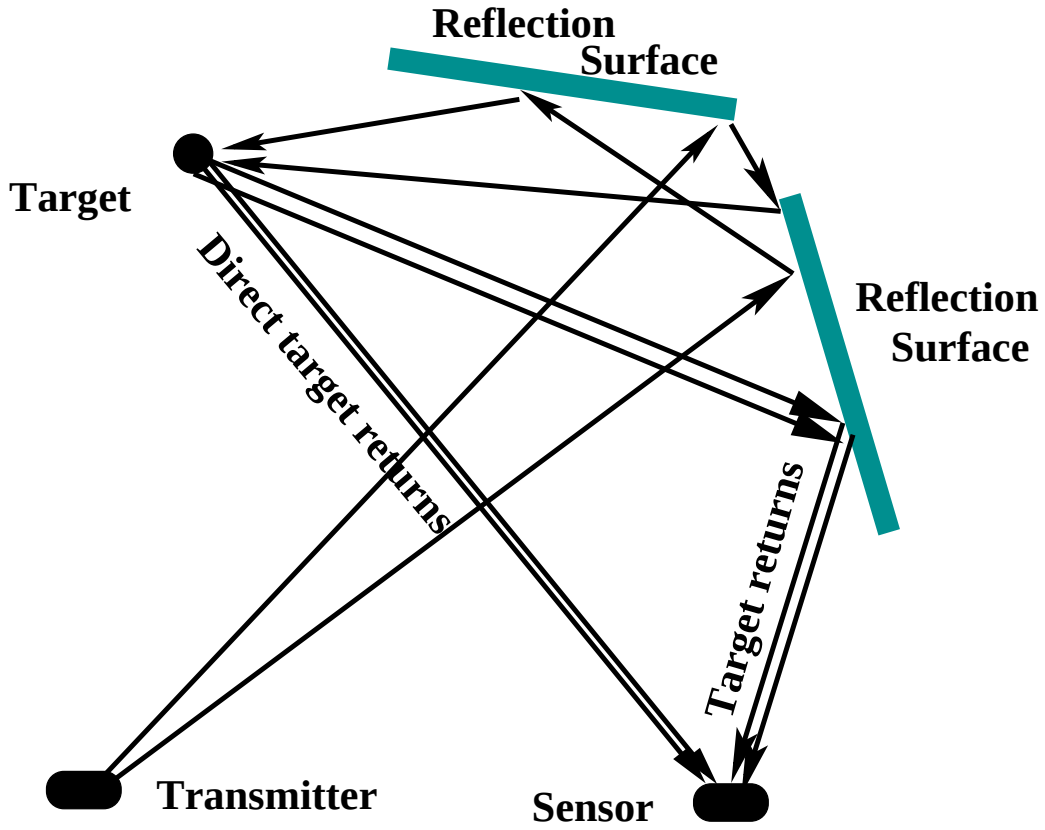

Figure 5.4: Multipath reflection scenarios: Multiple wall reflections.

- The reflections on the surface/wall are smooth and abide by the ray optical geometry principles.
- Uncertainties in the knowledge of the reflection surface parameters are known by its covariance. i.e., m' or the slope α and the intersect c' and their covariances are known.
- It is assumed that m' and c' are statistically independent, uniformly distributed with mean 0 and covariances of $\sigma^2_{m'}$ and $\sigma^2_{c'}$ respectively.

The measurements are bistatic range $r_d(k)$, multipath range $r_m(k)$, bearing from direct signal $\theta_d(k)$ and multipath reflected signal $\theta_m(k)$. The measurement equations are given below. At a given time step k, the bistatic range measurement from the direct target return

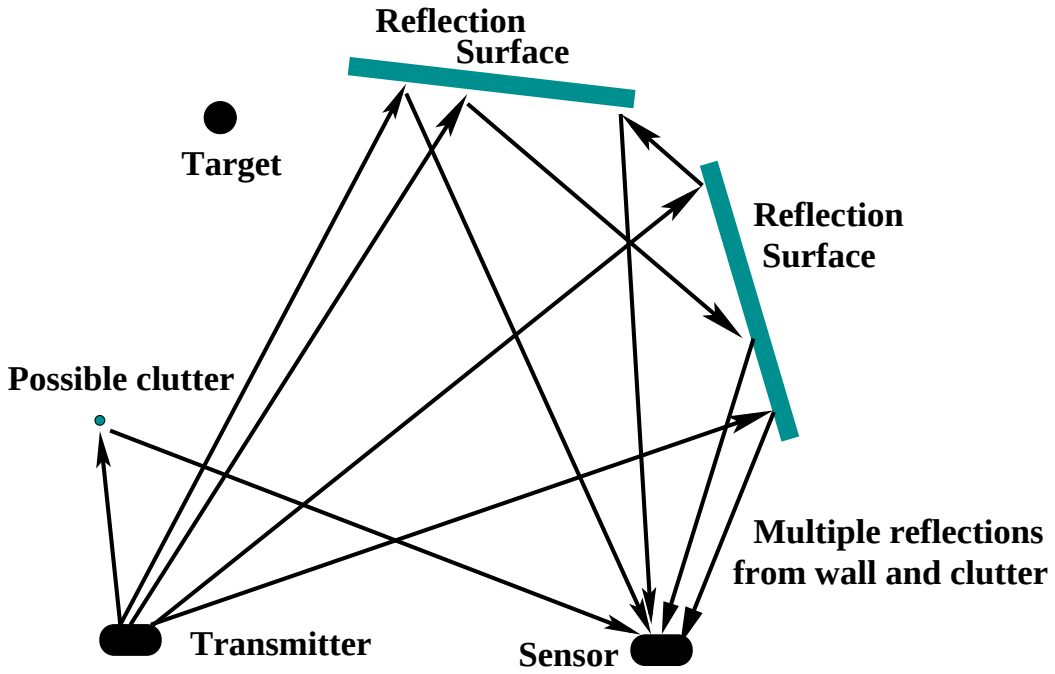

Figure 5.5: Multipath reflection scenarios: Non-target returns.

can be given by,

$$\begin{aligned} r_d(k) &= \left(\sqrt{(x(k)-x_t(k))^2+(y(k)-y_t(k))^2}\right)+ \\ &\quad \left(\sqrt{(x(k)-x_r(k))^2+(y(k)-y_r(k))^2}\right)+ \\ &\quad -\left(\sqrt{(x_t(k)-x_r(k))^2+(y_t(k)-y_r(k))^2}\right)+\omega_\tau(k) \end{aligned} \tag{5.1}$$

The DOA of the signal received directly from the target is given by

$$\theta_d(k) = \tan^{-1}\left[\frac{(y(k)-y_r(k))}{(x(k)-x_r(k))}\right]+\omega_\theta(k) \tag{5.2}$$

In the above case, no multipath reflection occur between the target and the sensor in the signal propagation path. When there are reflection between target and the sensor, the multipath range measurement can be given by

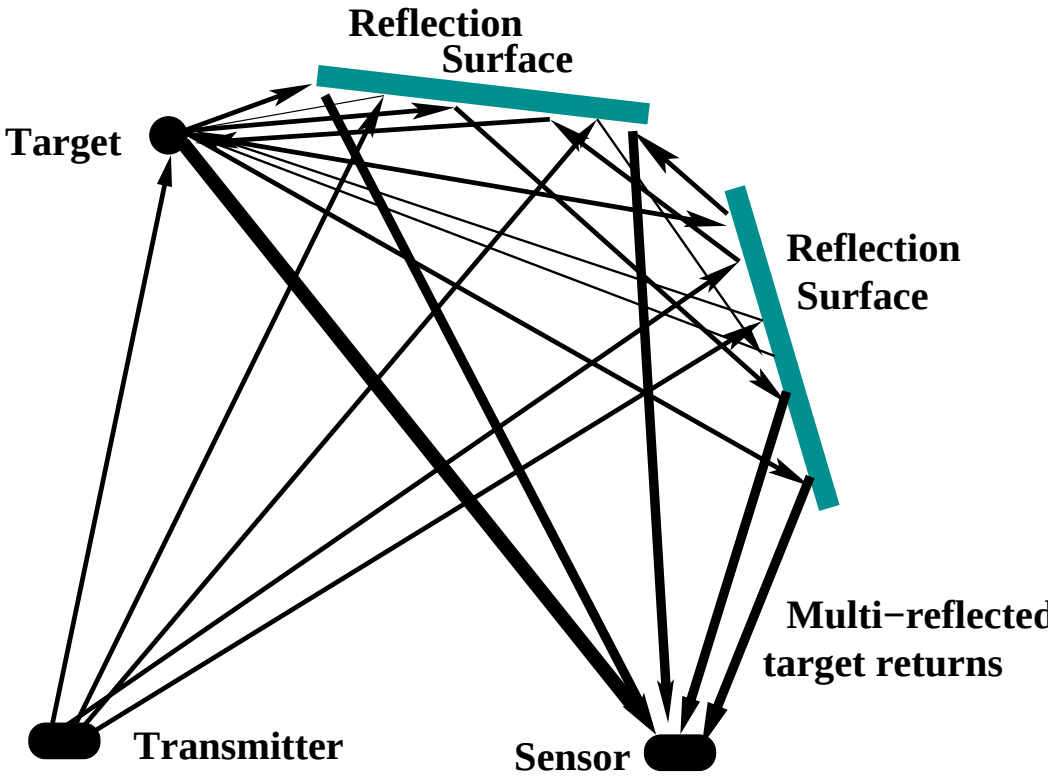

Figure 5.6: Multipath reflection scenarios: Complex reflections.

$$\begin{aligned} r_m(k) &= \left(\sqrt{(x(k)-x_t(k))^2+(y(k)-y_t(k))^2}\right)+\left(\sqrt{(x_{rs}(k)-x(k))^2+(y_{rs}(k)-y(k))^2}\right)+ \\ &+\left(\sqrt{(x_{rs}(k)-x_r(k))^2+(y_{rs}(k)-y_r(k))^2}\right)+ \\ &-\left(\sqrt{(x_t(k)-x_r(k))^2+(y_t(k)-y_r(k))^2}\right)+\omega_m(k) \end{aligned} \tag{5.3}$$

In this case, the DOA of the signal received by the sensor after reflected from a point on the reflection surface is given by

$$\theta_m(k) = \tan^{-1}\left[\frac{(y_{rs}(k)-y_r(k))}{(x_{rs}(k)-x_r(k))}\right]+\omega_\theta(k) \tag{5.4}$$

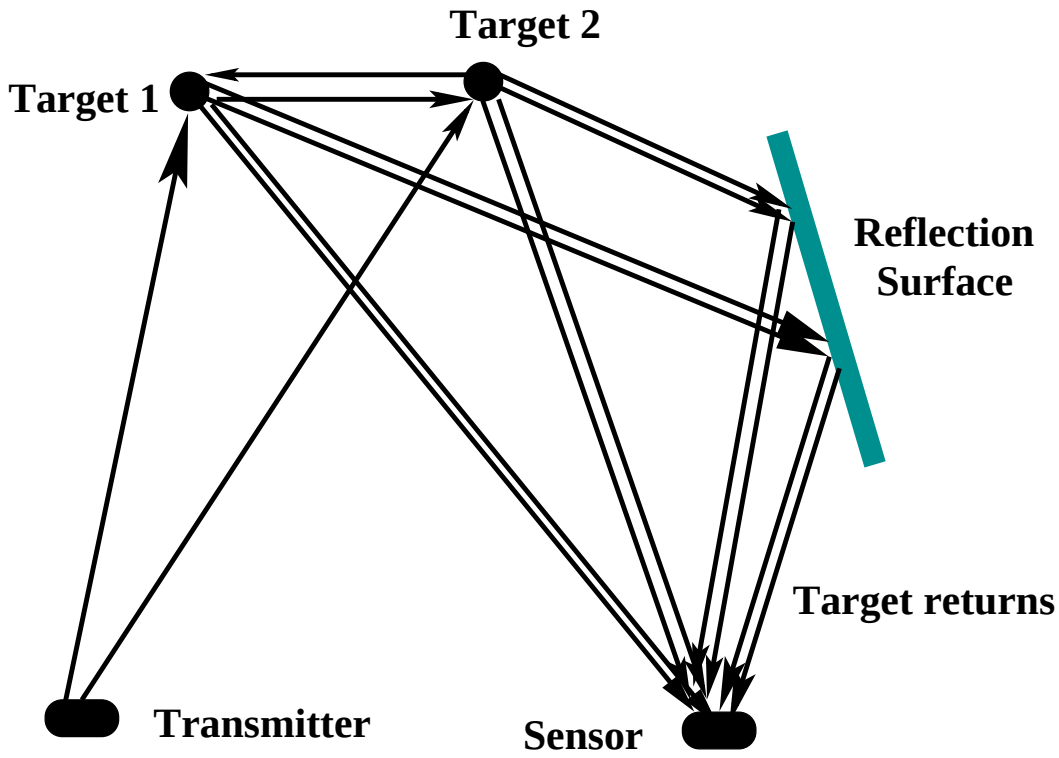

Figure 5.7: Multipath reflection scenarios: Target return reflections.

The measurement after two reflection between the target and the sensor can be given by

$$\begin{aligned} r_m(k) &= \left(\sqrt{(x(k)-x_t(k))^2+(y(k)-y_t(k))^2}\right)+ \\ &+\left(\sqrt{(x_{rs_1}(k)-x(k))^2+(y_{rs_1}(k)-y(k))^2}\right)+ \\ &+\left(\sqrt{(x_{rs_1}(k)-x_{rs_2}(k))^2+(y_{rs_1}(k)-y_{rs_2}(k))^2}\right)+ \\ &+\left(\sqrt{(x_{rs_2}(k)-x_r(k))^2+(y_{rs_2}(k)-y_r(k))^2}\right)+ \\ &-\left(\sqrt{(x_t(k)-x_r(k))^2+(y_t(k)-y_r(k))^2}\right)+ \\ &+\omega_m(k) \end{aligned} \tag{5.5}$$

The DOA signal received after two multipath reflection from the target is given by

$$\theta(k) = \tan^{-1}\left[\frac{(y_{rs_2}(k) - y_r(k))}{(x_{rs_2}(k) - x_r(k))}\right] + \omega_\theta(k) \tag{5.6}$$

Depends on the reflection scenario assumptions, the appropriate range and DOA measurement equations will be driven. The measurement $z(k)$ can be given by the following equation.

$$z(k) \quad = \quad \begin{bmatrix} r(k) \\ \theta(k) \end{bmatrix} \tag{5.7}$$

where $r(k) = r_d(k)$ and $\theta(k) = \theta_d(k)$ when the target return signal propagation mode is direct and $r(k) = r_m(k)$ and $\theta(k) = \theta_m(k)$ when the target return signal propagation mode is multipath.

5.2 Multipath Reflections on Smooth Surface

Figure 5.2 shows a simple multipath reflection scenarios. Based on the ray optical geometry, the reflection points $(x_{rs}(k), y_{rs}(k))$ on the reflection surface is evaluated when the reflection surface information and their covariances are known. Considering a smooth reflecting surface defined by $y = mx + c$ as shown in Figure 5.2. Figure 5.2 also shows the ray reflection path geometry where $(\frac{\pi}{2} - \phi)$ is the incident angle on the smooth surface, $\theta_m(k)$ is the DOA of the wall-reflected signal at the receiver at $(x_r(k), y_r(k))$, and $\theta_m^{rs}(k)$ is the direction of arrival angle at the reflection point. Then the reflection points $(x_{rs}(k), y_{rs}(k))$ on the reflection wall or surface can be defined by the following way.

Figure 5.2 shows a simple multipath reflection scenario where the sensor receives a

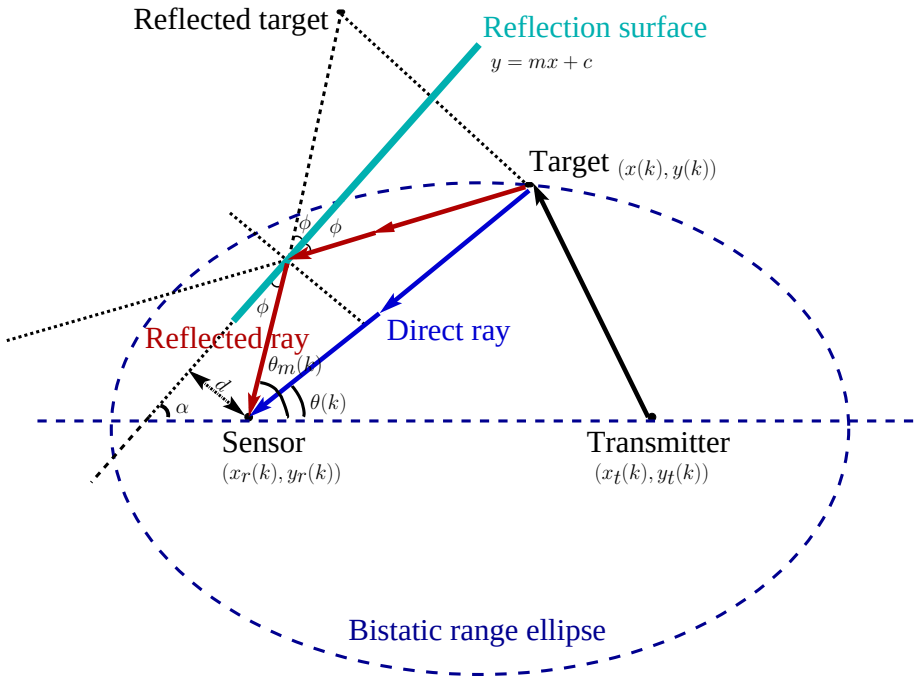

Figure 5.8: Direct and multipath reflected signals.

single direct and one multipath wall reflected signal. When the multipath range and its DOA is known, the track can be initiated. As the direct signal's range and DOA is known, these information can also be used to initialize the track. Consider the reflection scenario described in Figure 5.2. Let S be the sensor location and PS be the projection of S on the line $y = mx + c$. Here, d is the distance between the point S and its orthogonal projection point PS on the line $y = mx + c$.

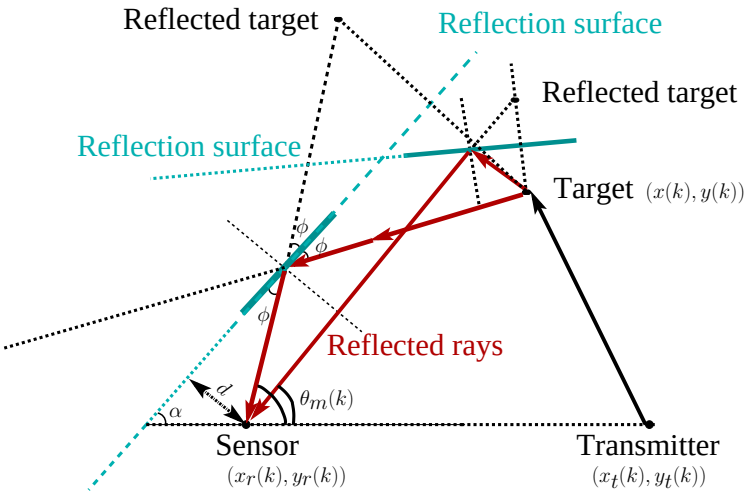

Figure 5.9: Two multipath reflected signals.

$$\theta_m(k) = \phi + \alpha \tag{5.8}$$

$$\theta_m^{rs}(k) = \alpha - \phi \tag{5.9}$$

$$\theta_m(k) = \tan^{-1}\left[\frac{(y_{rs}(k) - y_r(k))}{(x_{rs}(k) - x_r(k))}\right] + \omega_\theta(k)$$

$$\frac{y_{PS} - y_r(k)}{x_{PS} - x_r(k)} = -\frac{1}{m} \tag{5.10}$$

$$d = \frac{|y_r(k) - mx_r(k) - c|}{\sqrt{1+m^2}} \tag{5.11}$$

$$y_{PS} - mx_{PS} - c = 0 \tag{5.12}$$

$$my_{PS} - my_r(k) + x_{PS} - x_r(k) = 0 \tag{5.13}$$

where the point (x_{PS}, y_{PS}) is the coordinate of PS. The point (x_{PS}, y_{PS}) is on $y = mx + c$.

$$x_{PS} = \frac{my_r(k) + x_r(k) - cm}{(1+m^2)} \tag{5.14}$$

$$y_{PS} = \frac{m^2 y_r(k) + mx_r(k) + c}{(1+m^2)} \tag{5.15}$$

The reflected ray's straight line geometric equation can be given by

$$\tan\theta_m(k) = \frac{y - y_r(k)}{x - x_r(k)} \tag{5.16}$$

Hence

$$y - \tan\theta_m(k)x - y_r(k) + x_r(k)\tan\theta_m(k) = 0 \tag{5.17}$$

$$\tag{5.18}$$

Hence the intersect of the above equation at $y - mx - c = 0$ can be found. That is the reflection point $(x_{rs}(k), y_{rs}(k))$ on the reflection surface. Therefore the reflection points can be expressed as follows.

$$x_{rs}(k) = \frac{y_r(k) - x_r(k)\tan\theta_m(k) - c}{(m - m\tan\theta_m(k))} \tag{5.19}$$

$$\tag{5.20}$$

$$y_{rs}(k) = \frac{my_r(k) - mx_r(k)\tan\theta_m(k) - c\tan\theta_m(k)}{(m - m\tan\theta_m(k))} \tag{5.21}$$

$$\tag{5.22}$$

$$\sin\Phi = \frac{d}{\sqrt{(x_r(k) - x_{rs}(k))^2 + (y_r(k) - y_{rs}(k))^2}} \tag{5.23}$$

Let d' be the distance between the target and its orthogonal projection PT on the line $y = mx + c$. Hence

$$d' = \frac{|y(k) - mx(k) - c|}{\sqrt{1 + m^2}} \tag{5.24}$$

The point (x_{pt}, y_{pt}) be the projection point PT of the target on $y - mx - c = 0$. Hence

$$x_{PT} = \frac{my(k) + x(k) - cm}{(1 + m^2)} \tag{5.25}$$

$$\tag{5.26}$$

$$y_{PT} = \frac{m^2y(k) + mx(k) + c}{(1 + m^2)} \tag{5.27}$$

$$x_{PT} = \frac{(x_{RT} + x_t)}{2} \tag{5.28}$$

$$\tag{5.29}$$

$$y_{PT} = \frac{(y_{RT} + y_t)}{2} \tag{5.30}$$

$$\tag{5.31}$$

$$x_{PS} = \frac{(x_{RS} + x_r)}{2} \tag{5.32}$$

$$\tag{5.33}$$

$$y_{PS} = \frac{(y_{RS} + y_r)}{2} \tag{5.34}$$

$$\frac{y_{PS} - y_{RS}(k)}{x_{PS} - x_{RS}(k)} = -\frac{1}{m} \tag{5.35}$$

Based on the reflection scenario described in Figure 5.2, the following equations can be driven. Let d_{PStoRS}, d_{StoPS}, d_{RStoPT}, d_{TtoPT} be the distances between PS to RS, S to PS, RS to PT and T to PT, respectively.

Hence,

$$\frac{d_{PStoRS}}{d_{StoPS}} = \frac{d_{RStoPT}}{d_{TtoPT}} \tag{5.36}$$

The points PS, RS, PT are on the line $y = mx + c$. Also the reflection points RS can be expressed as

$$x_{RS} = x_{PT} - d_{RStoPT}\cos(\tan^{-1} m) \tag{5.37}$$

$$\tag{5.38}$$

$$\begin{aligned} y_{RS} &= y_{PT} - d_{RStoPT}\sin(\tan^{-1} m) \\ &= y_{PT} + d_{PStoRS}\sin(\tan^{-1} m) \\ &= y_{PT} + \frac{d_{PStoRS} m}{\sqrt{1+m^2}} \end{aligned} \tag{5.39}$$

Hence, d_{PStoRS} can be driven as given below.

$$d_{PStoRS} = \frac{d_{StoPS}\sqrt{(x_{PT}-x_{PS})^2 + (y_{PT}-y_{PS})^2}}{d_{StoPS} + \sqrt{(x_{PT}-x_{PS})^2 + (y_{PT}-y_{PS})^2}} \tag{5.40}$$

The signal reflection points $(x_{RS}(k), y_{RS}(k))$ and the target projection points $(x_{PT}(k), y_{PT}(k))$ are functions of the target. Hence, we can write the Jacobian of it with respect to the target location. Also for the tracking, the Jacobian can be written as,

$$\frac{\partial d_{PStoRS}}{\partial x} = \frac{\partial}{\partial x}\left(\frac{d_{StoPS}\sqrt{(x_{PT}-x_{PS})^2+(y_{PT}-y_{PS})^2}}{d_{StoPS}+\sqrt{(x_{PT}-x_{PS})^2+(y_{PT}-y_{PS})^2}}\right) \tag{5.41}$$

Figure 5.10 shows a multipath range ellipse and a bistatic range ellipse. The possible target location will be one intersect of the ellipses. Based on the smooth surface assumption, we can draw a multipath range ellipse as shown in Figure 5.10. This ellipse's one focus is the transmitter $(x_t(k), y_t(k))$ and the other is the point RS, and its coordinate is $(x_{RS}(k), y_{RS}(k)$. In Figure 5.10, the focus point $(x_f(k), y_f(k)$ of the multipath range ellipse is the point RS. That is the coordinate of the reflected sensor S on the line $y = mx + c$. Similar to the bistatic range ellipse in bistatic/multistatic radar tracking, the multipath range ellipse can be used to track the target in multipath reflection environment.

5.3 Tracking Algorithm

The target motion model and measurement models are using the following non-linear relationship in the Cartesian coordinate system.

$$x(k+1) = f_k\left(x(k)\right) + v(k) \tag{5.42}$$

$$\tag{5.43}$$

$$z(k) = h_k\left(x(k)\right) + w(k) \tag{5.44}$$

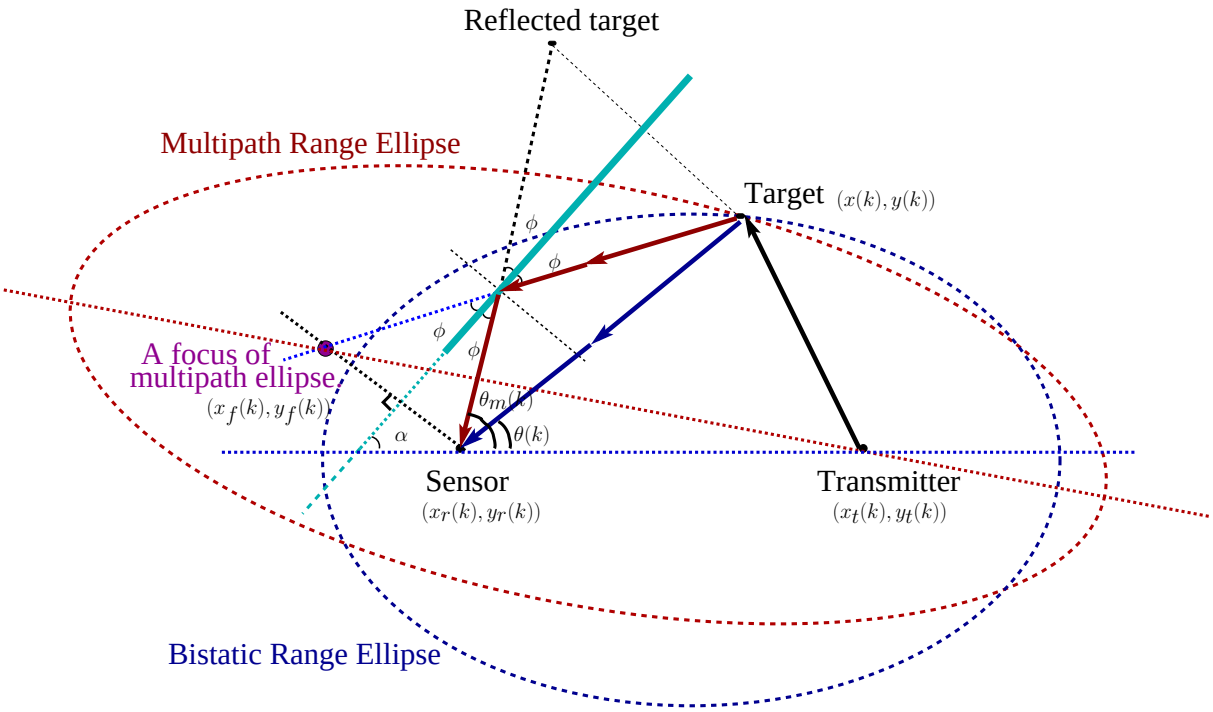

Figure 5.10: Multipath range ellipse and bistatic range ellipse.

where $x(k) = [x(k)\ \dot{x}(k)\ y(k)\ \dot{y}(k)]^T$ is the state of the moving target at discrete time step k. Here $x(k)$ and $y(k)$ are the positions and $\dot{x}(k)$ and $\dot{y}(k)$ are the velocities in the direction of X and Y coordinates. Here, f_k and h_k are state and measurement models defining the non-linear functions, and $v(k)$ and $w(k)$ are process and measurement noise, which are assumed to be drawn from a zero mean, statically independent and Gaussian white noise with covariances Q_k and R_k, respectively.

5.4 Simulation and Results

In this section, different reflection scenarios are considered and the track and RMSE information are compared. In the simulation, parameter setting are: transmitter position =

[49925, -10899]m; receiver position = [0, 0]m; the reflection surface equation is given by $y = mx + c$. Here $m = m' + e_{m'}$ and $c = c' + e_{c'}$ $m' = -1, c' = 100000$ m. The $e_{m'}$ and $e_{c'}$ are 0.001 and 100 m, respectively; the measurement interval is 1 second; measurement variances $\sigma_r^2 = 10$ m^2 and $\sigma_\theta^2 = 0.0001$ radians^2; probability of detection is 0.98; 10 false alarms at each sampling. The target trajectories, transmitter and receiver locations are given in Figures 5.11 and 5.12. There are two targets in the surveillance region, one enters the region at $k = 3$ and the other enters at $k = 6$.

Figure 5.11 shows the S-D association comparison of the tracking by not considering the multipath reflection model. In both cases S-D association and multipath S-D association are used. Figure 5.11 shows that when multipath measurements are available and if they are not utilized within the tracker, then there are spurious tracks formed.

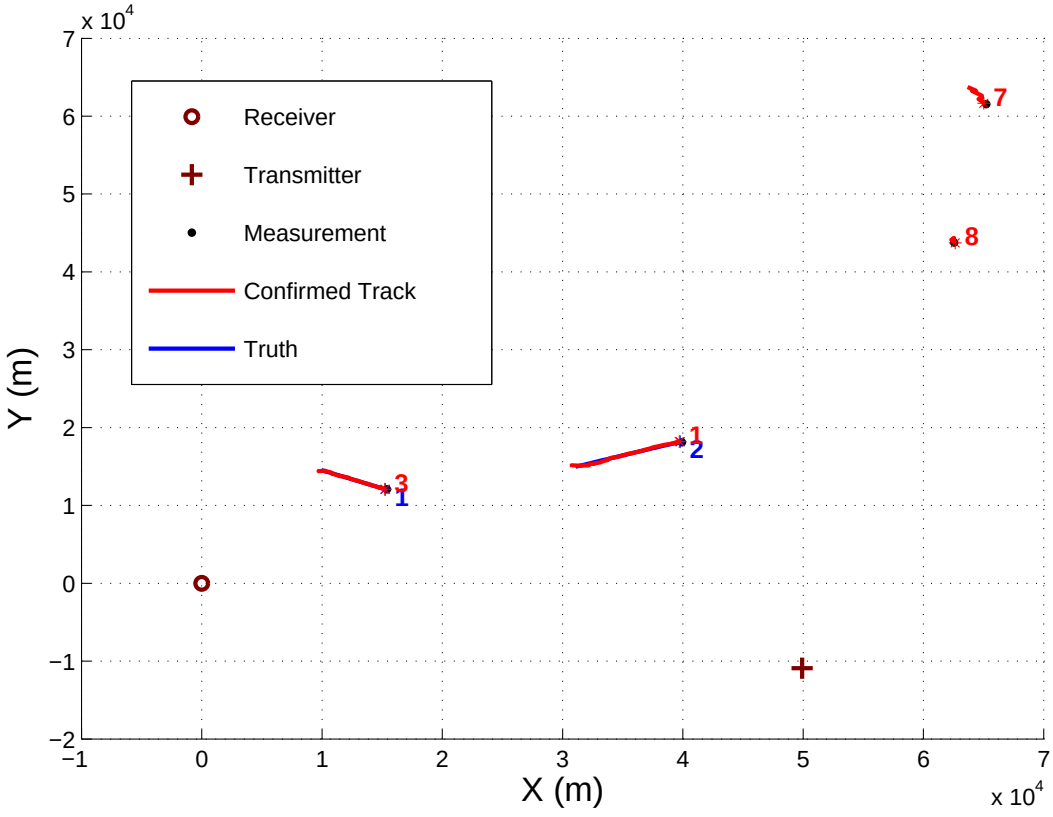

Figure 5.11: Estimated target tracks without incorporating multipath.

Figure 5.12 shows the S-D association comparison of the tracking by considering the multipath reflection model. Figure 5.12 shows that with a correct propagation mode assumption by considering the multipath reflection surface uncertainty. Integrating multipath information into the tracker can help improve the accuracy of tracking and reduce the number of false tracks.

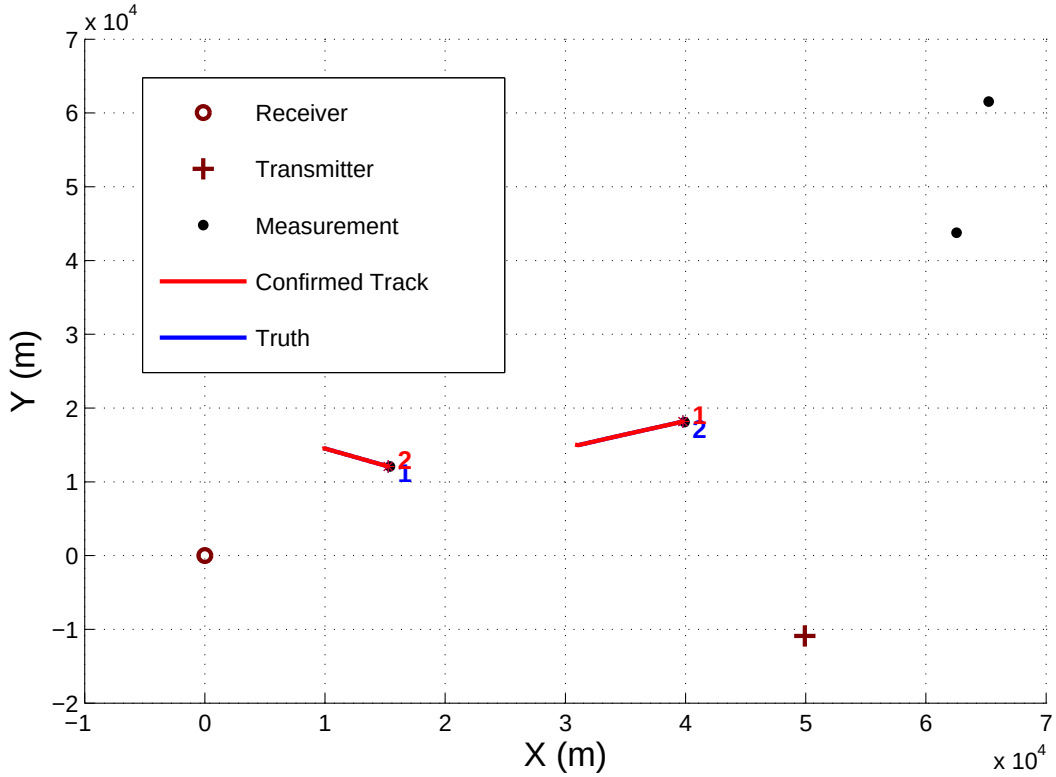

Figure 5.12: Estimated target tracks with incorporating multipath.

The root mean square error (RMSE) values are compared in Figure 5.13 and 5.14.

The RMSE values are lower for fused tracks that were obtained through multipath multiframe assignment technique that incorporated the reflection surface parameter uncertainty.

It shows that the multipath S-D association based tracking algorithm converges as the

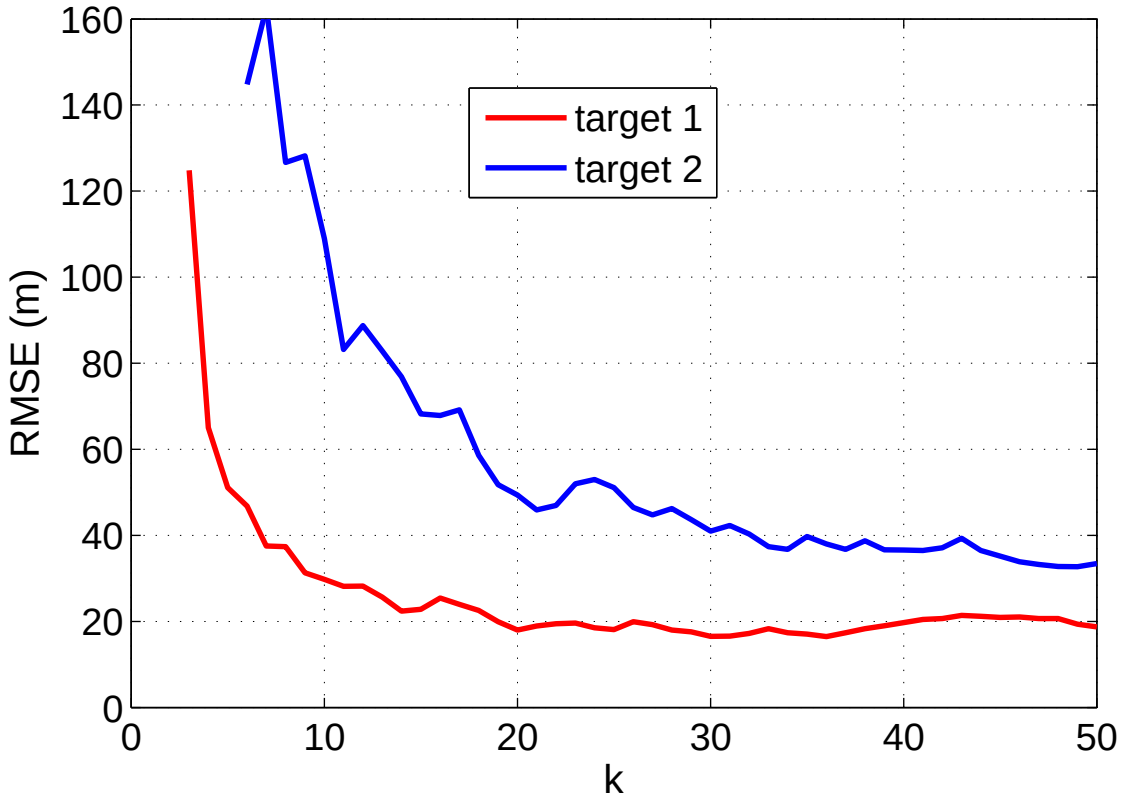

Figure 5.13: RMSE values without incorporating multipath.

RMSE goes lower over the time. The RMSE curves show that in tracking, multipath S-D association filter outperform when the multipath reflection modes information is incorporated appropriately.

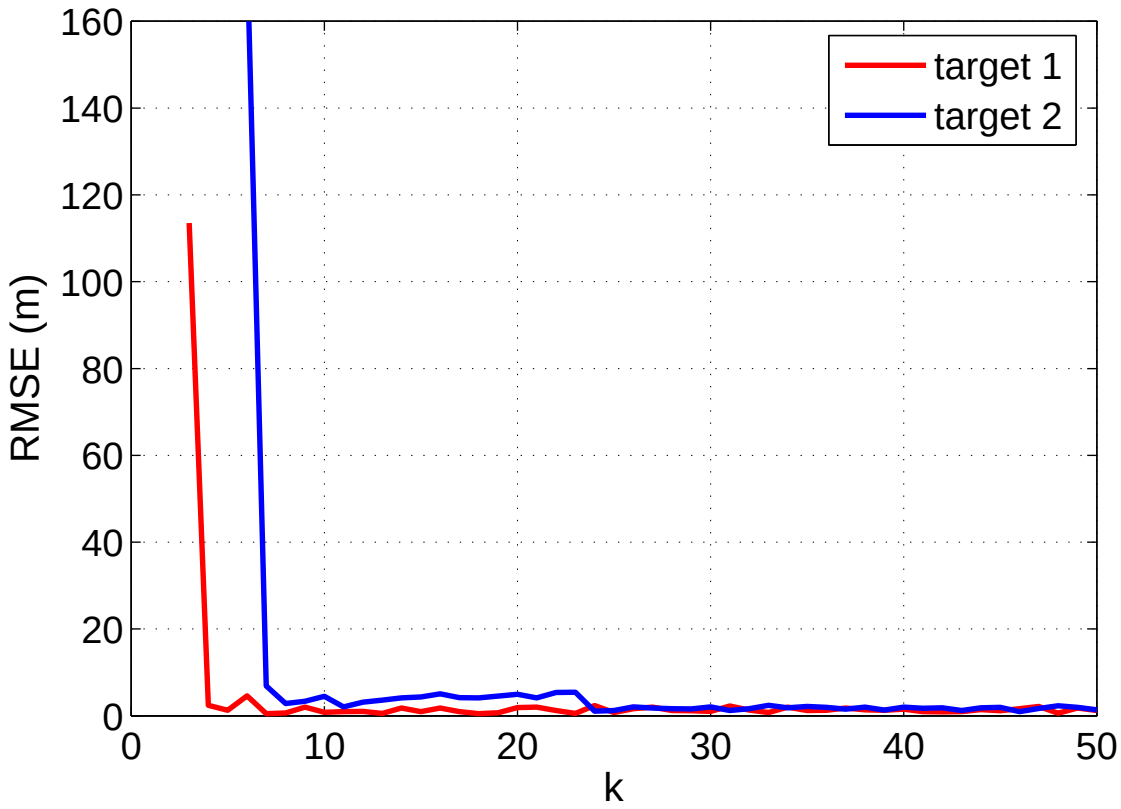

Figure 5.14: RMSE values with and without multipath.

5.5 Performance Evaluations of Multipath Multitarget Tracking using PCRLB

In this section, the performance of the multipath-assisted multitarget tracking using multiframe assignment for initiating and tracking multiple targets by employing one or more transmitters and receivers is studied. The basis of the technique is to use the posterior Cramer-Rao lower bound (PCRLB) to quantify the optimal achievable accuracy of target state estimation. When resolved multipath signals are present at the sensors, if proper measures are not taken, multiple tracks will be formed for a single target. In multipath environment, in every scan the number of sensor measurements from a target is equal to the number of resolved signals received by different propagation modes. The data association becomes more complex as this is in contrary to the standard data association problem whereas the total number of sensor measurements from a target is equal to at most one. This leads to a challenging problem of fusing the direct and multipath measurements from the same target. We showed in our evaluations that incorporating multipath information improves the performance of the algorithm significantly in terms of estimation error. Simulation results are presented to show the effectiveness of the proposed method.

5.6 Posterior Cramer-Rao Lower Bound in Multipath Tracking

This section study the performance of the multipath-assisted multitarget tracking using multiframe assignment for initiating and tracking multiple targets. MSD algorithm tracks targets with uncertainty in reflection-path-model (uncertain-origin) measurement. Optimally solving this problem is highly complex. It will be interest to evaluate the performance

of the tracker and is quantified by the PCRLB which is defined as the inverse of the Fisher information matrix (FIM). The PCRLB provides a mean square error lower bound on the performance of any unbiased estimator of the unknown target state and for additional reading (80) (87) (89) (90) (91) (93) (95) may be used. This discovers how close its mean square estimate is to the lower bound. An unbiased estimator can achieve the minimum variance for state estimates described by the PCRLB.

Let the measurement be $Z_k = [z_1, z_2, ..., z_k]$ and the unbiased estimator of x_k be $\hat{x}_k(Z_k)$. It is assumed targets are well separated, hence there is no measurement origin uncertainty in terms of targets. The PCRLB is defined as $J(k)^{-1}$, the inverse of the Fisher Information Matrix (FIM).

The lower bound on the error co-variance of $\hat{x}_k(Z_k)$, such that,

$$C_k \triangleq \mathbf{E}[\hat{x}_k(Z_k) - \hat{x}_k(Z_k)][\hat{x}_k(Z_k) - \hat{x}_k(Z_k)]^T \geq J(k)^{-1} \tag{5.45}$$

where $\mathbf{E}$ is the expectation over (x_k, Z_k).

The recursive PCRLB equations are given by (95)

$$J(k+1) = D_k^{22} - D_k^{21}(J(k) + D_k^{11})^{-1} D_k^{12} + J_z(k+1) \tag{5.46}$$

where

$$D_k^{11} = \mathbb{E}\big\{ -\Delta_{x_k}^{x_k} \ln p(x_{k+1}|x_k) \big\} \tag{5.47}$$

$$D_k^{12} = \mathbb{E}\big\{ -\Delta_{x_k}^{x_{k+1}} \ln p(x_{k+1}|x_k) \big\} \tag{5.48}$$

$$D_k^{21} = (D_k^{12})^T \tag{5.49}$$

$$D_k^{22} = \mathbb{E}\big\{ -\Delta_{x_{k+1}}^{x_{k+1}} \ln p(x_{k+1}|x_k) \big\} \tag{5.50}$$

$$J_z(k+1) = \mathbb{E}\big\{ -\Delta_{x_{k+1}}^{x_{k+1}} \ln p(z_{k+1}|x_{k+1}) \big\} \tag{5.51}$$

and Δ is a second-order partial derivative operator.

5.6.1 Multipath PCRLB

Lets consider the targets moving independently. The state equation can be written into M separate equations.

$$x_{x+1}^t = F_k^t x_k^t + v_k^t, \quad t = 1, 2, ..., M \tag{5.52}$$

where F_k^t is a linear function and v_k^t is an independent white noise sequence.

At each sampling time k, the j-th measurement $z_k^i(j)$ has the form

$$z_k(j) = \begin{cases} h_k^d(x_k^t, x_r, x_t) + \omega_k^t(j) & \text{if originated from target } t\text{, direct path} \\ h_k^m(x_k^t, x_r, x_t, x_{rs}) + \omega_k^t(j) & \text{if originated from target } t\text{, multipath} \\ \upsilon_k(j) & \text{if false alarm} \end{cases} \tag{5.53}$$

where $h_k^d(x_k^t, x_r, x_t)$ and $h_k^m(x_k^t, x_r, x_t, x_{rs})$ are (in general) nonlinear functions, $\omega_k^t(j)$ is a zero mean Gaussian random variable with covariance Σ_k and $\upsilon_k(j)$ is uniformly distributed throughout the field of view (V) of the sensor (87). The number of false alarms in the sensor's field of view is Poisson-distributed with mean λV.

It can be shown that if ν_k^t is Gaussian with zero mean and covariance Γ_k^t, then the FIM of target t, $J^t(k+1)$, can be written as (86)

$$J^t(k+1) = \underbrace{\left[\Gamma_k^t + F_k^t J^t(k)^{-1}(F_k^t)^T\right]^{-1}}_{J_x^t(k+1)} + J_z^t(k+1) \tag{5.54}$$

where $J_z^t(k+1)$ denotes the measurement information regarding target t at sampling time $k+1$, which is given by

$$J_z^t(k) = J_{z_d}^t(k) + \sum_{i=1}^{n} J_{z_m^i}^t(k) \tag{5.55}$$

where $J^t_{z_d}(k)$ is the information from direct path, $J^t_{z^i_m}(k)$ is the information from reflection point i and n is the number of reflection surfaces.

The $J^t_{z_d}(k)$ is given by

$$J^t_{z_d}(k) = \mathbb{E}\Big[q^{d,t}_k \big(H^{d,t}_k\big)^T \Sigma^{-1}_k H^{d,t}_k\Big] \tag{5.56}$$

with the (a,b)th element of matrix H^t_k being given by

$$H^{d,t}_k(a,b) = \frac{\partial h^d_k(x^t_k, x_r, x_t)(a)}{\partial x^t_k(b)} \tag{5.57}$$

$\big[h^i_k\big]^t(a)$ is the a-th component of the measurement vector and $x^t_k(b)$ is the b-th component of the state vector of target t. The variable $q^{d,t}_k$ is the Information Reduction Factor (IRF) for direct path that depends on the measurement noise (Σ_k), false alarm rate (λ), probability of detection $(P^t_D(k,i))$ and the gated field of view (V) (87).

Similarly, $J^t_{z^i_m}(k)$ is given by

$$J^t_{z^i_m}(k) = \mathbb{E}\Big[q^{i,t}_k \big(H^{i,t}_k\big)^T \Sigma^{-1}_k H^{i,t}_k\Big] \tag{5.58}$$

where $q^{i,t}_k$ is the IRF for multipath form reflection surface i.

In order to improve the overall tracking performance, this algorithm exploits multipath target returns from distinct propagation modes that are resolved by the receiver. We derived multipath PCRLB in a multipath reflection environment when the reflection surface information or points are known to the receiver with an assumption that the targets are well separated. The above equations can be used to calculate the multipath PCRLB for all the cases. Only the IRF will change with different assumption on reflection point information. When the reflection points are accurately known, the IRF can be calculated similar to direct path. When there is uncertainty in reflection surface parameters, calculating the IRM in

this case is much more complicated, since we must consider the effect of reflection path model uncertainty in addition to uncertainty in the data association.

5.7 Simulation and Results

In this section, a multipath reflection scenarios is considered and the track and the RMSE information are compared against the PCRLB. In the simulation, parameter setting are: transmitter position = [49925, -10899]m; receiver position = [0, 0]m; the reflection surface equation is given by $y = mx + c$. Here $m = -1, c = 100000$ m, the measurement interval is 1 second; measurement variances $\sigma_r^2 = 10$ m^2 and $\sigma_\theta^2 = 0.0001$ radians^2; probability of detection is 0.98; 10 false alarms at each sampling.

The target trajectories, transmitter and receiver locations are given in Figure 5.15 when multipath information is not incorporated. There are two targets in the surveillance region, one enters the region at $k = 3$ and the other enters at $k = 6$.

The target trajectories, transmitter and receiver locations are given in Figure 5.16 when multipath information is incorporated. Unscented Kalman filter (UKF) is used to track the targets by incorporating multipath measurements.

The measurements are associated to the targets and the appropriate multipath models. To associate the measurements to already established targets, multipath $S - D$ association (MSD) algorithm is used for UKF. Figures 5.18 and 5.17 were plotted for 100 Monte-Carlo runs.

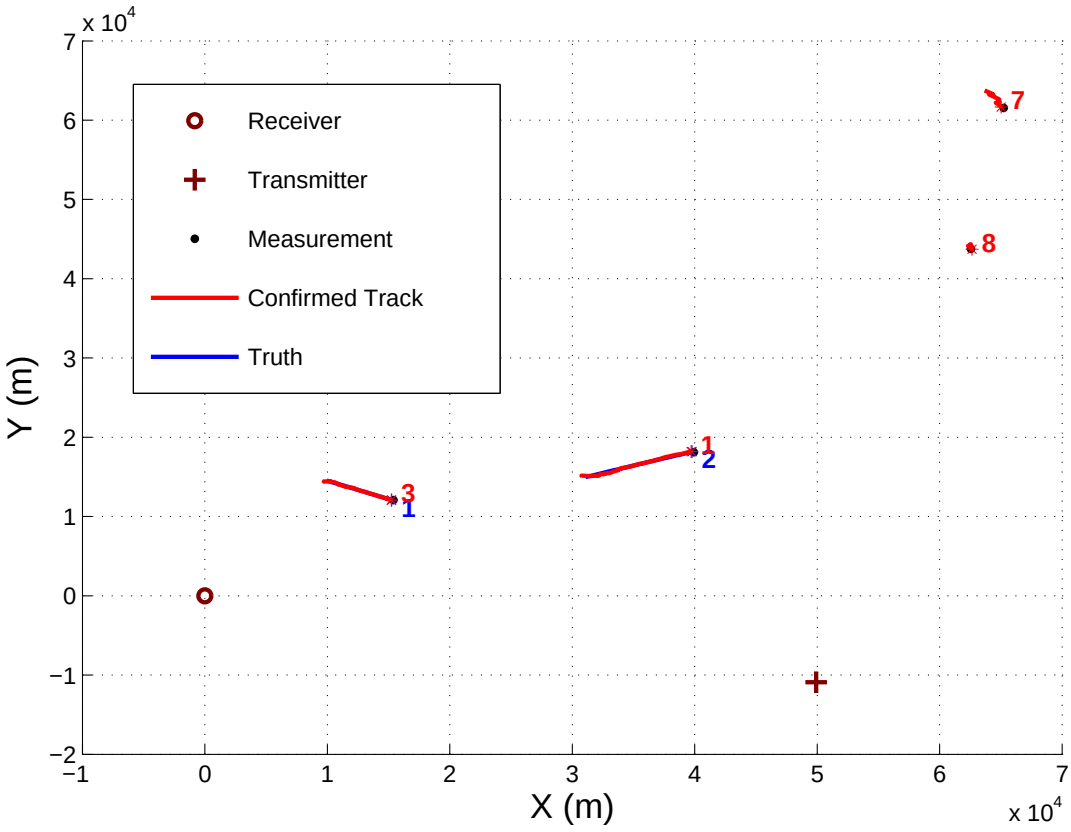

Figure 5.15: Estimated target tracks without incorporating multipath.

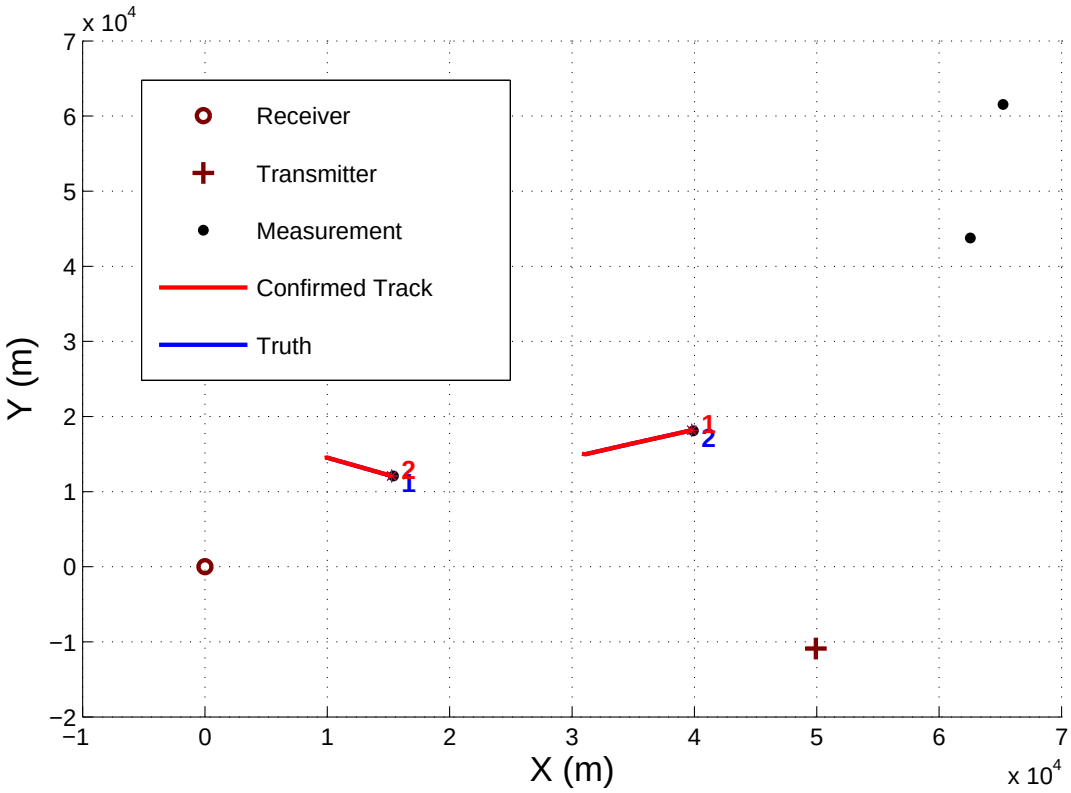

Figure 5.16: Estimated target tracks with incorporating multipath.

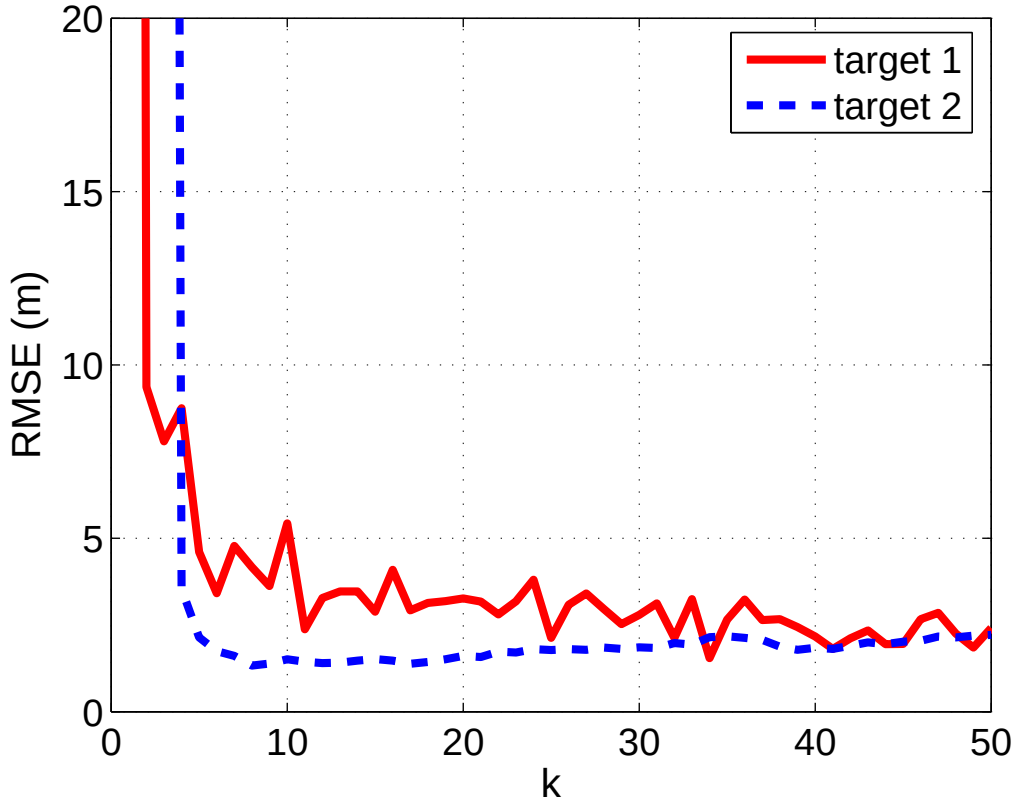

Figure 5.17: RMSE values for comparisons.

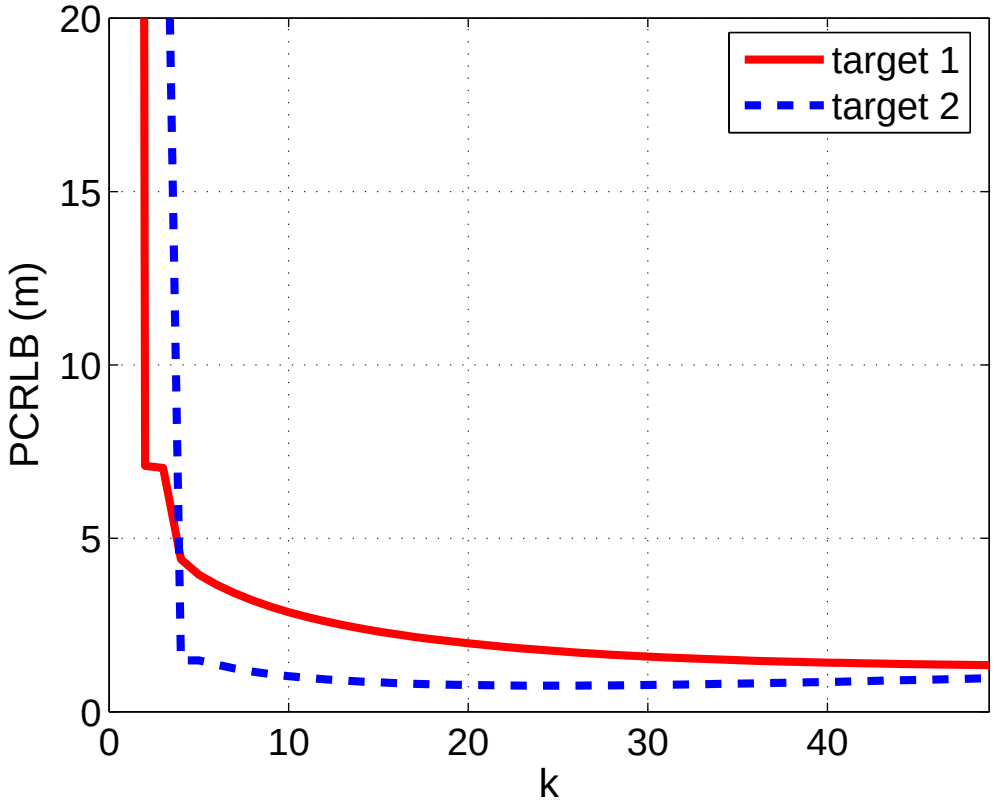

Figure 5.18: PCRLB values for comparisons.

Chapter 6

Conclusions and Future Work

6.1 Conclusions

In this thesis, the feasibility of tracking multiple targets using transmitters of opportunity was studied. The challenges are to handle low probability of detection of targets of interest, high nonlinearity due to high measurement errors, reflection path uncertainty and lack of elevation information. In this thesis, the converted measurement Kalman filter, unscented Kalman filter and particle filter based PHD filter are implemented for PCL radar measurements and their performances are compared. Simulation results showed that the unscented Kalman filter and particle filter based PHD filter are the desirable choices for PCL systems with small and large measurement errors, respectively.

We also implemented a bias estimation and removal technique in direction of arrival measurement for a PCL system. Due to the bias measurements, the measurement model exhibits a high nonlinearity. Most of the nonlinear filter based tracking require approximations. Errors in the DOA measurement leads to higher errors in tracking accuracy. Noise and the precision of DOA estimation are main issues in a PCL system. We demonstrate

that with an expensive computation, the SMC implementation of the PHD filter tracking algorithm provides a better approximation in target tracking. This approach was tested using simulated track data. The simulation results are presented to show the effectiveness of the proposed algorithm with an example of tracking airborne targets.

The algorithm for multipath-assisted multitarget tracking using multiframe assignment is proposed for initiating and tracking multiple targets. This algorithm was exploiting multipath target returns from distinct propagation modes that are resolvable by the receiver. When resolved multipath returns were not utilized within the tracker, i.e., discarded as clutter, potential information conveyed by the multipath detections of the same target was wasted. In this case, spurious tracks were formed using target-originated multipath measurements, but with an incorrect propagation mode assumption. We proposed a multiframe assignment technique to incorporate multipath information. The simulation results were presented to show the effectiveness of the proposed algorithm with an example of tracking ground targets.

The algorithm for multipath-assisted multitarget tracking using multiframe assignment is considered when there are uncertainties in multipath reflection points at the receiver. We considered the case when the target reflections are bounced off from smooth reflecting wall/surface. When these measurements are not utilized within the tracker, i.e., discarded as clutter, these target return information from these multipath detections of the same target were wasted. We proposed a multiframe assignment technique to incorporate multipath information when there were uncertainties in reflection surface information.

The simulation results were presented to show the effectiveness of the proposed algorithm with an example of tracking two targets with target reflected signals in a smooth multipath

reflection surface environment.

We studied the performance of the multipath-assisted multitarget tracking using multi-frame assignment for initiating and tracking multiple targets.

In contrary to the standard data association problem, this algorithm has to handle uncertainties in the target as well as the reflection path/mode. The simulation results are presented to show the effectiveness of the proposed algorithm with an example of tracking two targets in a multipath reflection environment.

We derived multipath PCRLB in a multipath reflection environment when the reflection surface information or points are known to the receiver with an assumption that the targets are well separated, and showed that the RMSE values follows the PCRLB. We showed that incorporating multipath information improves the performance of the algorithm significantly in terms of estimation error.

6.2 Future Work

Tracking using range (i.e., multipath range and bistatic range) and angle measurements and appropriately combining them by considering the multipath reflection is challenging when the reflection surface parameters are unknown. Performing the tracking when the reflection surface information or territorial information is completely unknown will be considered as future work.

Calculating the multipath PCRLB for the closely spaced targets and when there are uncertainties in the reflection points or surface parameters will be considered in the future works. Target tracking using complex multipath reflection signals from multistatic

configuration in multitarget environment will be also considered in the future work.

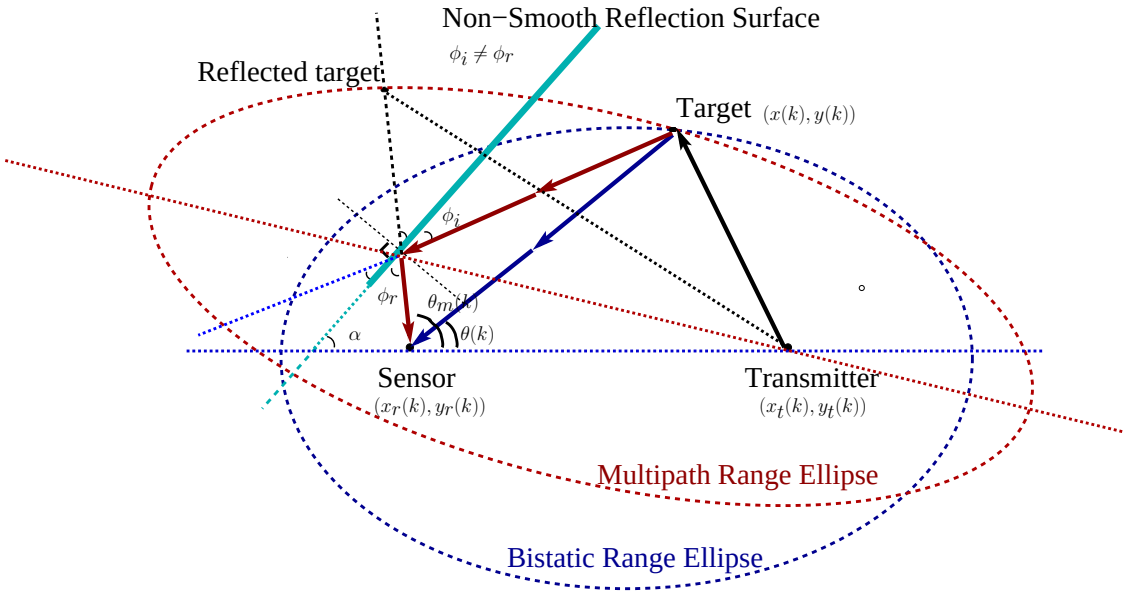

Figure 6.1: Reflection on non-smooth surface.

Figure 5.10 shows a reflection model on a smooth surface whereas Figure 6.2 shows the reflection on a non-smooth surface. When the sensor receives the TDOA and DOA measurements consistently from signals reflecting from a non-smooth surface, for a specific value of a multipath range, the target lies on multipath range ellipse as shown in Figure 6.2. When the reflection surface is not smooth, we cannot assume that the incident and reflection angles are equal. In the case when the surface is not smooth, the incident rays scatter on the surface and reflect in different directions. The concentrated energy's reflection angle depending on various factors such as the nature of the reflection surface and incident angle. In Figure 6.2, $\phi_i \neq \phi_r$.

On a smooth surface reflection, the focus of this multipath range ellipse will be the

transmitter and the other focus is the mirror location of the sensor on the reflection surface defined by $y = mx + c$.

On a non-smooth surface reflection, the received TDOA measurement will be used to calculate the new multipath range to find possible target's location that will lie on the multipath range ellipse as shown in Figure 6.2. In this case, one focus of the multipath range ellipse will be the transmitter and the other focus is the reflection point on the surface defined by $y = mx + c$. The initialization and tracking the target in such environment is left for future work.

A range of very simple to more complex reflection scenarios that may occur during a multipath reflection environment were illustrated in Figures 5.2 5.3 5.4, 5.5, 5.6 5.7. In this thesis, the case as in Figure 5.2 was considered. However, other scenarios that are discussed in Figures 5.3, 5.4, 5.5, 5.6 and 5.7 can be considered for tracking. These can be done easily by modifying this developed algorithms. This will be considered for future work.

Bibliography

[1] H. D. Griffiths, N. R. W. Long, "Television-based bistatic radar", *IEE Proceedings on Communications, Radar and Signal Processing*, vol. 133 - Part F, no. 7, pp. 649–657, December 1986.

[2] P. E. Howland, D. Maksimiuk and G. Reitsma, " FM radio based bistatic radar ", *IEE Proceedings on Radar Sonar Navigation*, vol. 152, no. 3, pp. 107–115, June 2005.

[3] M. Malanowski, "Comparison of Adaptive Methods for Clutter Removal in PCL Radar" *Proceedings International Radar Symposium 2nd Microwave and Radar Week*, pp. 237–240, Poland, May 2006.

[4] C. L. Zoeller, M. C. Budge and M. J. Moody, "Passive Coherent Location Radar Demonstration", *Proceedings of the Thirty-Fourth Southeastern Symposium - System Theory* pp. 358–362, March 2002.

[5] P. E. Howland, "Target tracking using television-based bistatic radar", *IEE Proceedings on Radar Sonar Navigation*, vol. 146, no. 3, pp. 166–174, June 1999.

[6] M. N. Petsios, E. G. Alivizatos and N. K. Uzunoglu, "Manoeuvring Target Tracking using Multiple Bistatic Range and Range-rate Measurements", *Signal Processing*, vol. 87, no. 3, pp. 665–686, August 2007.

[7] K. S. Kulpa and Z. Czekala, "Masking effect and its removal in PCL radar", *IEE Proceedings Radar, Sonar and Navigation*, vol. 152 , issue 3, pp 174–178, Warszawa, Poland, June 2005.

[10] H. D. Griffiths, C. J. Baker, "Passive coherent location radar systems. Part 1: Performance prediction", *IEE Proceedings Radar, Sonar and Navigation*, vol. 152, no. 3, pp 153–159, June 2005.

[9] C. J. Baker, H. D. Griffiths, I. Papoutsis,"Passive coherent location radar systems. Part 2: Waveform properties", *IEE Proceedings Radar, Sonar and Navigation*, vol. 152, no. 3, pp 160–168, June 2005.

[10] H. D. Griffiths, C. J. Baker, "Measurement and Analysis of Ambiguity Functions of Passive Radar Transmissions", *Radar Conference, IEEE International* pp. 321–325, May 2005.

[11] H. D. Griffiths, C. J. Baker, H. Ghaleb, R. Ramakrishnan and E. Willman, "Measurement and Analysis of Ambiguity Functions of off-air Signals for Passive Coherent Location" , *IEE Electronics Letters* vol. 39, no. 13, pp. 1005–1007, June 2003.

[12] T. Xiaoming, H. You, D. Shijia and N. Jinlin, "Doppler compensation for passive coherent location", *6th International Conference on Signal Processing*, Naval Aeronautical Engineering Institute China, Yantai, China, pp 1457–1460 vol. 2, August 2002.

[13] A. Jafargholi, M. R. Mousavi and M. M. Nayebi, "High Accurate Multiple Target Detection in PCL Radar Systems", *CIE 06. International Conference on Radar*, pp 1–4, Department of Electrical Engineering, K. N. Toosi University of Technology, Tehran, October 2006.

[14] R. H. Anderson, S. Kraut, and J. L. Krolik, "Robust Altitude Estimation for Over-the-Horizon Radar Using a State-Space Multipath Fading Model", *IEEE Transactions on Aerospace and Electronic Systems*, vol. 39, no. 1 pp. 192–201, January 2003.

[15] R. H. Anderson and J. L. Krolik, "Track Association for Over-the-Horizon Radar With a Statistical Ionospheric Model", *IEEE Transactions on Signal Processing*, vol. 50, no. 11, PP. 2632–2643, November 2002.

[16] Y. Bar-Shalom and X.R. Li, *Multitarget-Multisensor Tracking: Principles and Techniques*, YBS Publishing, Storrs, CT, 1995.

[17] P. Blanc-Benon and C. Jauffret, "TMA From Bearings and Multipath Time Delays", *IEEE Transactions on Aerospace and Electronic Systems*, vol. 33, no. 3, pp. 813–824, July 1997.

[18] R. E. Bogner, A. Bouzerdoum, K. J. Pope, and J. Zhu, "Association of Tracks from Over The Horizon Radar", *IEEE AES Systems Magazine*, pp. 31–35, September 1998.

[19] S. B. Colegrove, A. W. Davis, and J. K. Ayliffe, "Track initiation and nearest neighbors incorporated into probabilistic data association." *Journal of Electric and Electronic Engineering, Australia,* vol. 6, no. 3, pp. 191-198, September 1986.

[20] Y. Bar-Shalom and E. Tse, "Tracking in a cluttered environment with probabilistic data association",*Automatica*, vol. II, pp. 451-460, September 1975.

[21] R. Ignetik and B. J. Jarvis, "On the importance of earth geometry for over-the-horizon radar coordinate registration", *In Proceedings of the International Conference Radar*, Paris, 398-402, 1994.

[22] G. W. Pulford and R. J. Evans, "A Multipath Data Association Tracker for Over-the-Horizon Radar", *IEEE Transaction on Aerospace and Electronic Systems*, vol. 34, no. 4, pp. 1165–1183, October 1998.

[23] H. Liu, Y. Liang, Q. Pan and Y. Cheng, "A Multipath Viterbi Data Association Algorithm for OTUR", *College of Automation,Northwestem Polytechnical University Xi'an Shaanxi, 710072,China,* IEEE 0-7803-9582-4 2006.

[24] B. Friedlander, "Accuracy of Source Localization Using Multipath Delays", *IEEE Transactions on Aerospace and Electronic Systems*, vol. 24. no. 4, pp. 346–359, July 1998.

[25] K. W. Lo, B. G. Ferguson, Y. Gao, and A. Maguer, "Aircraft Flight Parameter Estimation Using Acoustic Multipath Delays", *IEEE Transactions on Aerospace and Electronic Systems*, vol. 39, no. 1, pp. 259–268, January 2003.

[26] K. Min and W. Guohong, "Research on Multi-Mode Fusion Tracking of OTHR based on Auction Algorithm", *2007 International Conference on Computational Intelligence and Security Workshops*, DOI 10.1109/CIS.Workshops.2007.115, pp. 393–396, 2007.

[27] S. S. Blackman and R. Popoli, *Design and analysis of modern tracking systems*, Artech House, Boston, MA, 1999.

[28] Y. Bar-Shalom, X. Li and T. Kirubarajan, *Estimation with Applications to Tracking and Navigation*, Wiley, New York, 2001.

[29] B. Oksendal, *Stochastic differential equations, 6th edition*, Springer Verlag, Heidelberg, 2003.

[30] V. Krishnan, *Nonlinear Filtering and Smoothing : An Introduction to Martingales, Stochastic Integrals and Estimation*, Dover, 2005.

[31] B. Grocholsky, "Information-theoretic control of multiple sensor platforms", *PhD thesis*, Department of Aerospace, Mechatronic and Mechanical Engineering, The University of Sydney, Australia, 2002.

[32] N. J. Gordon, D. J. Salmond and A. F. M. Smith, "Novel approach to nonlinear/non-Gaussian Bayesian state estimation", *IEE Proceedings Part F: Radar and Signal Processing,* , vol. 140, no. 2, pp. 107–113, April 1993.

[33] A. Doucet, S. J. Godsill and C. Andrieu. "On sequential Monte Carlo sampling methods for Bayesian filtering", *Statistics and Computing*, vol. 10, no. 3, pp. 197–208, 2000.

[34] M. S. Arulampalam, S. Maskell, N. Gordon and T. Clapp, "A tutorial on particle filters for online nonlinear/non-Gaussian Bayesian tracking", *IEEE Transactions on Signal Processing*, vol. 50, no. 2, pp. 174–188, February 2002.

[35] A. Doucet, B. Vo, C. Andrieu and M. Davy, "Particle filtering for multitarget tracking and sensor management", *Proceedings of the 5th International Conference on Information Fusion*, vol. 1, pp. 474–481, Annapolis, Maryland, July 2002.

[36] D. Crisan and A. Doucet, "A survey of convergence results on particle Filtering for practitioners", 2002.

[37] Y. Bar-Shalom and T. E. Fortmann, "Tracking and data association", *Academic Press*, Orlando, FL, 1988.

[38] S. S. Blackman, *Multiple-target tracking with radar applications*, Artech House, Norwood, MA, 1986.

[39] A. Farina , F. A. Studer, *Radar data processing*, Vols. I and II, Research Studies Press, England, 1985.

[40] A. S. Farina and S. Pardini, "Survey of radar data-processing techniques in air-traffic-control and surveillance systems", *IEE Proceedings of Communications, Radar and Signal Processing*, vol. 127, pp. 190–204, June 1980.

[41] T. Fortmann, Y. Bar-Shalom and M. Scheffe, "Sonar tracking of multiple targets using joint probabilistic data association", *IEEE Journal of Oceanic Engineering*, vol. 8, pp. 173–184, July 1983.

[42] D. B. Reid, "An Algorithm for Tracking Multiple Targets", *IEEE Transactions on Automatic Control*, vol. AC-24, no. 6, pp. 843–854, December 1979.

[43] R. Singer, R. Sea, K. Housewright, "Derivation and evaluation of improved tracking filter for use in dense multitarget environments", *IEEE Transactions on Information Theory*, vol. 20, issue 4, pp. 423–432, July 1974.

[44] R. W. Sittler, "An optimal data association problem in surveillance theory", *IEEE Transactions on Military Electronics*, vol. 8, issue 2, pp. 125–139, April 1964.

[45] M. Yeddanapudi, K. Pattipati, Y. Bar-Shalom, "A generalized S-D assignment algorithm for multisensor-multitarget state estimation", *IEEE Transactions on Aerospace and Electronic Systems*, vol. 33, pp. 523–538, Storrs, CT, April 1997.

[46] K. R. Pattipati, R. L. Popp, and T. Kirubarajan,"Survey of assignment techniques for multitarget tracking", in *Multitarget-Multisensor Tracking: Applications and Advances, Volume III*, Y. Bar-Shalom and W. D. Blair, eds., ch. 2, pp. 77159, Artech House, Norwood, MA, 2000.

[47] O. E. Drummond, "Multiple target tracking with multiple frame, probabilistic data association", *Proceedings of the SPIE Conference on Signal and Data Processing of Small Targets*, vol. 1954, pp. 394–408, 1993.

[48] O. E. Drummond, "Multiple sensor tracking with multiple frame, probabilistic data association", *Proceedings of the SPIE Conference on Signal and Data Processing of Small Targets*, vol. 2561, pp. 322–336, 1995.

[49] J. A. Roecker, "Multiple scan joint probabilistic data association", *IEEE Transactions on Aerospace and Electronic Systems*, vol. 31, issue 3, pp. 1204–1210, July 1995.

[50] R. J. Fitzgerald, "Development of practical PDA logic for multitarget tracking by microprocessor", *American Control Conference*, pp. 889–898, Raytheon Company, Missile Systems Division, Bedford, MA, 1986.

[51] B. Zhou and N. K. Bose, "An efficient algorithm for data association in multitarget tracking", *IEEE Transactions on Aerospace and Electronic Systems*, vol. 31, issue 1, pp. 458–468, University Park, PA, January 1995.

[52] M. I. Skolnik, *Introduction to Radar Systems*, McGraw-Hill, New York, NY, December 2002.

[53] G. A. Gilbert and Associates, "Historical Development of the Air Traffic Control System", *IEEE Transactions on Communications*, pp. 364–375, vol. 21, no. 5, May 1973.

[54] C. R. Drane and C. Rizos, *Positioning systems in intelligent transportation systems*, Artech House, Norwood, MA, 1998.

[55] B. McQueen and J. McQueen, *Intelligent transportation systems architectures*, Artech House, Norwood, MA, 1999.

[56] L. Slezak, M. Kvasnicka, M. Pelant, J. Vavra and R. Plesk, "Passive coherent location systems: simulation and evaluation", *Proceedings of the SPIE on Photonics Applications in Astronomy, Communications, Industry, and High-Energy Physics Experiments IV*, vol. 6159, Poland, June 2006.

[57] E. A. Wan and R. Van der Merwe, "The unscented Kalman filter", *in Kalman filtering and Neural Networks*, (S. Haykin, ed.), pp. 1210-1217, Wiley & Sons, New York, NY, USA, October 2001.

[58] Y. Bar-Shalom, T. Kirubarajan and C. Gokberk, "Tracking with classification-aided multiframe data association", *IEEE Transactions on Aerospace and Electronic Systems*, pp. 131–142, vol. 41, no. 3, July 2005.

[59] R. Mahler, "Multitarget moments and their application to multitarget tracking", *Proceedings of the Workshop on Estimation, Tracking and Fusion: A Tribute to Yaakov Bar-Shalom*, Monterey, CA, pp. 134–166, May 2001.

[60] H. Wang, T. Kirubarajan and Y. Bar-Shalom, "Precision large scale air traffic surveillance using an IMM estimator with assignment", *IEEE Transactions on Aerospace and Electronic Systems*, pp. 255-266, vol. 35, no. 1, January 1999.

[61] K. Punithakumar, A. Sinha and T. Kirubarajan, "A multiple model probability hypothesis density filter for tracking maneuvering targets", *IEEE Transactions on Aerospace and Electronic Systems*, vol. 44, no. 1, pp. 87–98, 2008.

[62] A. Sinha, Z.J. Ding, T. Kirubarajan and M. Farooq, "Track quality based multitarget tracking algorithm", *Proceedings of the SPIE Conference on Signal and Data Processing of Small Targets*, vol. 6236, Orlando, FL, April 2006.

[63] S-W. Yeom, T. Kirubarajan and Y. Bar-Shalom, "Track segment association, fine-step IMM and initialization with Doppler for improved track performance", *IEEE Transactions on Aerospace and Electronic Systems*, vol. 40, no. 1, pp. 293–309, January 2004.

[64] M. Longbin, S. Xiaoquan, Z. Ynu, S. Z. Kang and Y. Bar-Shalom, "Unbiased Converted

Measurements for Tracking", *IEEE Transactions on Aerospace and Electronic Systems*, vol. 34, no. 3, pp. 1023–1027, July 1998.

[65] S. J. Julier, J. K. Uhlmann, "A new extension of the Kalman filter to nonlinear systems", *Proceedings of the SPIE on Signal Processing, Sensor Fusion and Target Recognition VI*, vol. 3068, pp. 182–193, Orlando, FL, April 1997.

[66] M. Tobias and A. D. Lanterman, "A probability hypothesis density-based multitarget tracker using multiple bistatic range and velocity measurements", *Proceedings of the Thirty-Sixth Southeastern Symposium on System Theory*, Atlanta, GA, pp. 205–209, March 2004.

[67] B.-N. Vo, S. Singh, and A. Doucet, "Sequential Monte Carlo methods for multi-target filtering with random finite sets", *IEEE Transactions on Aerospace and Electronic Systems*, vol. 41, no. 4, pp. 1224–1245, October 2005.

[68] L. Lin, Y. Bar-Shalom and T. Kirubarajan, "Track labeling and PHD filter for multitarget tracking", *IEEE Transactions on Aerospace and Electronic Systems*, vol. 42, no. 3, pp. 778–795, July 2006.

[69] K. R. Pattipati, T. Kirubarajan and R. L. Popp, "Survey of assignment techniques for multitarget tracking", *Proceedings of the Workshop on Estimation, Tracking, and Fusion: A Tribute to Yaakov Bar-Shalom*, Monterey, CA, May 2001.

[70] R. Tharmarasa, K. Punithakumar, T. Kirubarajan and Y. Bar-Shalom, "Sensor data fusion with application to multi-target tracking", chapter in *Handbook on Array Processing and Sensor Networks* edited by S. Haykin and R. Liu, IEEE-Wiley, December 2009.

[71] N. J. Willis, *Bistatic Radar*, SciTech Publishing Inc., Raleigh, NC, 2005.

[72] M. I. Skolnik, "An Analysis of Bistatic Radar", *IRE Transactions on Aerospace and Navigational Electronics*, vol. ANE-8 , issue 1, pp. 19–27, Res. Div., Electronic Communications, Inc., Timonium, MD, March 1961.

[73] N. J. Willis and H. D. Griffiths, *Advances in Bistatic Radar*, SciTech Publishing Inc., Raleigh, NC, 2007.

[74] M. C. Jackson, "The geometry of bistatic radar systems", *IEE Proceedings of Communications, Radar and Signal Processing*, vol. 133 , issue 7, pp. 604–612, Marconi Co. Ltd., Research Centre, Chelmsford, UK, December 1986.

[75] K. Milne, "Principles and concepts of multistatic surveillance radars", *Proceedings of the IEE International Conference*, vol. A79-10281 01-04, pp. 46–52, London, UK, October 1977.

[76] "Lockheed Martin silent sentry", *Aviation Week & Space Technology*, Trade Publication, vol. 150 Issue 19, p75, October 1999.

[77] C. Baker, D.W. O'Hagan, H.D. Griffiths, M. Inggs, R. Lord and N. Morrison, "Passive radar tracking", *IET Seminar on the Future of Civil Radar*, pp. 57–67, London, UK, June 2006.

[78] D. P. Bertsekas, " The auction algorithm: A distributed relaxation method for the assignment problem ", *Annals of Operations Research* , vol. 14, pp. 105–123, June 1988.

[79] O. E. Drummond, "Track and tracklet fusion filtering using data from distributed sensors", *Proceeding of the Estimation, Tracking and Fusion: A Tribute to Yaakov Bar-Shalom*, pp. 167–186, Monterey, CA, May 2001.

[80] M. L. Hernandez, T. Kirubarajan and Y. Bar-Shalom, "Multisensor resource deployment using posterior Cramér-Rao bounds", *IEEE Transactions on Aerospace and Electronic Systems*, vol. 40, no. 2, pp. 399–416, April 2004.

[81] R. L. Popp, K. R. Pattipati, Y. Bar-Shalom, R. R. Gassner, "An adaptive m-best SD assignment algorithm and parallelization for multitarget tracking", *IEEE Aerospace Conference*, vol. 5, pp. 71–84, urlington, MA, March 1998.

[82] A. Farina, "Tracking function in bistatic and multistatic radar systems", *IEE Proceedings on Communications, Radar and Signal Processing*, vol. 133 - Part F, no. 7, pp. 630–637, December 1986.

[83] H. D. Griffiths, "Bistatic radar - principles and practice", *SBMO International Microwave Conference*, vol. 2, pp. 519–526, Sao Paulo, Brazil, August 1993.

[84] H. Tan, M. Ren, Bo Liu and J. Song. "PCL System with Illuminator of Opportunity", *International Conference on Radar*, October 2006.

[85] K. R. Pattipati,S. Deb, Y. Bar-Shalom and R. B. Washburn, "A new relaxation algorithm and passive sensor data association", *IEEE Transactions on Automatic Control*, vol. 37, no. 2, pp.198–213, Storrs, CT Feb 1992.

[86] B. Ristic, S. Zollo, and S. Arulampalam, "Performance bounds for maneuvering target tracking using asynchronous multi-platform angle-only measurements", *Proceedings of the 4th International Conference on Information Fusion*, Montreal, QC, Canada, August 2001.

[87] X. Zhang and P. K. Willett, " Cramer-Rao bounds for discrete time linear filtering with measurement origin uncertainty ", *Proceedings of the Workshop on Estimation,*

Tracking and Fusion: A Tribute to Yaakov Bar-Shalom , pp. 546–561, Monterey, CA, May 2001.

[88] R. P. S. Mahler, "Multitarget Bayes filtering via first-order multitarget moments", *IEEE Transactions on Aerospace and Electronic Systems*, vol. 39, No. 4, pp. 1152–1178, October 2003.

[89] R. Tharmarasa, T. Kirubarajan, M. L. Hernandez and A. Sinha, "PCRLB-Based Multisensor Array Management for Multitarget Tracking", *IEEE Transactions on Aerospace and Electronic Systems*, vol. 43, no. 2, pp. 539–555, 2007.

[90] K. Punithakumar, T. Kirubarajan and M. L. Hernandez,"Multisensor Deployment Using PCRLB, Incorporating Sensor Deployment and Motion Uncertainties", *IEEE Transactions on Aerospace and Electronic Systems*, vol. 42, No. 4, pp. 1474-1485, October 2006.

[91] R. Tharmarasa, T. Kirubarajan and M.L. Hernandez,"PCRLB Based Multisensor Array Management for Multitarget Tracking", *Proc. SPIE Conference on Signal and Data Processing of Small Targets*, vol. 5428, Orlando, FL, April 2004.

[92] E. J. Dela Cruz, A. T. Alouani, W. D. Blair, T.R. Rice, "Estimation of tilt errors in multisensor systems", Proceedings of IEEE Southeastcon '92, vol. 1 pp. 205 - 209 12-15 April 1992.

[93] P. Tichavsky, "Posterior Cramér-Rao bounds for adaptive harmonic retrieval", *IEEE Transactions on Signal Processing*, vol. 43, no. 5, pp. 1299–1302, May 1995.

[94] A. B. Poore and A. J. Robertson, "A new Lagrangian Relaxation based algorithm for a class of multidimensional assignment problems", *Computational Optimization and Applications*, vol. 8, issue 2, pp. 129–150, September 1997.

[95] P. Tichavsky, C. H. Muravchik, and A. Nehorai, "Posterior CramerRao bounds for discrete-time nonlinear filtering", *IEEE Transactions on Signal Processing*, vol. 46, no. 5, pp. 13861396, May 1998.